In presenting the dissertation as a partial fulfillment of the requirements for an advanced degree from the Georgia Institute of Technology, I agree that the Library of the Institute shall make it available for inspection and circulation in accordance with its regulations governing materials of this type. I agree that permission to copy from, or to publish from, this dissertation may be granted by the professor under whose direction it was written, or, in his absence, by the Dean of the Graduate Division when such copying or publication is solely for scholarly purposes and does not involve potential financial gain. It is understood that any copying from, or publication of, this dissertation which involves potential financial gain will not be allowed without written permission.

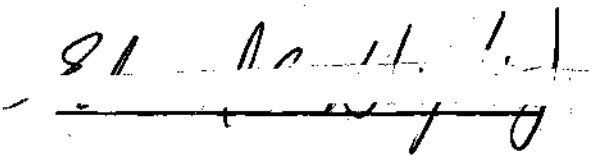

7/25/68

PARAMETRIC EXCITATION OF NONPLANAR MOTIONS OF AN ELASTIC ROD

A THESIS

Presented to

The Faculty of the Graduate Division

by

Edward Charles Haight, Jr.

In Partial Fulfillment

of the Requirements for the Degree

Doctor of Philosophy in the

School of Engineering Science and Mechanics

Georgia Institute of Technology

February 1969

PARAMETRIC EXCITATION OF NONPLANAR MOTIONS OF AN ELASTIC ROD

Approved:

Chairman

Date approved by Chairman: 3/19/69

This thesis is dedicated to

Judy, Ned, and Ann.

ACKNOWLEDGMENTS

I wish to thank Dr. Wilton W. King, my thesis advisor, for his ideas, direction, and encouragement. I wish also to thank Dr. D. V. Ho and Dr. G. M. Rentzepis for reading my thesis. Particular thanks are due to James A. Shiflett for preparing the computer program for determining δ_{mn} and to John W. Shipley for assisting with the experiments.

TABLE OF CONTENTS

TABLE OF CONTENTS (Continued)

LIST OF TABLES

LIST OF ILLUSTRATIONS

LIST OF ILLUSTRATIONS (Continued)

LIST OF PRINCIPAL SYMBOLS

A	Area of the rod cross-section
A_b	Amplitude of the base displacement function for axial excitation
$\bar{A}_b$	A_b/ℓ. Nondimensional axial base excitation amplitude
A_n	Steady-state amplitude of the planar response
$\bar{A}_n$	A_n/ℓ. Nondimensional steady-state amplitude
$(A_n)_{cr}$	Steady-state amplitude of the planar response for which motion changes from a stable to an unstable state
A_{1n}, A_{2n}	$A_{1n}^2 + A_{2n}^2 = A_n^2$
$\bar{A}_{1n}$, $\bar{A}_{2n}$	$\bar{A}_{1n} = A_{1n}/\ell$, $\bar{A}_{2n} = A_{2n}/\ell$
B_b	Amplitude of the base displacement function for transverse excitation
$\bar{B}_b$	B_b/ℓ. Nondimensional transverse base excitation amplitude
E	Modulus of elasticity
I_η, I_2, I_3	Moments of inertia of the rod cross-section about the η, χ_2, and χ_3 axes, respectively
L	Lagrangian function
M	Mass per unit length of the rod
N	Normal force on the rod cross-section
P	Point at which the response curve has a vertical tangent

S	Deformed arc length
T	Kinetic energy
T_{2n}, T_{3m}	nth and mth generalized coordinates
V	Potential energy
X_1, X_2, X_3	Inertial coordinates of the rod centerline in its undeformed configuration
$X_n(S), X_m(S)$	nth and mth spatial modes
$a_m^{(2)}$	$\frac{4\beta_m^{(2)}}{\alpha}$
$a_n^{(3)}$	$\frac{4\beta_n^{(3)}}{\alpha}$
b_m, b_n	$b_m = \frac{4\gamma_m \ell}{\alpha}$, $b_n = \frac{4\gamma_n \ell}{\alpha}$
c_m, c_n	$c_m = \frac{\delta_m \ell^2}{\alpha}$, $c_n = \frac{\delta_n \ell^2}{\alpha}$
c_{mn}	$\frac{\Delta_{mn} \ell^2}{\alpha}$
f_n	$f_n = \frac{4\epsilon_n}{\alpha}$
$\bar{i}, \bar{j}, \bar{k}$	Unit vectors in the x_1, x_2, x_3 directions, respectively
ℓ	Length of the rod
m,n	Mode numbers
s	Undeformed arc length
t	Time
u,v,w	Displacement components in the x_1, x_2, x_3 directions, respectively
x_1, x_2, x_3	Inertial coordinates of the rod centerline in its deformed configuration

x_{3m}	Perturbation function
β_n	Parameter defined as $[M\omega_n^2/EI]^{\frac{1}{4}}$
$\alpha, \beta_n^{(3)}, \beta_m^{(2)}, \gamma_n, \gamma_m, \delta_n, \delta_m, \Delta_{mn}, \Delta_{nm}$	Constants defined in Appendix B
Δ_n	Logarithmic decrement for the nth mode
ϵ	Extensional strain of the rod centerline
ϵ_1, ϵ_2	Coefficients in the Mathieu equation
ϵ_n	Damping constant
ζ	4τ
η	2τ
$\varkappa$	Principal curvature of the rod centerline
τ	Non-dimensional time, $\tau = \frac{\omega t}{2}$
φ_n	Parameter, given in Table 1
ω	Frequency of the excitation
$\omega_n^{(3)}$	nth eigenfrequency for the response in the x_1, x_2-plane
$\omega_m^{(2)}$	mth eigenfrequency for the response in the x_1, x_3-plane
$\dot{(\ )}$	$\frac{\partial(\ )}{\partial t}$
$(\ )'$	$\frac{\partial(\ )}{\partial S}$ or $\frac{d(\ )}{d\tau}$. The distinction is clear from the context.

SUMMARY

A theoretical and experimental examination has been made of the loss due to parametric coupling of the stability of the planar steady-state forced response of a long slender elastic rod. Attention has been given to two methods of excitation. In the first, the rod is harmonically driven in the axial direction and the principal planar motion is the parametrically induced half-order subharmonic response. The second method for exciting the rod is to force it harmonically in a direction perpendicular to the rod axis; this excitation directly induces a harmonic plane steady-steady response. In both cases, nonplanar motions are parametrically coupled to the principal planar oscillations. It is the stability of the planar motions with respect to disturbances perpendicular to the original response plane which is investigated.

For the case of the axially driven rod, the analysis shows that provided an arbitrarily small viscous damping term is present, plane motion is stable for all values of the parameters when the natural frequency ratio for motions in the two principal planes is unity. Only when the natural frequencies are detuned does the original planar response lose its stability. It is shown that when the frequency ratio is near unity there is a critical excitation frequency which causes the original planar response to exhibit an amplitude jump and a simultaneous plane shift to stable motions in the other principal plane. For sufficiently large detuning, the responses in the two principal planes are separated by a frequency interval in which the straight configuration of the rod is

stable. An argument is presented to show that a whirling motion of the axially excited rod will not be observed in the laboratory. The effect of adding a viscous damping term is to decrease the regions in which plane motion is unstable.

When the rod is driven transversely, there are values of the exciting frequency which cause a loss of planar stability even when the natural frequency ratio is unity. The amplitude jump which is always present in the nonlinear analysis of plane motion of the transversely excited rod may now occur at a frequency lower than, inside of, or greater than the frequency interval for which the planar response is unstable, depending on the natural frequency ratio. Again, the effect of damping is to decrease the zone for which the planar response is unstable. Large detuning combined with viscous damping can cause the planar response to be stable for all values of the parameters.

The experiments verify that the theory correctly predicts the qualitative response of the rod for both types of excitation. Good quantitative agreement for both the amplitudes and frequencies at which the planar response becomes unstable is obtained for the transversely forced case. For the axially driven rod, the theory accurately predicts critical frequencies, but the theoretical amplitudes are considerably higher than the experimental ones, especially for large amplitudes. It is possible that more accurate amplitude predictions may result from a more sophisticated damping model or from a higher order approximate analysis.

CHAPTER I

INTRODUCTION

This research concerns the analytical and experimental investigation of parametrically excited nonplanar motions of an elastic system undergoing plane steady-state oscillations. Several physical problems can be fitted to this basic idea; among these are the vibrating string, the spherical pendulum, and the vibrating rigid container of fluid. The system which is treated herein is the elastic rod.

At this point it is prudent to amplify the meaning of "parametric" when used in the above context since the term "parametric oscillation" does not adequately explain the phenomenon. The term arises from the fact that the functions which cause the parametric oscillation appear as non-constant coefficients in the differential equation of motion. This is illustrated by $\ddot{\theta}(t) + \left(-\frac{g}{\ell} + \frac{1}{m\ell} P(t)\right)\theta(t) = 0$ which is the equation given by Stoker [1]* for the parametric excitation of the inverted pendulum of length ℓ and bob mass m. $P(t)$ is the parametric load.

Several features distinguish parametric resonance from directly excited resonance. First, in the parametric case, a vector which represents the excitation is perpendicular to a vector associated with the resulting displacement while in the direct resonance case these vectors are parallel. Second, the frequencies of the excitation causing parametric resonance are continuously distributed as contrasted to the

*Numbers in brackets refer to references listed in Literature Cited.

discrete frequencies of the excitation which cause resonance in the directly forced case.

For a comprehensive literature review relating to parametric behavior of elastic bodies, the reader is referred to Beylin and Dzhaneldize [2], 1952, and Evan-Iwanowski [3], 1965. Apparently the first to report on his observations of parametric resonance was Faraday [4], 1831. He discussed extensively a class of acoustical and mechanical oscillations but presented no quantitative data. The easily reproduced classical Melde experiment [5], 1859, consisted of attaching a horizontal thread to a vertical tine of a tuning fork. When the fork was struck, Melde observed that the string executed vibrations in a vertical direction at a frequency half that of the fork frequency. Lord Rayleigh [6], 1887, discussed the problem mathematically.

The earliest work on the structural aspect of dynamic stability is credited to Beliaev [7], 1924. He analyzed an elastic rod, hinged at both ends, and excited by an axial force of the form $P(t) = P_0 + P_1\cos\Omega t$, where P_0 and P_1 are constants and Ω is the frequency of the periodic load. Beliaev calculated the principal instability region for this problem.

It is notable that the pioneering developments in the field of dynamic stability of structures were made by Russian researchers; these advances were followed by German work. The first significant English language study was presented by Lubkin and Stoker [8], 1943, when they considered the stability of parametrically excitedplane motions of rods and strings.

Early studies were simplified by assumptions or approximations which caused the governing differential equations to be linear. However,

Gol'denblat [9], 1947, showed that while a linear formulation is sufficient for the prediction of the instability regions, it is incapable of determining the amplitudes of the vibrations in the resonance regions. Bolotin, in a number of articles, incorporated a nonlinear theory to more satisfactorily explain the phenomenon; these studies are summarized in his unique book [10], 1956. The (nonlinear) effect of longitudinal inertia upon the parametric response of columns was discussed by Evensen and Evan-Iwanowski [11], 1966.

Material dealing with the stability of planar motions with respect to nonplanar disturbances is less plentiful. The most relevant article on this specialization of dynamic stability is a study by Henry and Tobias [12], 1961, of a pair of quasi-linear, coupled, ordinary differential equations of a special form, representing free vibrations of an undamped, two degree of freedom system. This paper was prompted by an earlier one by Tobias [13], 1957, concerning the coupling effects in imperfect discs. In the 1961 paper, Henry and Tobias demonstrated that it is possible for motion to be confined entirely to one mode and they determined a criterion for stability of the mode at rest.

Even though the Henry and Tobias study is closely related to this one, their research does not deal with several of the essential features of this thesis. The complications in this study arise first because this system is an elastic one undergoing general three-dimensional motion; this gives rise to three nonlinear partial differential equations as opposed to two ordinary nonlinear ones. Secondly, this system is externally excited as contrasted to their freely vibrating system. Therefore, a larger variety of responses is possible in the present problem.

The majority of the literature dealing with physical systems of the types mentioned on Page 1 incorporates direct rather than parametric excitation of the basic system [14, 15, 16]. These papers show that a string, for example, having fixed ends and being excited in a direction perpendicular to the axis may reach a condition for which the particles cease to vibrate solely in the plane of the driving force. When this condition is reached, the string acquires a component of motion in the direction perpendicular to the driving force plane. That is, planar motion is unstable over some frequency interval of the driving force. This phenomenon may be considered as a parametric excitation of the non-planar motions by the planar response. (See the discussion in Chapter V.)

The writer is aware of four papers which specifically confront the issue of parametrically excited systems which exhibit nonplanar responses. Hemp and Sethna [17], 1964, investigated the vertically excited spherical pendulum, but they restricted the frequency of the support motion to be much larger than the linear natural frequency of the pendulum in plane motion. In another paper, Hemp and Sethna [18], 1964, studied the gyroscopic pendulum subjected to a vertical disturbance of arbitrary frequency. They considered motions that are in the neighborhood of steady precession motions. Quick [19], 1964, excited an elastic string longitudinally and showed that elastic asymmetry causes the string to move out of the plane of vibration and into thin elliptical orbits. Ebner [20], 1968, studied the parametric oscillation of imperfect simply supported thin-walled columns with open cross-section and included in his analysis twisting deformations as well as lateral bending deformation. Using the analog computer, he determined the stability regions and the amplitude-time response.

Tso [21], 1968, analyzed the related topic of the parametric torsional stability of a bar subjected to axial excitation. His equations. which account for the coupling between longitudinal and torsional vibrations, have a form similar in many respects to the ones shown in Chapter V of this thesis. Another related study is by Evensen [22], 1965. He studied coupled-mode bending vibrations in the plane of a thin circular ring; his experiments show generally good agreement with his theory.

One might also suppose that the vertical excitation of an upright, rigid, right circular cylindrical tank filled with a liquid might cause the liquid to swirl. However, Dodge, Kana, and Abramson [23], 1965, point out that there is "no evidence of any time-dependent rotation, periodic or otherwise, of the plane of the liquid motion as occurs with large-amplitude sloshing resulting from transverse excitation." We comment further on this observation in Chapter VII.

CHAPTER II

THE EQUATIONS OF MOTION

Consider a long, slender, initially straight, perfectly elastic rod oriented so that the base is clamped and the opposite end is free. We note here that the above-mentioned end conditions are chosen to expedite the experiments; other end conditions can be handled analytically in a similar manner. Let the cross-sectional dimensions and the material properties of the rod be constant with S.

In order to minimize any twisting motion that the rod might undergo, the restriction is made that the rod cross-section is closed; furthermore, it is assumed that the lowest eigenfrequency of twisting motion about the longitudinal axis is much larger than any of the bending response eigenfrequencies with which we shall be concerned. In light of these assumptions, we omit the twisting response from the analysis.

Let x_2 and x_3 be the principal centroidal axes of the rod cross-section and let the base be excited harmonically according to $A_b \cos \omega t$. The coordinate system is shown in Figures 1 and 2. Let the undeformed arc length of the center line be S and the deformed arc length be $s(S,t)$. The undeformed position of a particle on the rod is $X_i(S,t)$, $i = 1,2,3$; the deformed position of the particle is $x_i(S,t)$. We choose to formulate the problem in Lagrangian or material coordinates.

Hamilton's Principle is used to obtain the equations of motion. With shear deformation neglected, the total potential energy of the rod

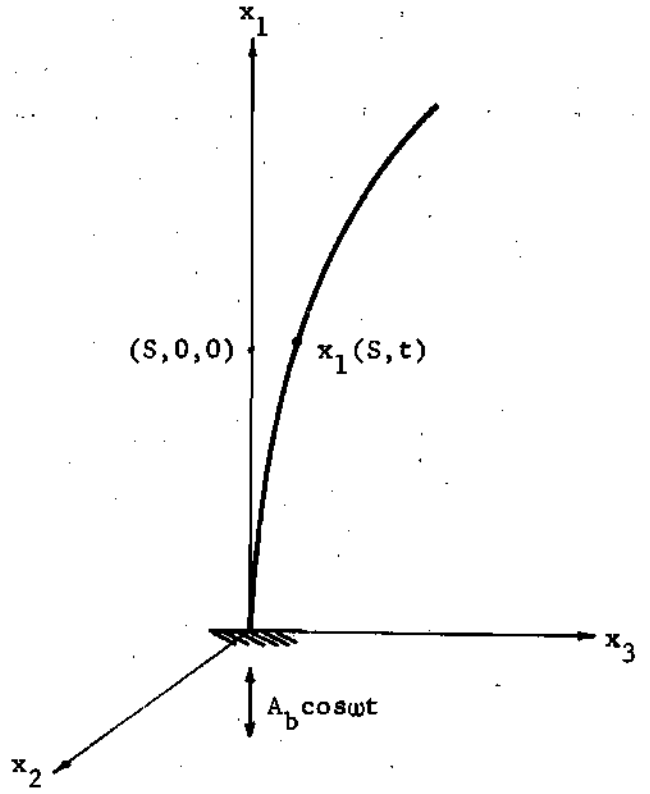

Figure 1. Orientation of the Coordinate System.

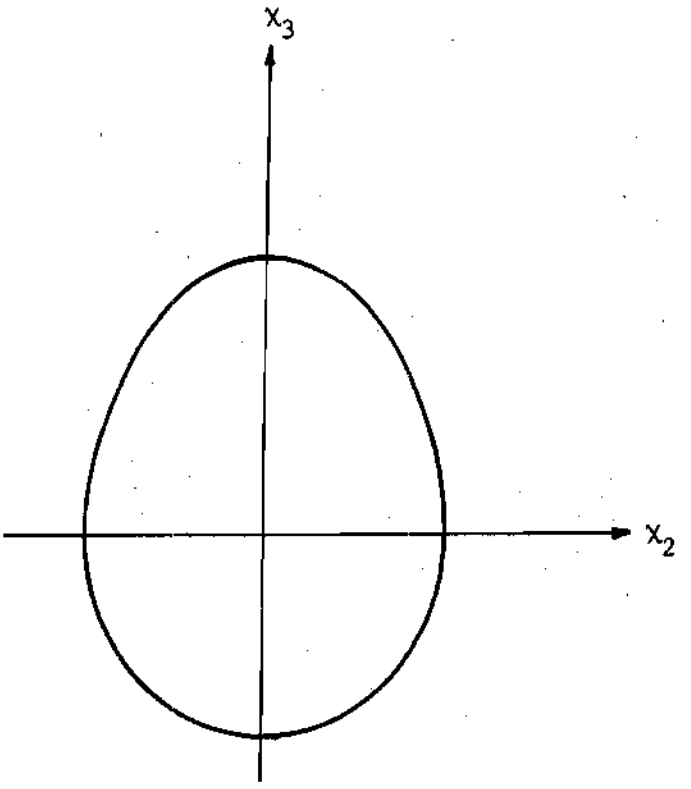

Figure 2. Orientation of the Coordinate System.

is the elastic potential energy due to bending plus the elastic potential energy due to stretching of the centerline. That is,

$$V(t) = \frac{1}{2}\int_0^{\ell} EI_{\eta}(S,t)\varkappa^2(S,t)dS + \frac{1}{2}\int_0^{\ell} EA\ \epsilon^2(S,t)dS. \qquad (2\text{-}1)$$

In the above equation, $\varkappa(S,t)$ is the principal curvature of the centerline at point S, $I_{\eta}(S,t)$ is the moment of inertia of the cross-section about the instantaneous bending axis at S, and $\epsilon(S,t)$ is the extensional strain of the centerline at S. In Appendix A, the bending potential energy term is converted to a form which involves the moments of inertia of the cross-section about the χ_2 and χ_3 principal axes. Since the latter two moments of inertia are constant, the analysis becomes simpler than it would be had we used $I_{\eta}(S,t)$.

Assuming that the cross-sectional dimensions are small compared to the length of the rod, we write the kinetic energy as

$$T(t) = \frac{1}{2}\int_0^{\ell} M[\dot{u}^2(S,t) + \dot{v}^2(S,t) + \dot{w}^2(S,t)]dS\ , \qquad (2\text{-}2)$$

where $\dot{(\ )} = \frac{\partial(\ )}{\partial t}$, and $u(S,t)$, $v(S,t)$, and $w(S,t)$ are displacement components in the x_1, x_2, and x_3 directions, respectively. Hence, the Lagrangian function is given by

$$L(t) = T(t) - V(t) = \int_0^{\ell} \left\{\frac{M}{2}[\dot{u}^2(S,t) + \dot{v}^2(S,t) + \dot{w}^2(S,t)]\right.$$

$$\left. - \frac{EI_{\eta}(S,t)}{2}\varkappa^2(S,t) - \frac{EA}{2}\epsilon^2(S,t)\right\}dS\ . \qquad (2\text{-}3)$$

We now seek to express $\epsilon(S,t)$ and $\varkappa(S,t)$ in terms of the displacement components $u(S,t)$, $v(S,t)$, and $w(S,t)$. To do this, define extensional

strain of the centerline as

$$\epsilon(S,t) = \frac{1}{2}\frac{ds^2-dS^2}{dS^2} . \qquad (2-4)$$

Using this definition, it can be shown [24] that the expression for $\epsilon(S,t)$ in terms of displacement components is

$$\epsilon(S,t) = u'(S,t) + \frac{1}{2}[u'^2(S,t) + v'^2(S,t) + w'^2(S,t)] , \qquad (2-5)$$

where

$$(\ )' = \frac{\partial(\ )}{\partial S} .$$

The curvature of the centerline $\kappa(S,t)$ must also be given in terms of $u(S,t)$, $v(S,t)$ and $w(S,t)$. The well-known curvature expression in Eulerian or spatial coordinates is

$$\kappa(s,t) = \left(\frac{\partial^2 x_i(s,t)}{\partial s^2}\frac{\partial^2 x_i(s,t)}{\partial s^2}\right)^{\frac{1}{2}} , \quad i = 1,2,3 . \qquad (2-6)$$

First the independent variables are changed from (s,t) to (S,t) and then equations (2-4) and (2-5) are used. After performing the calculations (the details are presented in Appendix A), we find:

$$\begin{aligned}\kappa(S,t) = [(1+u')^2+v'^2+w'^2]^{-2}\Big[&\Big\{[(1+u')^2+v'^2+w'^2]u'' \\ &- \frac{1+u'}{2}\frac{\partial}{\partial S}[(1+u')^2+v'^2+w'^2]\Big\}^2 + \Big\{[(1+u')^2+v'^2+w'^2]v'' \\ &- \frac{v'}{2}\frac{\partial}{\partial S}[(1+u')^2+v'^2+w'^2]\Big\}^2 + \Big\{[(1+u')^2+v'^2+w'^2]w'' \\ &- \frac{w'}{2}\frac{\partial}{\partial S}[(1+u')^2+v'^2+w'^2]\Big\}^2\Big]^{\frac{1}{2}} , \end{aligned} \qquad (2-7)$$

where u, v, w are functions of (S,t).

Clearly, equation (2-7) is too complicated to deal with in a concise manner. If we make the simplifying assumptions

$$\left.\begin{aligned} &|\epsilon(S,t)| \ll \tfrac{1}{2} && (2\text{-}8)\\ &\frac{\partial \epsilon(S,t)}{\partial S} = 0 \quad \text{for } 0 \le S \le \ell \text{ and } t \ge 0 , && (2\text{-}9)\\ &|u'(S,t)| \ll \tfrac{1}{2} && (2\text{-}10) \end{aligned}\right\} ,$$

we find that

$$\kappa(S,t) \doteq [v''^2(S,t) + w''^2(S,t)]^{\frac{1}{2}} \qquad (2\text{-}11)$$

and

$$\epsilon(S,t) = u'(S,t) + \tfrac{1}{2}[v'^2(S,t) + w'^2(S,t)] . \qquad (2\text{-}12)$$

The meaning of equations (2-8) and (2-9) is that we assume not only that the centerline strain can be neglected compared to $\frac{1}{2}$ but that its rate of change as we move along the rod is so small that it can be neglected. Assumption (2-10) implies that the contribution to ϵ due to v'^2 and w'^2 far surpasses the contribution to ϵ due to u'^2.

Now equations (2-11), (2-12) and (A-22) can be used in equation (2-3) to yield

$$\begin{aligned} L(t) = \int_0^{\ell} \{ & \tfrac{M}{2}[\dot{u}^2(S,t) + \dot{v}^2(S,t) + \dot{w}^2(S,t)] \\ & - \tfrac{E}{2}[I_3 v''^2(S,t) + I_2 w''^2(S,t)] \\ & - \tfrac{EA}{2}[u'(S,t) + \tfrac{1}{2}(v'^2(S,t) + w'^2(S,t))]^2 \} dS . \end{aligned} \qquad (2\text{-}13)$$

According to Hamilton's Principle, we must determine the functions $u(S,t)$, $v(S,t)$ and $w(S,t)$ which render stationary $\int_{t_o}^{t_1} L(t)dt$. A straightforward application of the methods of the calculus of variations yields the equations of motion:

$$- EA \frac{\partial}{\partial S}\left\{u'(S,t) + \frac{1}{2}[v'^2(S,t) + w'^2(S,t)]\right\} + M\ddot{u}(S,t) = 0 \qquad (2\text{-}14)$$

$$EI_3 v''''(S,t) - EA \frac{\partial}{\partial S}\left\{u'(S,t) + \frac{1}{2}[v'^2(S,t) + w'^2(S,t)]\right\}v'(S,t)$$

$$- EA\left\{u'(S,t) + \frac{1}{2}[v'^2(S,t) + w'^2(S,t)]\right\}v''(S,t) + M\ddot{v}(S,t) = 0 \qquad (2\text{-}15)$$

$$EI_2 w''''(S,t) - EA \frac{\partial}{\partial S}\left\{u'(S,t) + \frac{1}{2}[v'^2(S,t) + w'^2(S,t)]\right\}w'(S,t)$$

$$- EA\left\{u'(S,t) + \frac{1}{2}[v'^2(S,t) + w'^2(S,t)]\right\}w''(S,t) + M\ddot{w}(S,t) = 0. \qquad (2\text{-}16)$$

The dependent variable $u(S,t)$ can be eliminated from this set of equations by the following manipulations. Integrate equation (2-14) to get

$$EA\left\{u'(S,t) + \frac{1}{2}[v'^2(S,t) + w'^2(S,t)]\right\} = + \int_o^S M\ddot{u}(\xi,t)d\xi + C(t), \qquad (2\text{-}17)$$

where $C(t)$ is an arbitrary time dependent function. The normal force on any rod cross-section is

$$N(S,t) = EA\ \epsilon\ (S,t)\ . \qquad (2\text{-}18)$$

From equation (2-12), we find

$$N(S,t) \doteq EA\left\{u'(S,t) + \frac{1}{2}[v'^2(S,t) + w'^2(S,t)]\right\}\ . \qquad (2\text{-}19)$$

Now since $N(\ell,t) = 0$, we combine this with equations (2-17) and (2-19) to conclude that

$$N(S,t) = -\int_s^\ell M\ddot{u}(\xi,t)d\xi \ . \tag{2-20}$$

Using equations (2-19) and (2-20) in the equations of motion gives

$$EI_3v'''' - M\ddot{u}v' + v''\int_s^\ell \ddot{u}(\xi,t)d\xi + M\ddot{v} = 0 \tag{2-21}$$

$$EI_2w'''' - M\ddot{u}w' + w''\int_s^\ell \ddot{u}(\xi,t)d\xi + M\ddot{w} = 0 \ . \tag{2-22}$$

This pair of equations agrees with the one found by Evensen and Evan-Iwanowski [11] when the above equations are reduced to the plane motion case by letting $w(S,t) \equiv 0$.

We now determine the function $u(S,t)$ so that it can be eliminated from equations (2-21) and (2-22). Note that

$$ds^2 = dx_1^2 + dx_2^2 + dx_3^2 \tag{2-23}$$

$$x_1(S,t) = S + u(S,t) \tag{2-24}$$

$$x_2(S,t) = v(S,t) \tag{2-25}$$

$$x_3(S,t) = w(S,t) \ , \tag{2-26}$$

therefore,

$$dx_1^2 = \left[\left(\frac{\partial s}{\partial S}\right)^2 - \left(\frac{\partial v}{\partial S}\right)^2 - \left(\frac{\partial w}{\partial S}\right)^2\right]dS^2 \ . \tag{2-27}$$

An expression for $\left(\frac{\partial s}{\partial S}\right)^2$ is obtained from equation (2-4) by rearranging terms to get

$$\left(\frac{\partial s}{\partial S}\right)^2 = 1 + 2\epsilon(S,t) \ . \qquad (2\text{-}28)$$

Assumption (2-8) applied to equation (2-28) implies that

$$\left(\frac{\partial s}{\partial S}\right)^2 \doteq 1 \ . \qquad (2\text{-}29)$$

The use of equation (2-29) in equation (2-27) and one integration with respect to S shows that

$$x_1(S,t) \doteq \int_0^S [1 - v'^2(\xi,t) - w'^2(\xi,t)]^{\frac{1}{2}} d\xi + C_1(t) \ . \qquad (2\text{-}30)$$

The end displacement condition is that $x_1(0,t) = A_b \cos \omega t$, hence

$$x_1(S,t) \doteq \int_0^S [1 - v'^2(\xi,t) - w'^2(\xi,t)]^{\frac{1}{2}} d\xi + A_b \cos \omega t \ . \qquad (2\text{-}31)$$

Finally, we combine equations (2-31) and (2-24) to obtain the formula for u(S,t):

$$u(S,t) \doteq \int_0^S [1 - v'^2(\xi,t) - w'^2(\xi,t)]^{\frac{1}{2}} d\xi - S + A_b \cos \omega t \ . \qquad (2\text{-}32)$$

In keeping with the first order approximation policy used herein, we expand the integrand of equation (2-32) in a binomial series and retain only terms up to, and including, the linear one in $[v'^2(S,t) + w'^2(S,t)]$. This shows that

$$u(S,t) \doteq -\frac{1}{2} \int_0^S [v'^2(\xi,t) + w'^2(\xi,t)] d\xi + A_b \cos \omega t \ . \qquad (2\text{-}33)$$

The governing integro-differential equations which determine v(S,t) and w(S,t) are found by using equation (2-33) in equations (2-21) and (2-22). The equations are:

$$EI_3 v'''' + M\ddot{v} + \frac{Mv'}{2}\frac{\partial^2}{\partial t^2}\int_o^s [v'^2(\xi,t) + w'^2(\xi,t)]d\xi + Mv'A_b\omega^2\cos\omega t$$

$$- \frac{Mv''}{2}\int_o^{\ell}\left\{\frac{\partial^2}{\partial t^2}\int_o^{\xi}[v'^2(\eta,t) + w'^2(\eta,t)]d\eta\right\}d\xi$$

$$- Mv''A_b\omega^2(\ell - S)\cos\omega t = 0 \qquad (2\text{-}34)$$

$$EI_2 w'''' + M\ddot{w} + \frac{Mw'}{2}\frac{\partial^2}{\partial t^2}\int_o^s [v'^2(\xi,t) + w'^2(\xi,t)]d\xi + Mw'A_b\omega^2\cos\omega t$$

$$- \frac{Mw''}{2}\int_o^{\ell}\left\{\frac{\partial^2}{\partial t^2}\int_o^{\xi}[v'^2(\eta,t) + w'^2(\eta,t)]d\eta\right\}d\xi$$

$$- Mw''A_b\omega^2(\ell - S)\cos\omega t = 0 \ . \qquad (2\text{-}35)$$

Notice that when $I_2 = I_3$ these equations are symmetric in v and w.

CHAPTER III

REDUCTION TO A FINITE NUMBER OF DEGREES OF FREEDOM USING THE GALERKIN METHOD

In this chapter, we apply the Galerkin method in order to reduce equations (2-34) and (2-35) to ordinary differential equations. The eigenfunctions of the linear fixed-free vibrating rod are chosen as coordinate functions. A solution to equations (2-34) and (2-35) could be sought in the form

$$v(S,t) = \sum_{i=1}^{\infty} T_{2ni}(t) X_{ni}(S)$$

$$w(S,t) = \sum_{i=1}^{\infty} T_{3mi}(t) X_{mi}(S) \ ,$$

but as a first approximation we restrict this form to

$$v(S,t) \doteq T_{2n}(t)\ X_n(S) \tag{3-1}$$

$$w(S,t) \doteq T_{3m}(t)\ X_m(S) \ . \tag{3-2}$$

Notice that this solution form, which results in two ordinary differential equations for the determination of $T_{2n}(t)$ and $T_{3m}(t)$, admits (when $m \neq n$) the possibility that the spatial mode shape in the x_1, x_3-plane is different from the spatial mode shape in the x_1, x_2-plane.

The choice of the eigenfunctions for the linear vibration problem as coordinate functions in the Galerkin analysis is of considerable

convenience due to the fact that many of the resulting integrals have been tabulated by Young and Felgar [25]. The functions $X_n(S)$ are

$$X_n(S) = \cosh \beta_n S - \cos \beta_n S - \varphi_n(\sinh \beta_n S - \sin \beta_n S) ,$$

$$n = 1,2,.... \tag{3-3}$$

where

$$\beta_n^4 = \frac{M\omega_n^2}{EI}$$

and φ_n is a parameter, the values of which are given in Table 1.

Table 1. Values of φ_n and $\beta_n \ell$.

n	φ_n	$\beta n \ell$
1	0.7341	1.8751
2	1.0185	4.6941
3	0.9992	7.8548
4	1.0000	10.9955
5	1.0000	14.1372

A routine application of Galerkin's method gives

$$\alpha\ddot{T}_{2n} + (\beta_n^{(3)} + \gamma_n A_b \omega^2 \cos \omega t)T_{2n} + \delta_n T_{2n}(T_{2n}\ddot{T}_{2n} + \dot{T}_{2n}^2)$$

$$+ \Delta_{nm} T_{2n}(T_{3m}\ddot{T}_{3m} + \dot{T}_{3m}^2) = 0 \tag{3-4}$$

$$\alpha\ddot{T}_{3m} + (\beta_m^{(2)} + \gamma_m A_b \omega^2 \cos \omega t)T_{3m} + \delta_m T_{3m}(T_{3m}\ddot{T}_{3m} + \dot{T}_{3m}^2)$$

$$+ \Delta_{mn} T_{3m}(T_{2n}\ddot{T}_{2n} + \dot{T}_{2n}^2) = 0 . \tag{3-5}$$

The constants appearing in equations (3-4) and (3-5) are defined by

$$\alpha = M \int_o^{\ell} X_n^2(S)dS \tag{3-6}$$

$$\beta_n^{(3)} = \int_o^{\ell} [EI_3 X_n(S) X_n''''(S)]dS \tag{3-7}$$

$$\beta_m^{(2)} = \int_o^{\ell} [EI_2 X_m(S) X_m''''(S)]dS \tag{3-8}$$

$$\gamma_j = \int_o^{\ell} [MX_j(S)X_j'(S) - M(\ell - S)X_j(S)X_j''(S)]dS , \qquad j = m,n \tag{3-9}$$

$$\delta_j = \int_o^{\ell} \left[M \int_o^s X_j'^2(\xi)d\xi \right] X_j(S)X_j'(S)dS$$

$$- \int_o^{\ell} \left\{ M \int_s^{\ell} \left[\int_o^{\xi} X_j'^2(\eta)d\eta \right] d\xi \right\} X_j(S)X_j''(S)dS , \qquad j = m,n \tag{3-10}$$

$$\Delta_{ij} = \int_o^{\ell} \left[M \int_o^s X_j'^2(\xi)d\xi \right] X_i(S)X_i'(S)dS$$

$$- \int_o^{\ell} \left\{ M \int_s^{\ell} \left[\int_o^{\xi} X_j'^2(\eta)d\eta \right] d\xi \right\} X_i(S)X_i'(S)dS , \qquad \begin{matrix} i = m,\ j = n \\ \text{or} \\ i = n,\ j = m \end{matrix} \tag{3-11}$$

The values of the above integrals are presented in Appendix B.

Non-dimensional time τ is introduced by defining $\tau = \frac{\omega t}{2}$. Using this, equations (3-4) and (3-5) become

$$T_{2n}'' + \left(\frac{4\beta_n^{(3)}}{\alpha\omega^2} + \frac{4\gamma_n}{\alpha} A_b \cos 2\tau \right) T_{2n} + \frac{\delta_n}{\alpha} T_{2n}(T_{2n}\, T_{2n}'' + T_{2n}'^2)$$

$$+ \frac{\Delta_{nm}}{\alpha} T_{2n}(T_{3m}\, T_{3m}'' + T_{3m}'^2) = 0 \tag{3-12}$$

$$T''_{3m} + \left(\frac{4\beta_m^{(2)}}{\alpha\omega^2} + \frac{4\gamma_m}{\alpha} A_b \cos 2\tau\right)T_{3m} + \frac{\delta_m}{\alpha} T_{3m}(T_{3m} T''_{3m} + T'^2_{3m})$$

$$+ \frac{\Delta_{mn}}{\alpha} T_{3m}(T_{2n} T''_{2n} + T'^2_{2n}) = 0 , \qquad (3\text{-}13)$$

where

$$( )' = \frac{d( )}{d\tau} .$$

For use at a later point, we show the form of equations (3-12) and (3-13) for the special, but important, case m = n. Note that m = n implies $\delta_n = \delta_m = \Delta_{mn} = \Delta_{nm}$; the common quantity is represented by δ. The special equations are, after dropping the alphabetic subscript for clarity:

$$T''_2 + \left(\frac{\beta^{(3)}}{\alpha\omega^2} + \frac{4\gamma}{\alpha} A_b \cos 2\tau\right)T_2 + \frac{\delta}{\alpha} T_2(T_2T''_2+T'^2_2+T_3T''_3+T'^2_3) = 0 \qquad (3\text{-}14)$$

$$T''_3 + \left(\frac{\beta^{(2)}}{\alpha\omega^2} + \frac{4\gamma}{\alpha} A_b \cos 2\tau\right)T_3 + \frac{\delta}{\alpha} T_3(T_2T''_2+T'^2_2+T_3T''_3+T'^2_3) = 0 . \qquad (3\text{-}15)$$

Equations (3-12) and (3-13)can be compared with results derived by others by observing that the plane motion case, say $T_{3m}(\tau) \equiv 0$, is a solution of the equations. This reduces the pair of equations to

$$T''_{2n} + \left(\frac{4\beta_n^{(3)}}{\alpha\omega^2} + \frac{4\gamma_n}{\alpha} A_b \cos 2\tau\right)T_{2n} + \frac{\delta_n}{\alpha} T_{2n}(T_{2n} T''_{2n} + T'^2_{2n}) = 0, \qquad (3\text{-}16)$$

which again is the form obtained by Evensen and Evan-Iwanowski [11].

The simplifying assumptions pertaining to the curvature have reduced the expression (2-11) to the one used in small deflection beam theory. This has resulted in the disappearance of the nonlinear elasticity

terms[1] from equation (3-16). When retained, this effect appears, in the first approximation, as a cubic term in T_{2n} [10]. The only nonlinearity present in our equations is the so-called nonlinear inertia term $\frac{\delta_n}{\alpha} T_{2n}(T_{2n}T''_{2n}+T'^{2}_{2n})$ which arises due to the inclusion of the longitudinal inertia of an element of the rod. Bolotin [10] has shown in Chapter 4, Section 17 that, for rods of this type, the predominant nonlinear effect is that of nonlinear inertia. Moody [26] also concludes that nonlinear inertia effects are far more significant than nonlinear elasticity effects on the parametric response of thin rods.

Equations (3-12) and (3-13) further show that the essential coupling between motions in the two perpendicular planes is due exclusively to the nonlinear terms. If the equations are linearized, motion in one plane is independent of motion in the other plane. It is important to realize that, as is frequently the case, a linearized theory is incapable of accounting for the phenomenon of interest.

---

1 Here we use Bolotin's terminology and define nonlinear elasticity terms as nonlinear terms that do not certain derivatives of displacements with respect to time.

CHAPTER IV

THE SUBHARMONIC RESPONSE AND THE STABILITY ANALYSIS FOR THE AXIALLY EXCITED ROD

The principal planar motion of the axially excited long slender rod is the well-known plane, steady-state, half-order subharmonic response. It is the stability of this planar motion to out-of-plane perturbations that we investigate.

To help make the ensuing analysis more lucid, we begin with a summary of the stability analysis procedure. The starting assumption is that the initially straight rod is executing plane, steady-state, half-order subharmonic motion of the form

$$T_{2n}(\tau) = A_{1n} \sin \tau + A_{2n} \cos \tau \qquad (4\text{-}1)$$

$$T_{3m}(\tau) = 0 \, . \qquad (4\text{-}2)$$

The use of this solution form in equations (3-12) and (3-13) and the application of the Ritz averaging method produces the amplitude-frequency or response relation for plane motion. Stability of the plane motion solution to disturbances perpendicular to the plane of motion can be investigated by substituting the perturbed solution

$$T_{2n}(\tau) = A_{1n} \sin \tau + A_{2n} \cos \tau + 0 \qquad (4\text{-}3)$$

$$T_{3m}(\tau) = 0 + x_{3m}(\tau) \qquad (4\text{-}4)$$

into equations (3-12) and (3-13) and applying the "infinitesimal" stability criterion as described by Stoker, [1], Chapter IV, §11.

Note that the plane motion restriction (4-2) reduces equations (3-12) and (3-13) to equation (3-16) which is repeated here for convenience:

$$T''_{2n} + \left(\frac{4\beta_n^{(3)}}{\alpha\omega^2} + \frac{4\gamma_n}{\alpha} A_b \cos 2\tau\right) T_{2n} + \frac{\delta_n}{\alpha} T_{2n}\left(T_{2n}T''_{2n} + T'^2_{2n}\right) = 0 . \quad (4\text{-}5)$$

This equation governs the x_1, x_2-plane response of the rod when $T_{3m}(\tau) \equiv 0$. To this we apply the averaging method of W. Ritz[1] [27] and obtain the algebraic result

$$\bar{A}_{1n}\left[\bar{A}_{1n}^2 + \bar{A}_{2n}^2 - \frac{2}{c_n}\left(\frac{(2\omega_n^{(3)})^2}{\omega^2} - 1 - \frac{b_n\bar{A}_b}{2}\right)\right] = 0 \quad (4\text{-}6)$$

$$\bar{A}_{2n}\left[\bar{A}_{1n}^2 + \bar{A}_{2n}^2 - \frac{2}{c_n}\left(\frac{(2\omega_n^{(3)})^2}{\omega^2} - 1 + \frac{b_n\bar{A}_b}{2}\right)\right] = 0 . \quad (4\text{-}7)$$

This pair of nonlinear algebraic equations, called the response equations, determines the relationship which exists between the amplitude of the response and the frequency of the exciting force when $T_{3m}(\tau) \equiv 0$. Here the notation has been simplified by introducing the dimensionless quantities

$$b_n = \frac{4\gamma_n \ell}{\alpha} \quad (4\text{-}8)$$

$$c_n = \frac{\delta_n \ell^2}{\alpha} \quad (4\text{-}9)$$

[1] In order to make this presentation as self-contained as possible, a summary of the Ritz averaging technique is presented in Appendix C.

$$\bar{A}_b = A_b/\ell,\ \bar{A}_n = A_n/\ell,\ \bar{A}_{1n} = A_{1n}/\ell,\ \bar{A}_{2n} = A_{2n}/\ell \tag{4-10}$$

and by observing from equation (3-3) and Appendix B that the constant $\frac{4\beta_n^{(3)}}{\alpha}$ is the square of twice the linear natural frequency for motions of the rod in the x_1,x_2-plane. That is,

$$\frac{4\beta_n^{(3)}}{\alpha} = (2\omega_n^{(3)})^2 . \tag{4-11}$$

Returning to equations (4-6) and (4-7), we note that two useful cases are present. ($\bar{A}_{1n} = \bar{A}_{2n} = 0$ is a trivial case.) In the first case, we choose $\bar{A}_{1n} \neq 0$ and $\bar{A}_{2n} = 0$ to obtain

$$\bar{A}_{1n}^2 - \frac{2}{c_n}\left[\frac{(2\omega_n^{(3)})^2}{\omega^2} - 1 - \frac{b_n\bar{A}_b}{2}\right] = 0 . \tag{4-12}$$

In the second case, $A_{1n} = 0$ and $A_{2n} \neq 0$ implies

$$\bar{A}_{2n}^2 - \frac{2}{c_n}\left[\frac{(2\omega_n^{(3)})^2}{\omega^2} - 1 + \frac{b_n\bar{A}_b}{2}\right] = 0 . \tag{4-13}$$

A third case, the one for which both $\bar{A}_{1n} \neq 0$ and $\bar{A}_{2n} \neq 0$, is not present unless $b_n\bar{A}_b = 0$. If $b_n\bar{A}_b = 0$(which occurs only if the base excitation amplitude $\bar{A}_b = 0$), the two equations are identical and yield the "backbone" or free vibration response curve.

For convenience, we drop the subscripts 1 and 2 in equations (4-12) and (4-13) and combine them as

$$\bar{A}_n^2 - \frac{2}{c_n}\left[\frac{(2\omega_n^{(3)})^2}{\omega^2} - 1 \mp \frac{b_n\bar{A}_b}{2}\right] = 0 . \tag{4-14}$$

An alternate way to accomplish this end is to let $\bar{A}_n^2 = \bar{A}_{1n}^2 + \bar{A}_{2n}^2$ and

substitute this into equations (4-6) and (4-7). Then the two cases $\bar{A}_{1n} \neq 0$, $\bar{A}_{2n} = 0$ and $\bar{A}_{1n} = 0$, $\bar{A}_{2n} \neq 0$ give the result, equation (4-14). In order to relate $\bar{A}_n$ to an actual amplitude on the rod, we refer to Young and Felgar [25] and note that $X_n(\ell) = 2.000$. This means that $2A_n$ equals the actual steady-state amplitude of the rod at its free end.

Equations (4-14) represent the two branches of the amplitude-frequency relationship and are shown in Figure 3. Bolotin [10] and others have discussed the well-known result that the left-most curve is unstable with respect to small in-plane disturbances and hence is never physically realized.

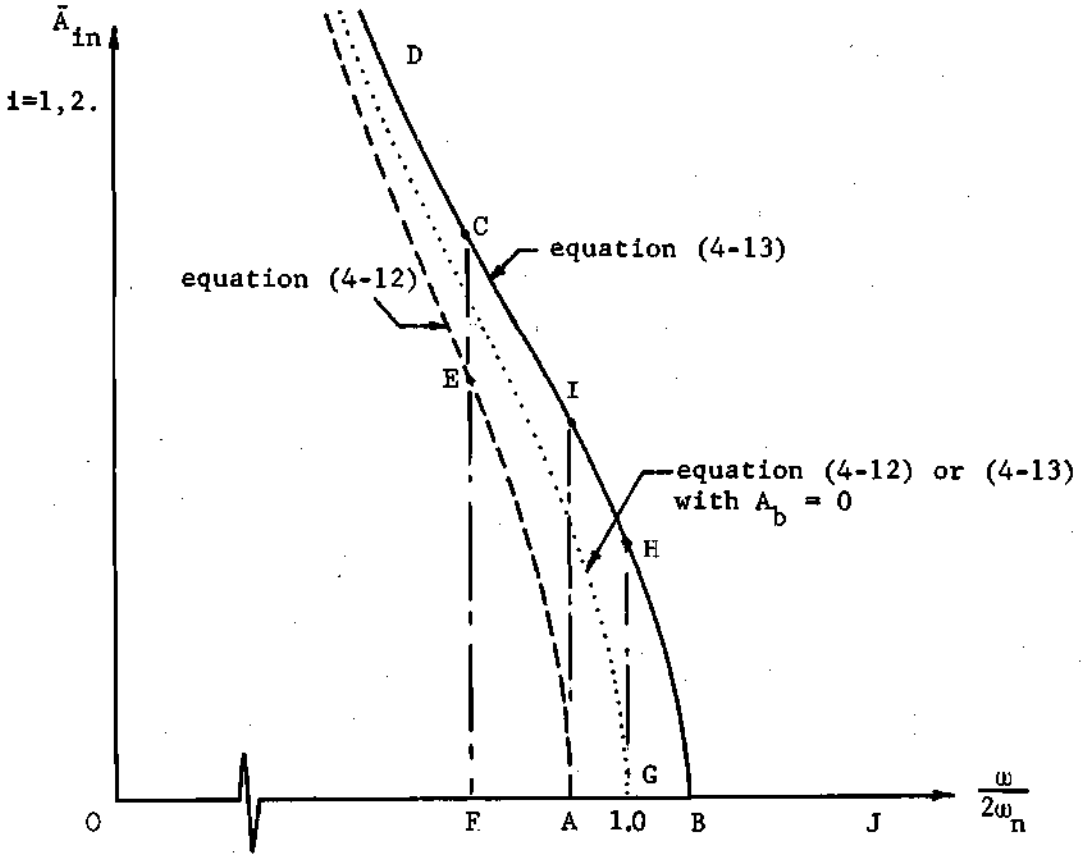

Figure 3. The Response Relation for Plane Motion of the Axially Excited Rod.

Before proceeding to the nonplanar aspect of the stability analysis it is important to understand the meaning of the information displayed in Figure 3; that is, one should understand the results of an analysis which tests the stability of the straight rod with respect to disturbances in the direction of the planar response with which we are concerned. As is frequently the case in the study of nonlinear phenomena, there are regions for which two or more amplitudes are predicted by the theory for a single given frequency. This situation occurs in the present case for frequencies to the left of point B in Figure 3. For instance, if the exciting frequency has the value given by point F, the theory predicts three possible response amplitudes. They are the zero amplitude response (that is, the rod remains straight), the amplitude given by point E (which is unstable and never physically realized), and the amplitude given by point C. Whether the amplitude at F or at C is the one which is present depends upon whether the frequency is being increased to F or decreased to F. The region between points A and B is one for which the straight configuration is unstable. Hence, if the frequency at G is selected, the rod can only respond with a steady-state amplitude given by H.

If one slowly and continuously increases the exciting frequency from zero, a point follows Figure 3 along the abscissa from O to A; in other words, the rod remains straight. When the frequency at A is reached, a vertical amplitude jump occurs and the rod begins a steady-state planar response having an amplitude given by I. If the frequency is further increased, the amplitude decreases along path I H B J and the rod becomes straight once more. Decreasing the frequency slowly from J to B causes the rod to remain straight until the frequency at B is reached; a further

decrease in frequency causes the amplitude of the response to increase along path B H I C D. Theoretically, the response amplitude continues to increase without bound, but in practice the damping which is inherent in all physical systems causes a downward jump from the frequency at D to zero amplitude. The presence of damping causes the curves given by equations (4-12) and (4-13) to be smoothly connected at a finite amplitude such as D.

The investigation of the above-mentioned planar response to out-of-plane disturbances is conducted by using the "infinitesimal" stability criterion. The names "variational method" and "method of small oscillations" are also applied to this technique. Even though the method is frequently employed to good advantage in stability analyses, its logical consistency is justly criticized by Stoker [28]. Before presenting a review of Stoker's criticizm, the method itself should be summarized.

Suppose the differential equation of motion for a one degree of freedom system is

$$N_1[g(t)] = f(t) \ , \tag{4-15}$$

where N_1 is a differential operator (not necessarily linear) and f is a function of time. Let g(t) be a solution of equation (4-15); it is the stability of g(t) that is to be tested. To accomplish this, a neighboring solution of the form $\bar{g}(t) = g(t) + x(t)$ is constructed such that the perturbation function x(t) is assumed to be so small that powers of it can be neglected when compared to the first power. The solution $\bar{g}(t)$ is substituted into equation (4-15), use is made of the fact that g(t) is also a solution, and all terms but those of the first power in x(t) are

neglected. This results in a linear homogeneous differential equation

$$L_2[x(t)] = 0 \tag{4-16}$$

which contains the known solution g(t) as a non-constant coefficient. In equation (4-16), L_2 is a linear differential operator. Now a motion is said to be stable if all solutions of equation (4-16) remain bounded for $t > 0$; otherwise, the motion is unstable.

The logical difficulty is that by assuming at the outset x(t) is small and by neglecting powers of it, nothing can be said about x(t) if it does indeed turn out to be small. Furthermore, if x(t) becomes large with increasing t one can not conclude that he has shown that the assumption of small x(t) was erroneous. What has been shown is that the neglect of higher order terms is unjustified. Stoker gives reference to an example for which the small oscillation criterion leads to an incorrect result. The method, however, is still useful even though it conclusively proves neither stability or instability. Its virtue is that one does not have to produce the solutions to the nonlinear differential equation being investigated. Correct results for the stability analysis are likely to be obtained from this almost universally used criterion, but in order to be certain of their validity in doubtful cases, these results should be experimentally tested.

The application to this problem proceeds as follows: A known solution to equations (3-12) and (3-13) is

$$T_{2n}(\tau) = A_{1n} \sin \tau + A_{2n} \cos \tau$$

$$T_{3m}(\tau) = 0 \ .$$

A neighboring solution is

$$\bar{T}_{2n}(\tau) = A_{1n} \sin \tau + A_{2n} \cos \tau + 0 \tag{4-17}$$

$$\bar{T}_{3m}(\tau) = 0 + x_{3m}(\tau) \ . \tag{4-18}$$

Upon substituting equations (4-17) and (4-18) into equations (3-12) and (3-13) and neglecting terms of higher order than the first in x_{3m}, we obtain

$$x''_{3m} + \left[\frac{\left(2\omega_m^{(2)}\right)^2}{\omega^2} + b_m \bar{A}_b \cos 2\tau + \frac{c_{mn}}{\ell^2} T_{1n} T''_{1n} + \frac{c_{mn}}{\ell^2} T'^2_{1n}\right] x_{3m} = 0, \tag{4-19}$$

where

$$\left(2\omega_m^{(2)}\right)^2 = \frac{4\beta_m^{(2)}}{\alpha} \tag{4-20}$$

$$b_m = \frac{4\gamma_m \ell}{\alpha} \tag{4-21}$$

$$c_{mn} = \frac{\Delta_{mn} \ell^2}{\alpha} \ . \tag{4-22}$$

Making use of the fact that

$$T_{2n}(\tau) = A_{1n} \sin \tau + A_{2n} \cos \tau$$

equation (4-19) yields

$$x''_{3m}(\tau) + \left[\frac{\left(2\omega_m^{(2)}\right)^2}{\omega^2} + (b_m \bar{A}_b + c_{mn} \bar{A}_{1n}^2 - c_{mn} \bar{A}_{2n}^2) \cos 2\tau \right.$$

$$\left. - 2\, c_{mn}\, \bar{A}_{1n} \bar{A}_{2n} \sin 2\tau\right] x_{3m}(\tau) = 0 \ . \tag{4-23}$$

This is called the stability equation. The solutions $x_{3m}(\tau)$ of equation (4-23) determine whether or not the system is stable with respect to disturbances in the x_3 (out-of-plane) direction.

The stability equation can be converted to the Mathieu equation by making use of the two cases $\bar{A}_{1n} \neq 0$, $\bar{A}_{2n} \neq 0$. However, since $\bar{A}_{1n} \neq 0$, $\bar{A}_{2n} = 0$ is always unstable with respect to in-plane disturbances, there is no need to test its stability with respect to out-of-plane disturbances. Hence, we devote our attention only to the case $\bar{A}_{1n} = 0$, $\bar{A}_{2n} \neq 0$ and obtain from equation (4-23)

$$x''_{3m}(\tau) + \left[\frac{\left(2\omega_m^{(2)}\right)^2}{\omega^2} + (b_m \bar{A}_b - c_{mn}\bar{A}_n^2)\cos 2\tau\right] x_{3m}(\tau) = 0 \ . \qquad (4\text{-}24)$$

Note that since $\bar{A}_{1n} = 0$, we have used the fact that $\bar{A}_{2n}^2$ is the same as $\bar{A}_n^2$.

Now the standard form of the Mathieu equation can be obtained from equation (4-24) by changing the independent variable according to

$$\eta = 2\tau \qquad (4\text{-}25)$$

and by letting

$$\epsilon_1 = \frac{\left(2\omega_m^{(2)}\right)^2}{4\omega^2} \qquad (4\text{-}26)$$

$$\epsilon_2 = \tfrac{1}{4}(b_m \bar{A}_b - c_{mn}\bar{A}_n^2) \ . \qquad (4\text{-}27)$$

This gives

$$\frac{d^2 x_{3m}(\eta)}{d\eta^2} + (\epsilon_1 + \epsilon_2 \cos \eta) x_{3m}(\eta) = 0 \ . \qquad (4\text{-}28)$$

As has been shown by McLachlan [29] and others, the solutions to

the Mathieu equation are either bounded or unbounded depending on the values of the parameters ϵ_1 and ϵ_2. In fact, values of ϵ_1 and ϵ_2 causing either stable or unstable solutions cover entire regions in the ϵ_1, ϵ_2-plane. These regions are illustrated in Figure 4.

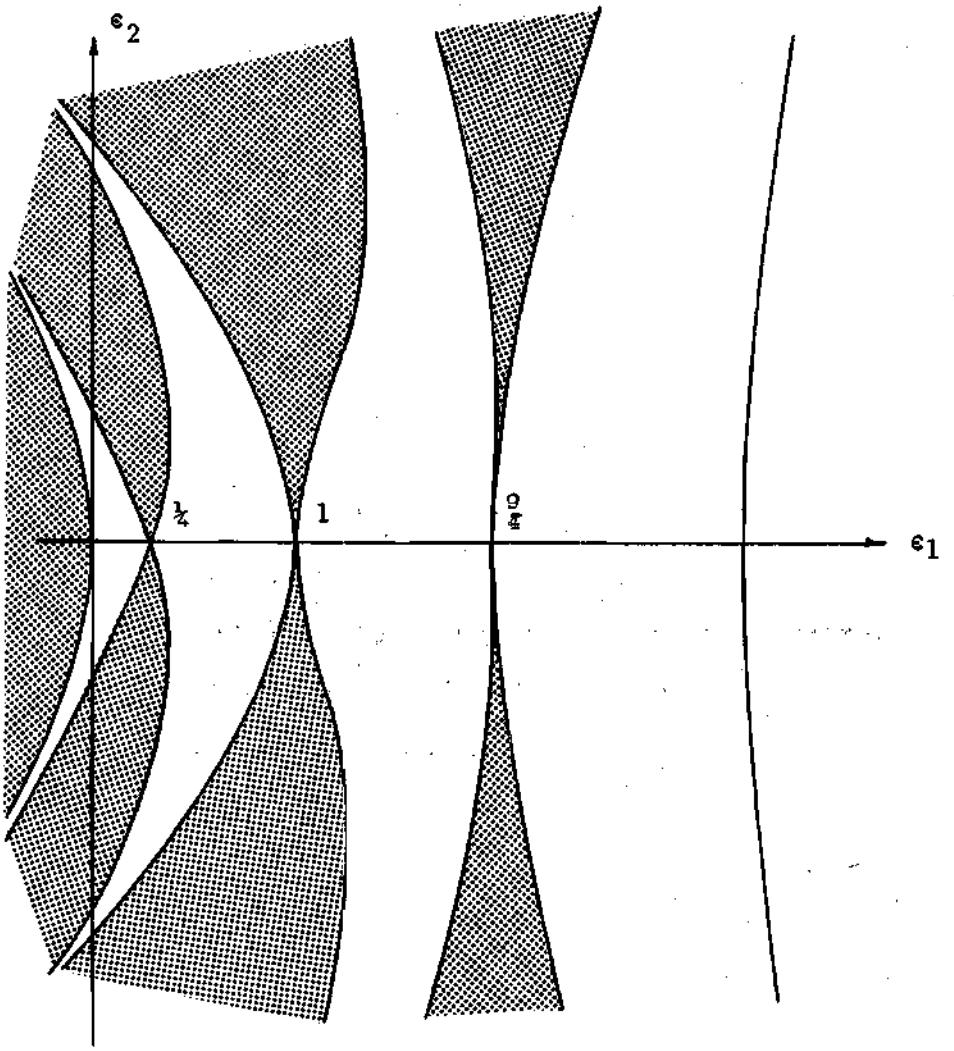

Figure 4. Stable and Unstable Regions for the Mathieu Equation.

Each point in the ϵ_1, ϵ_2-plane will be called a stability point. We say that a given motion is stable if the parameters which define the motion cause the stability point to fall in the portion (unshaded in Figure 4) of the ϵ_1, ϵ_2-plane which corresponds to bounded solutions of the Mathieu equation. Stability points lying in the shaded portion of the plane correspond to unbounded solutions (unstable motions) of the Mathieu equation. Points which lie on the boundaries of the stable or unstable regions are identified with unbounded solutions, also. Cunningham [30] shows that the boundary solutions have one or the other of the forms

$$x_{3m}(\eta) = AP(\eta) + B\eta Q(\eta)$$
$$x_{3m}(\eta) = Ae^{i\eta} P(\eta) + B\eta\, e^{i\eta} Q(\eta) .$$

If one restricts his attention to the portion of the ϵ_1, ϵ_2-plane in the neighborhood of $\epsilon_1 = \frac{1}{4}$, $\epsilon_2 = 0$, Cunningham [30] and others have shown that for small values of ϵ_2 a good first order approximation to the principal instability zone is given by

$$\epsilon_1 = \frac{1}{4} \pm \frac{1}{2} \epsilon_2 . \qquad (4\text{-}29)$$

These boundaries are shown in Figure 5.

Since we are interested in excitation frequencies near twice the linear natural frequency of the rod, it is clear from equation (4-26) that we are concerned with values of ϵ_1 near $\frac{1}{4}$. To see that ϵ_2 is small for our problem, we note that the base excitation amplitude will be restricted to $0 \leq \tilde{A}_b \leq 0.005$ and the steady-state response

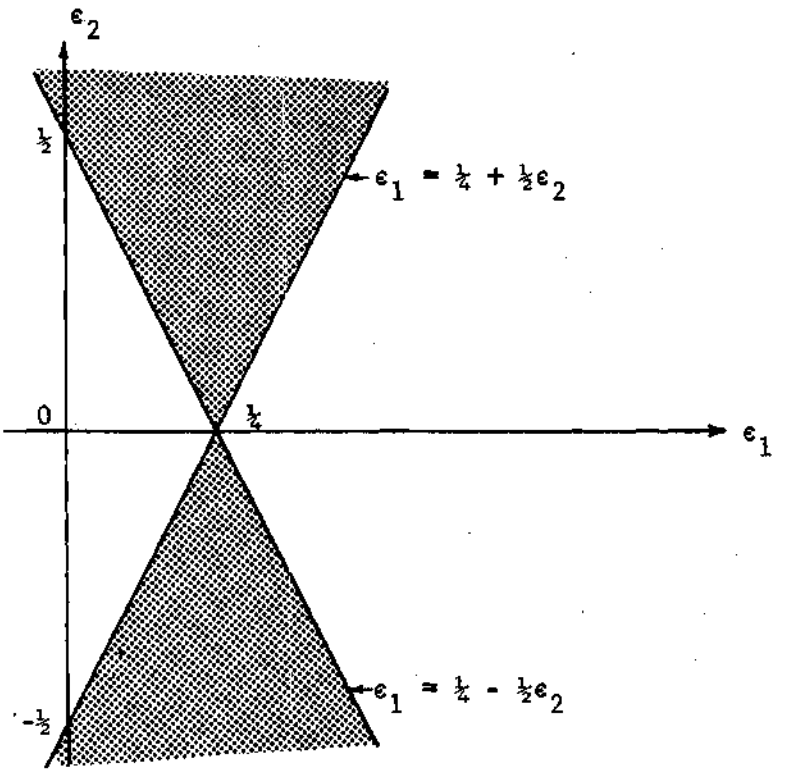

Figure 5. Approximate Principal Instability Region for the Mathieu Equation for Small Values of ϵ_2.

amplitude will be restricted to $0 \leq \bar{A}_n \leq 0.10$. Tables 4 and 5 show the first three values of b_m and c_{mn}. Substituting the above values into equation (4-27) shows that $-\frac{1}{2} < \epsilon_2 < \frac{1}{2}$ for this problem.

As has been mentioned, the values of the parameters ϵ_1 and ϵ_2 determine the stability of a planar motion. Therefore, one must determine which pairs of numbers $\bar{A}_n$ and $\frac{\omega}{2\omega_n^{(3)}}$ satisfying the response relation (4-14) lead to stable solutions of the stability equation (4-28). There are two methods for displaying this information. One might plot the response curve (4-14) on the ϵ_1, ϵ_2-plane; this would give a pair of parametric equations for the response curve in the ϵ_1, ϵ_2-plane with $\bar{A}_n$ as the parameter. On the other hand, one might map the ϵ_1, ϵ_2-plane onto

the $\frac{\omega}{2\omega_n^{(3)}}$, $\bar{A}_n$-plane. We begin by discussing the former approach.

Solving the stable branch of equation (4-14) for ω^2 gives

$$\omega^2 = \frac{\left(2\omega_n^{(3)}\right)^2}{1 - \frac{1}{2}(b_n\bar{A}_b - c_n\bar{A}_n^2)} . \tag{4-30}$$

Applying this to equations (4-26) and (4-27) yields the parametric equations (with $\bar{A}_n$ as a parameter) for the stable branch of the response curve in the ϵ_1, ϵ_2-plane. These are

$$\epsilon_1 = \frac{1}{8}\frac{I_2}{I_3}\left(\frac{\beta_m}{\beta_n}\right)^4 (c_n\bar{A}_n^2 + 2 - b_n\bar{A}_b) \tag{4-31}$$

$$\epsilon_2 = \frac{1}{4}(b_m\bar{A}_b - c_{mn}\bar{A}_n^2) . \tag{4-32}$$

Use has been made of the fact that

$$\frac{\left(2\omega_m^{(2)}\right)^2}{\left(2\omega_n^{(3)}\right)^2} = \frac{I_2}{I_3}\left(\frac{\beta_m}{\beta_n}\right)^4 .$$

Note that these equations represent a straight line in the ϵ_1, ϵ_2-plane. Each different value of the non-dimensional base amplitude $\bar{A}_b$ gives a different straight line in a family of parallel lines.

Elimination of $\bar{A}_n$ from equations (4-31) and (4-32) shows that

$$\epsilon_2 = -2\frac{c_{mn}}{c_n}\frac{I_3}{I_2}\left(\frac{\beta_n}{\beta_m}\right)^4 \epsilon_1 + \frac{1}{4}\left[b_m\bar{A}_b - \frac{c_{mn}}{c_n}(b_n\bar{A}_b - 2)\right] . \tag{4-33}$$

For the special case m = n, we recall that $c_{mn} = c_n$ and find from equation (4-33) that

$$\epsilon_2 = -2\frac{I_3}{I_2}\epsilon_1 + \frac{1}{2} . \tag{4-34}$$

It is easier to interpret the stability information given by equations (4-26) and (4-27) if one maps the ϵ_1, ϵ_2-plane on the $\frac{\omega}{2\omega_n^{(3)}}$, $\bar{A}_n$ - plane rather than to make the inverse mapping as discussed in the preceeding paragraphs. To effect this transformation, we eliminate ϵ_1 and ϵ_2 between equations (4-26) and (4-27) and the stability boundaries $\epsilon_1 = \frac{1}{4} \pm \frac{1}{2}\epsilon_2$. This gives

$$\frac{\omega^2}{\left(2\omega_m^{(2)}\right)^2} = \frac{1}{1 + \frac{1}{2}(b_m \bar{A}_b - c_{mn}\bar{A}_n^2)} \tag{4-35}$$

for the boundary given by $\epsilon_1 = \frac{1}{4} + \frac{1}{2}\epsilon_2$ and

$$\frac{\omega^2}{\left(2\omega_m^{(2)}\right)^2} = \frac{1}{1 - \frac{1}{2}(b_m \bar{A}_b - c_{mn}\bar{A}_n^2)} \tag{4-36}$$

for the boundary given by $\epsilon_1 = \frac{1}{4} - \frac{1}{2}\epsilon_2$. Note the similarities between equations (4-30) and (4-36).

Thus far, we have discussed only planar responses of the rod in the x_1, x_2-plane and disturbances of this planar response in the x_3-direction. Of course, it is possible for the rod to respond in the x_1, x_3-plane as well, and when it does, we shall then be concerned with disturbances in the x_2-direction. Clearly, the equations governing the stability of the x_1, x_3-plane response to x_2-direction perturbations can be found from equations (4-14), (4-35), and (4-36) by substituting n for m and 3 for 2 in the subscripts and superscripts.

The stability information contained in equations (4-14), (4-35) and (4-36) together with their counterparts obtained by exchanging n for m and 3 for 2 in the subscripts and superscripts can be interpreted by plotting these eight equations for a particular selection of the parameters

involved. Only the case for which m = n is treated from this point on. The reason is as follows: if the stability point determined by equation (4-24) (which governs the growth of small nonplanar disturbances) lies in the unstable region which is in the neighborhood of $\epsilon_1 = \frac{1}{4}$, $\epsilon_2 = 0$ of Figure 4, then the small nonplanar disturbances $x_{3m}(\tau)$ occur initially at half the exciting frequency [12], [13], [30]. This frequency is the same as the frequency of the planar response; that is, m = n. Experimental evidence accumulated during this research indicates the validity of this observation.

The eight equations with m = n are

$$\frac{\omega^2}{\left(2\omega_n^{(3)}\right)^2} = \frac{1}{1 - \frac{1}{2}(\pm\, b_n \bar{A}_b - c_n \bar{A}_n^2)} \quad \text{(response curve for the } x_1, x_2\text{-plane response)} \tag{4-37}$$

$$\frac{\omega^2}{\left(2\omega_n^{(2)}\right)^2} = \frac{1}{1 - \frac{1}{2}(\pm\, b_n \bar{A}_b - c_n \bar{A}_n^2)} \quad \text{(response curve for the } x_1, x_3\text{-plane response)} \tag{4-38}$$

$$\frac{\omega^2}{\left(2\omega_n^{(2)}\right)^2} = \frac{1}{1 \pm \frac{1}{2}(b_n \bar{A}_b - c_n \bar{A}_n^2)} \quad \text{(stability boundaries associated with equation (4-37))} \tag{4-39}$$

$$\frac{\omega^2}{\left(2\omega_n^{(3)}\right)^2} = \frac{1}{1 \pm \frac{1}{2}(b_n \bar{A}_b - c_n \bar{A}_n^2)} \quad \text{(stability boundaries associated with equation (4-38))} \tag{4-40}$$

The physical constants for the example problem, which consists of a long, slender originally circular cross-section rod with parallel flats of material removed from its sides as shown in Figure 6, are

ℓ = 32.9 in.

A_b = 0.075 in.

m = n = 2

original diameter = 0.188 in.

e = 0.005 in.

b_2 = 34.6, c_2 = 145 } from Tables 4 and 5

E = 30×10^6 psi.

Specific weight of the material = 485 lb/ft^3

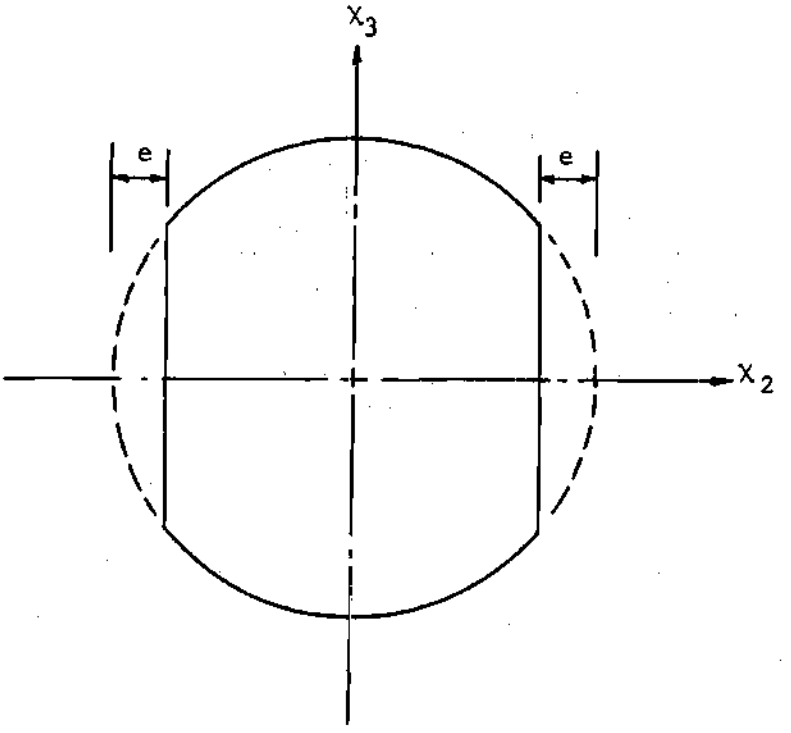

Figure 6. Cross-Section of the Rod.

The graph of the eight equations (4-37), (4-38), (4-39), (4-40) on the $\frac{\omega}{2\omega_2^{(2)}}$, $\bar{A}_2$-plane is presented in Figure 7.

We are now able to follow the response of the initially straight rod to a continuously increasing excitation frequency and to a continuously decreasing one. Suppose the excitation frequency is slowly and continuously increased from zero. A stability point then follows Figure 7 along path OLA; that is, the rod remains in a stable straight configuration. When the frequency at point A is reached, the straight configuration becomes unstable with respect to amplitude perturbations in the x_2-direction and an upward amplitude jump to point B takes place. The rod now is undergoing a stable, steady-state, half-order subharmonic vibration in the x_1, x_2-plane. As the frequency is further increased, the amplitude of the plane response decreases along path BCD.

Before continuing, one should recall from the earlier discussion of the response curves that in the region between frequencies A and K the straight rod configuration is unstable with respect to small disturbances in the x_2-direction, while in the region between frequencies J and G the straight rod is unstable with respect to x_3-direction disturbances.

Now, as the frequency increases to a value slightly higher than the frequency at D, there are four situations which must be given consideration. Firstly, we see that the x_1, x_2-plane response is unstable with respect to x_3-direction disturbances. Secondly, the straight configuration is unstable with respect to x_2-direction disturbances (in frequency range AK), and thirdly, the straight configuration is also unstable with respect to x_3-direction perturbations (in frequency range JG). Lastly, at this value of the exciting frequency we see that the

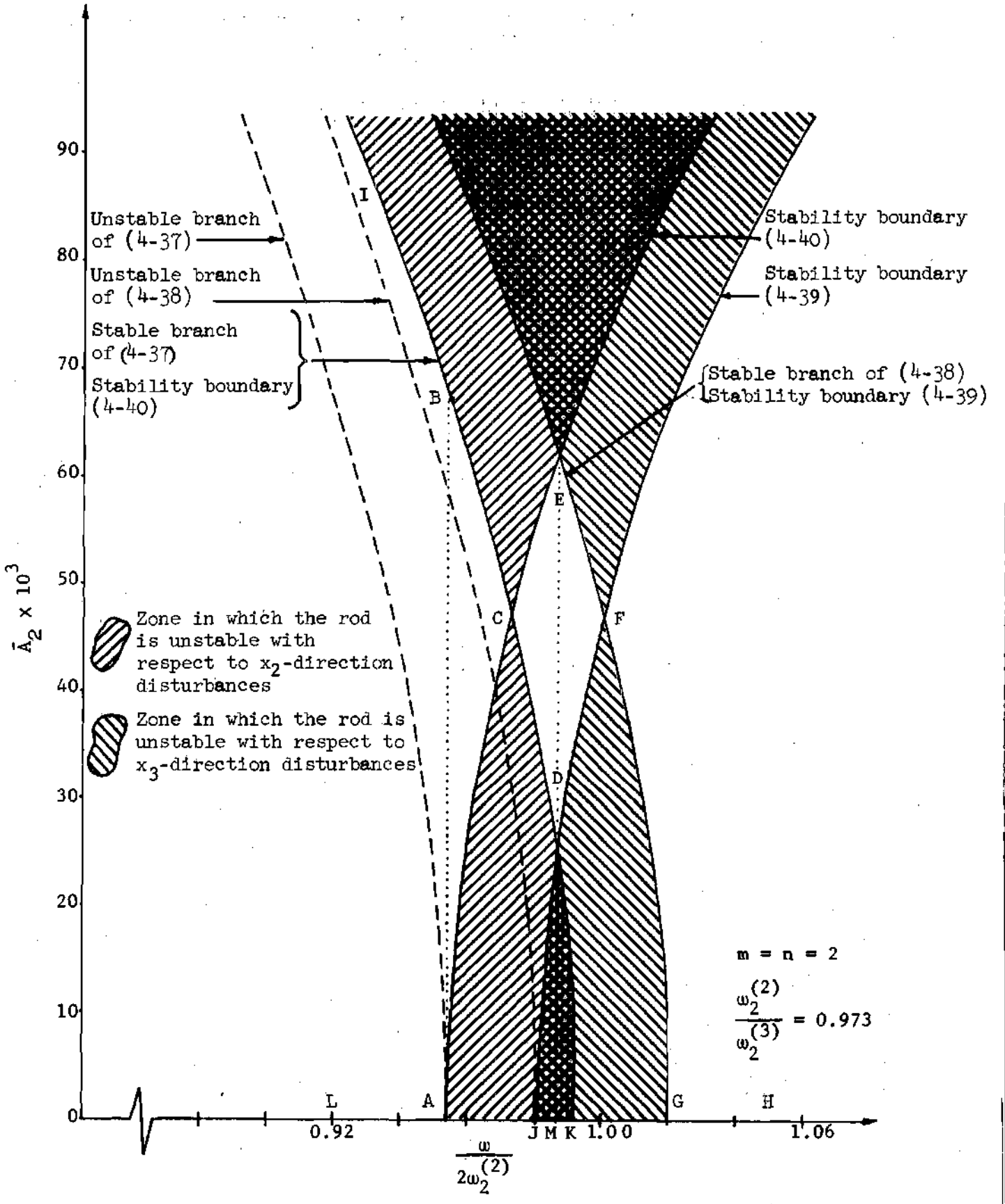

Figure 7. Response Equations and Stability Boundaries for the Axially Excited Rod.

x_1, x_3-plane response is stable with respect to x_2-direction disturbances. Therefore, a vertical amplitude jump occurs and the rod begins undergoing stable plane motion in the x_1, x_3-plane with the amplitude given by point E. A further increase in frequency causes the amplitude to decrease along path EFGH and the rod again returns to a stable straight configuration.

Suppose the exciting frequency is now slowly and continuously decreased. The straight configuration then is stable until frequency G is reached at which point the rod begins a stable, half-order subharmonic response in the x_1, x_3-plane. As the frequency is further lowered, the steady-state amplitude increases along path GFE. At a frequency value slightly lower than that given by point E, the stability point enters a zone for which the x_1, x_3-plane response is unstable with respect to x_2-direction disturbances, the straight configuration is unstable with respect to both x_2 and x_3 direction disturbances, and the x_1, x_2-plane response is stable with respect x_3-direction disturbances. Hence, a downward amplitude jump occurs and the rod begins executing stable x_1, x_2-plane oscillations with an amplitude given by point D. As the frequency is further reduced, the x_1, x_2-plane amplitude increases along path DCBI until the point is reached at which damping (not present in this analysis) causes the two branches of the x_1, x_2-plane response to join. Another downward amplitude jump then occurs and the rod returns to a stable straight configuration at point L.

We turn now to the special case for which both $m = n$ and $\omega_n^{(3)} = \omega_m^{(2)}$. Referring to either equation (4-34) or (4-36), one will observe that this special case causes the stable branch of the response curve to coincide with the stability boundary given by $\epsilon_1 = \frac{1}{4} - \frac{1}{2}\epsilon_2$. It was indicated

earlier in this chapter that stability points lying coincident with a boundary correspond to unbounded solutions. This seems to imply that, when $m = n$ and $\omega_n^{(3)} = \omega_m^{(2)}$, the planar response of the rod is unstable when disturbed in a nonplanar direction, regardless of the planar response amplitude. In addition to being intuitively unpalatable, this situation fails to occur in the laboratory. However, the apparent paradox can be resolved by the addition to the theory of a damping term. This damping term, no matter how small, causes the $m = n$ and $\omega_n^{(3)} = \omega_m^{(2)}$ case to have a planar response which is always stable with respect to nonplanar disturbances. In Appendix D, Figure 21, we show the effect of damping on the curves in $\frac{\omega}{2\omega_h}$, $\bar{A}_n$-plane for this special case.

Another interesting situation arises when the detuning is large, that is, when $\omega_n^{(3)}$ is much different from $\omega_m^{(2)}$. As the detuning increases, the cross-hatched regions in Figure 7 tend to separate. At a certain value of the detuning the region of overlapping JDK in Figure 7 decreases to zero and a qualitatively different response arises. We concentrate briefly on the case in which $K \leq J$.

The frequency at point J is given by

$$\omega^2 = \frac{\left(2\omega_m^{(2)}\right)^2}{1 + \frac{1}{2} b_m \bar{A}_b},$$

and the frequency at point K is given by

$$\omega^2 = \frac{\left(2\omega_n^{(3)}\right)^2}{1 - \frac{1}{2} b_n \bar{A}_b}.$$

The overlapping zone JDK disappears provided

$$\frac{\left(2\omega_n^{(3)}\right)^2}{1 - \frac{1}{2} b_n \bar{A}_b} \leq \frac{\left(2\omega_m^{(2)}\right)^2}{1 + \frac{1}{2} b_m \bar{A}_b} ,$$

that is, provided the detuning is such that

$$\frac{\left(\omega_n^{(3)}\right)^2}{\left(\omega_m^{(2)}\right)^2} \leq \frac{1 - \frac{1}{2} b_n \bar{A}_b}{1 + \frac{1}{2} b_m \bar{A}_b} . \tag{4-41}$$

The stability information for the previous example with the moments of inertia adjusted so that equation (4-41) is satisfied is shown in Figure 8. As frequency is increased from zero, the straight configuration is stable until frequency A is reached. At this frequency, an upward amplitude jump AB occurs and the rod begins stable x_1, x_2-plane oscillations. The amplitude decreases along path BCD as frequency is again increased. When frequency D is reached, the rod has returned to a stable straight configuration without undergoing the plane shift which occurred previously. The straight shape now remains stable until frequency D' is reached; there another upward amplitude jump occurs and the rod begins vibrating stably in the x_1, x_3-plane with an amplitude given by J. The amplitude then decreases along path JFG with increasing frequency until the stable straight configuration is reached once more at frequency G.

As the excitation frequency is slowly decreased, path HGFJE is followed. At a value of the frequency slightly lower than that at E, we find that the x_1, x_3-plane response is unstable with respect to x_2-direction disturbances but the straight configuration is stable with respect to disturbances in either direction. Hence a downward jump EM

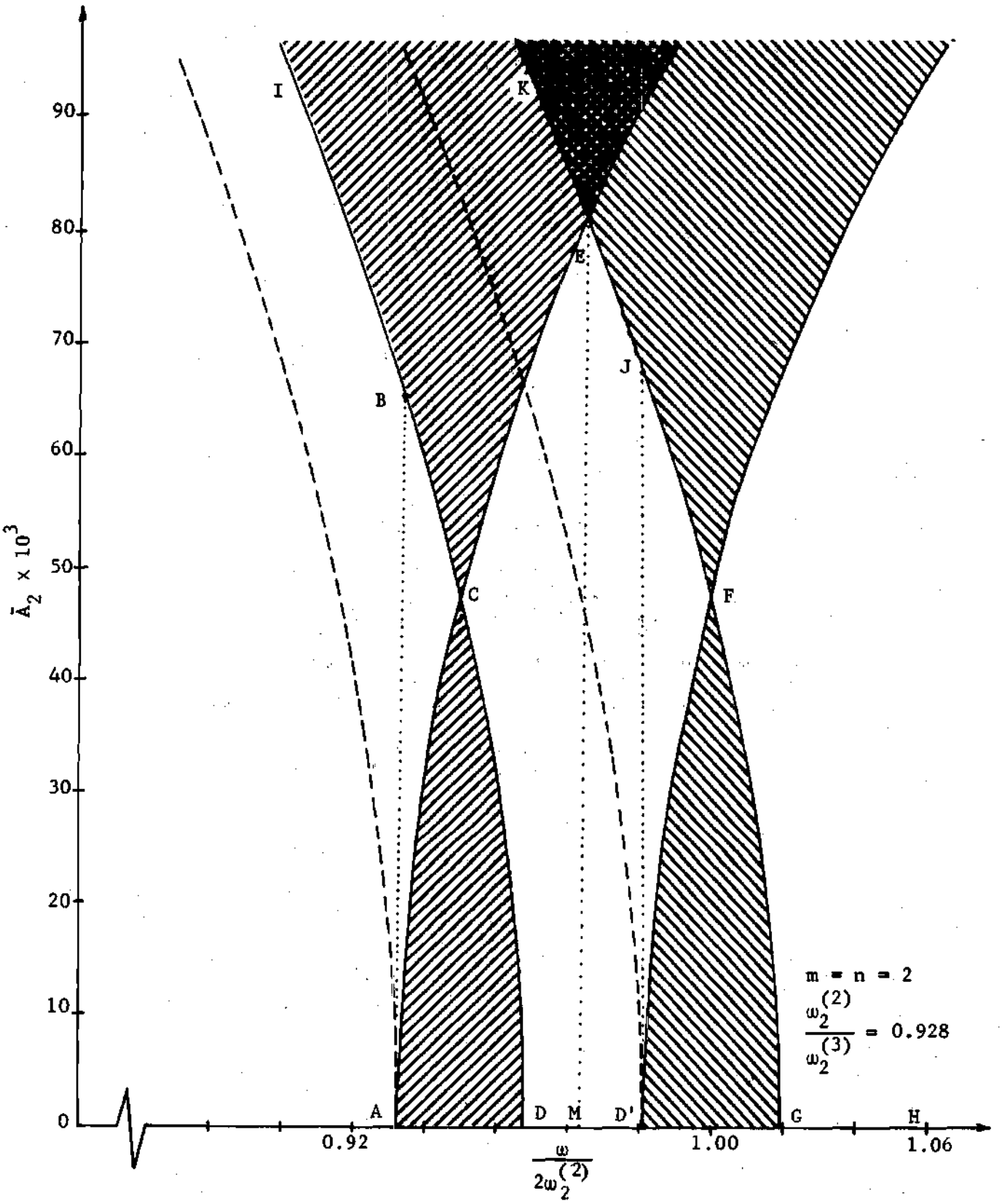

Figure 8. Response Equations and Stability Boundaries for the Axially Excited Rod When $\frac{\left(\omega_n^{(3)}\right)^2}{\left(\omega_n^{(2)}\right)^2} \leq \frac{1 - \frac{1}{2} b_n \bar{A}_b}{1 + \frac{1}{2} b_n \bar{A}_b}$.

occurs and the rod once more becomes straight. The rod then remains straight as frequency is lowered until D is reached. At this frequency, stable x_1, x_2-plane motions begin and increase in amplitude along path DCBI as frequency is further reduced. The amplitude increases until damping again causes a downward jump to the stable straight configuration.

As a final item of interest, we show that a "whirling motion" of the type predicted by Murthy and Ramakrishna [15] in their analysis of motions of an elastic string excited transversely is not possible for the axially excited rod. In order to account for the "whirling motion", a phase difference of $\frac{\pi}{2}$ is assumed between the motions in the x_1, x_2-plane and the x_1, x_3-plane. Hence we assume, as did Murthy and Ramakrishna, a solution of the form

$$v(s,t) = T_{2n}(t)X_n(S) = a_{n2}X_n(S)\cos\frac{\omega t}{2} \tag{4-42}$$

$$w(s,t) = T_{3n}(t)X_n(S) = a_{n3}X_n(S)\sin\frac{\omega t}{2}\ . \tag{4-43}$$

The Galerkin method applied to the spatial variable then shows as before that

$$T_2''(\tau) + \left[\frac{\left(2\omega_n^{(3)}\right)^2}{\omega^2} + b_n\bar{A}_b\cos 2\tau\right]T_2(\tau) + \frac{c_n}{\ell^2}T_2(\tau)\left[T_2(\tau)T_2''(\tau) + T_2'^2(\tau) + T_3(\tau)T_3''(\tau) + T_3'^2(\tau)\right] = 0 \tag{4-44}$$

$$T_3''(\tau) + \left[\frac{\left(2\omega_n^{(2)}\right)^2}{\omega^2} + b_n\bar{A}_b\cos 2\tau\right]T_3(\tau) + \frac{c_n}{\ell^2}T_3(\tau)\left[T_2(\tau)T_2''(\tau) + T_2'^2(\tau) + T_3(\tau)T_3''(\tau) + T_3'^2(\tau)\right] = 0\ . \tag{4-45}$$

We now let $T_{2n}(\tau) = a_{n2} \cos \tau$ and $T_{3n}(\tau) = a_{n3} \sin \tau$ and apply the method of harmonic balance (Cunningham [30]). This gives the algebraic result

$$a_{n2}\left[\frac{\left(2\omega_n^{(3)}\right)^2}{\omega^2} - 1 + \frac{b_n \bar{A}_b}{2} + \frac{c_n(a_{n3}^2 - a_{n2}^2)}{2\ell^2}\right] = 0 \qquad (4\text{-}46)$$

$$a_{n3}\left[\frac{\left(2\omega_n^{(2)}\right)^2}{\omega^2} - 1 - \frac{b_n \bar{A}_b}{2} - \frac{c_n(a_{n3}^2 - a_{n2}^2)}{2\ell^2}\right] = 0 \, . \qquad (4\text{-}47)$$

Since we are restricting our attention to the case $a_{n2} \neq 0$, $a_{n3} \neq 0$ (this insures the "whirling motion"), we divide equation (4-46) by a_{n2} and equation (4-47) by a_{n3} and add the results. This shows that

$$\omega^2 = 2\left(\omega_n^{(2)^2} + \omega_n^{(3)^2}\right) \, . \qquad (4\text{-}48)$$

In other words, there is a single discrete frequency at which the "whirling motion" could occur. This is tantamount to saying that the "whirling motion" can not be generated in the laboratory since equation (4-48) can not be exactly satisfied in practice. It is interesting to note that the frequency given by equation (4-48) is the frequency M for which the previously discussed plane shift occurs. That this latter statement is true can be readily seen by simultaneously solving the equations for curves CDK and JDF for ω^2 and by solving the equations for curves ACE and EFG for ω^2.

It is straight forward, of course, to calculate the values of the amplitudes such as D and E in Figure 7 at which the vertical amplitude jumps occur. One needs only to substitute equation (4-48) into the

appropriate stable branch of the response curves given by equation (4-30). The amplitude at E is

$$(\bar{A}_n^2)_{\substack{cr. \\ m=n}} = \frac{1}{c_n}\left[b_n \bar{A}_b + 2\left(\frac{\omega_n^{(2)^2} - \omega_n^{(3)^2}}{\omega_n^{(2)^2} + \omega_n^{(3)^2}}\right)\right] \tag{4-49}$$

and the amplitude at D is

$$(\bar{A}_n^2)_{\substack{cr. \\ m=n}} = \frac{1}{c_n}\left[b_n A_b - 2\left(\frac{\omega_n^{(2)^2} - \omega_n^{(3)^2}}{\omega_n^{(2)^2} + \omega_n^{(3)^2}}\right)\right] . \tag{4-50}$$

CHAPTER V

THE DIRECTLY EXCITED ROD WITH PARAMETRICALLY COUPLED NONPLANAR MOTION

In this chapter we formulate the problem for which the base of the rod is excited in a direction perpendicular to the rod centerline. Figure 9 defines the coordinate system and the direction of the base excitation for this case. As before, it is the stability of the planar response with respect to nonplanar disturbances that is to be investigated.

Although the planar response for this configuration is not parametrically excited, it is true that the nonplanar motions are excited parametrically by the planar response. That is, the amplitude of the planar response is the parameter which appears in the restoring force term of the stability equation. Of course, this is also the case in the previous problem, but in that problem the base excitation as well appears as a parameter in the restoring force term. The stability equations (4-24) and (5-18) are repeated below in order to help clarify the comparison.

$$x''_{3m}(\tau)+\left[\frac{\left(2\omega_m^{(2)}\right)^2}{\omega^2}+(b_m\bar{A}_b-c_{mn}\bar{A}_n^2)\cos 2\tau\right]x_{3m}(\tau)=0$$

(parametric excitation)

$$x''_{3m}(\tau)+\left[\frac{\left(2\omega_m^{(2)}\right)^2}{\omega^2}-4c_{mn}\bar{A}_n^2\cos 4\tau\right]x_{3m}(\tau)=0\ .\ \text{(direct excitation)}$$

One can say, for either case, that the nonplanar motion is parametrically coupled to the planar response.

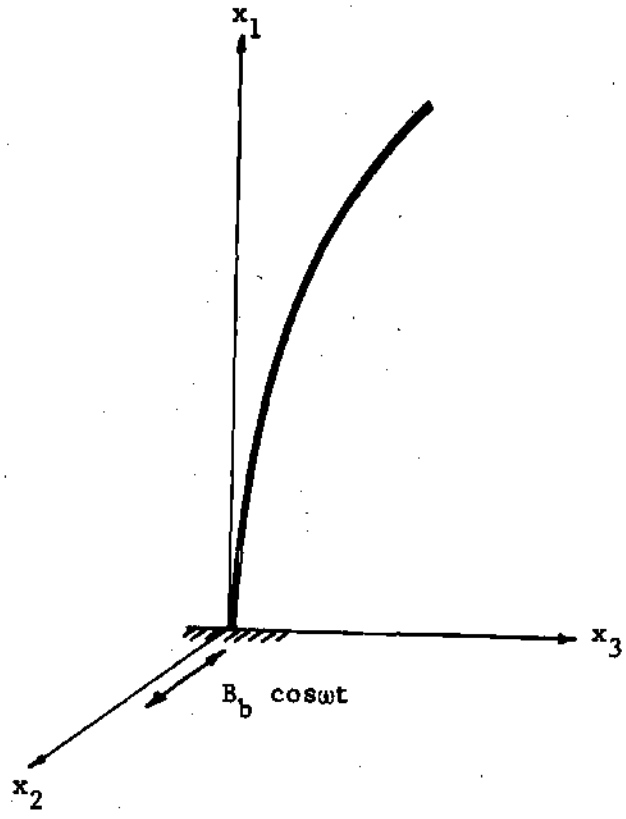

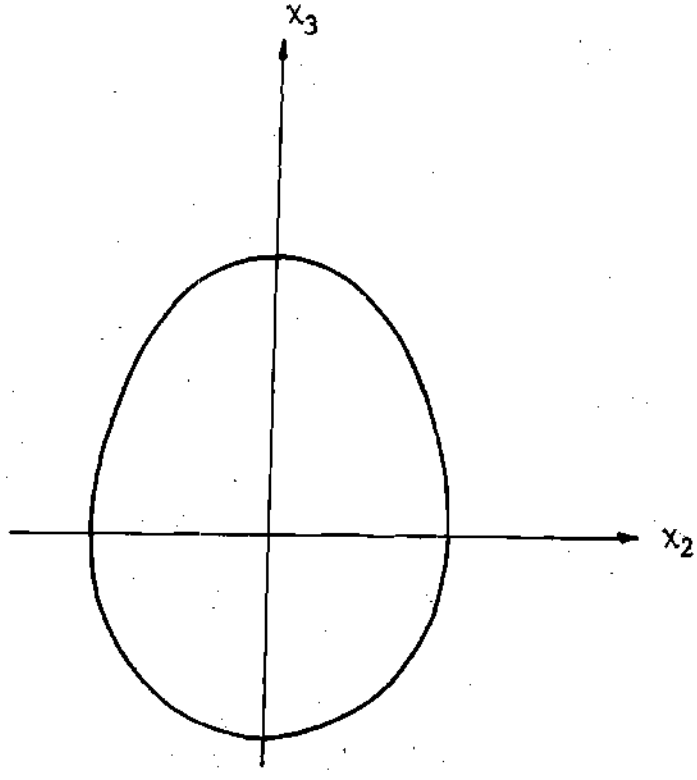

Figure 9. Orientation of the Coordinate System.

As mentioned in the introduction, literature concerning direct excitation is more prevalent than that dealing with parametrically excited systems. Murthy and Ramakrishna [15], 1965, excited a fixed-ended string along its length in a direction perpendicular to the string axis and witnessed a nonplanar whirling motion for sufficiently large in-plane amplitudes. Their analysis and experiments show good agreement. Miles, [14] and [16], analyzed both the spherical pendulum and the elastic string subjected to direct excitation and predicted a nonplanar response in both cases. He did not report on any experiments. Apparently, there is as yet no published literature dealing with the analogous elastic rod problem which we present in this chapter.

In order to obtain the equations of motion, we simply modify the previously derived ones. The governing partial differential equations are found immediately from equations (2-34) and (2-35) by setting $A_b = 0$. The result is

$$EI_3 v''''(S,t) + M\ddot{v}(S,t) + \frac{Mv'(S,t)}{2}\frac{\partial^2}{\partial t^2}\int_o^S [v'^2(\xi,t) + w'^2(\xi,t)]d\xi$$

$$- \frac{Mv''(S,t)}{2}\int_o^{\ell}\left\{\frac{\partial^2}{\partial t^2}\int_o^{\xi}[v'^2(\eta,t) + w'^2(\eta,t)]d\eta\right\}d\xi = 0 \quad (5\text{-}1)$$

$$EI_2 w''''(S,t) + M\ddot{w}(S,t) + \frac{Mw'(S,t)}{2}\frac{\partial^2}{\partial t^2}\int_o^S [v'^2(\xi,t) + w'^2(\xi,t)]d\xi$$

$$- \frac{Mw''(S,t)}{2}\int_o^{\ell}\left\{\frac{\partial^2}{\partial t^2}\int_o^{\xi}[v'^2(\eta,t) + w'^2(\eta,t)]d\eta\right\}d\xi = 0. \quad (5\text{-}2)$$

To introduce the base excitation, let

$$v(S,t) = v_1(S,t) + B_b \cos \omega t \quad (5\text{-}3)$$

where $v_1(S,t)$ now is the function to be determined. This substitution into equations (5-1) and (5-2) gives

$$EI_3 v_1''''(S,t) + M\ddot{v}_1(S,t) - \omega^2 MB_b \cos \omega t + \frac{Mv_1'(S,t)}{2} \frac{\partial^2}{\partial t^2} \int_o^s [v_1'^2(\xi,t) + w'^2(\xi,t)]d\xi - \frac{Mv_1''(S,t)}{2} \int_o^\ell \left\{ \frac{\partial^2}{\partial t^2} \int_o^\xi [v_1'^2(\eta,t) + w'^2(\eta,t)]d\eta \right\} d\xi = 0 \quad (5\text{-}4)$$

$$EI_2 w''''(S,t) + M\ddot{w}(S,t) + \frac{Mw'(S,t)}{2} \frac{\partial^2}{\partial t^2} \int_o^s [v_1'^2(\xi,t) + w'^2(\xi,t)]d\xi - \frac{Mw''(S,t)}{2} \int_o^\ell \left\{ \frac{\partial^2}{\partial t^2} \int_o^\xi [v_1'^2(\eta,t) + w'^2(\eta,t)]d\eta \right\} d\xi = 0. \quad (5\text{-}5)$$

The Galerkin analysis is carried out in an identical manner to the one in Chapter III. The resulting ordinary differential equations are

$$\alpha \ddot{T}_{2n}(t) + \beta_n^{(3)} T_{2n}(t) + \delta_n T_{2n}(t)[T_{2n}(t)\ddot{T}_{2n}(t) + \dot{T}_{2n}^2(t)] + \Delta_{nm} T_{2n}(t)[T_{3m}(t)\ddot{T}_{3m}(t) + \dot{T}_{3m}^2(t)] = \frac{2\omega^2 MB_b \varphi_n}{\beta_n} \cos \omega t \quad (5\text{-}6)$$

$$\alpha \ddot{T}_{3m}(t) + \beta_m^{(2)} T_{3m}(t) + \delta_m T_{3m}(t)[T_{3m}(t)\ddot{T}_{3m}(t) + \dot{T}_{3m}^2(t)] + \Delta_{mn} T_{3m}(t)[T_{2n}(t)\ddot{T}_{2n}(t) + \dot{T}_{2n}^2(t)] = 0 . \quad (5\text{-}7)$$

The coefficients α, $\beta_n^{(3)}$, etc. are the same as those defined by equations (3-6) through (3-11). In order to make the form of these equations as

much as possible like that of the previous ones, we let $\tau = \frac{\omega t}{2}$; now equations (5-6) and (5-7) become

$$T''_{2n} + \frac{4\beta_n^{(3)}}{\alpha\omega^2} T_{2n} + \frac{\delta_n}{\alpha} T_{2n}(T_{2n}T''_{2n} + T'^2_{2n}) + \frac{\Delta_{nm}}{\alpha} T_{2n}(T_{3m}T''_{3m} + T'^2_{3m})$$

$$= \frac{8B_b\varphi_n}{\beta_n \ell} \cos 2\tau \qquad (5\text{-}8)$$

$$T''_{3m} + \frac{4\beta_m^{(2)}}{\alpha\omega^2} T_{3m} + \frac{\delta_m}{\alpha} T_{3m}(T_{3m}T''_{3m} + T'^2_{3m})$$

$$+ \frac{\Delta_{mn}}{\alpha} T_{3m}(T_{2n}T''_{2n} + T'^2_{2n}) = 0 , \qquad (5\text{-}9)$$

where $(\ )'$ means $\frac{d(\ )}{d\tau}$. By setting $T_{3m}(\tau) \equiv 0$, we see that planar motion is governed by

$$T''_{2n} + \frac{4\beta_n^{(3)}}{\alpha\omega^2} T_{2n} + \frac{\delta_n}{\alpha} T_{2n}(T_{2n}T''_{2n} + T'^2_{2n}) = \frac{8B_b\varphi_n}{\beta_n \ell} \cos 2\tau . \qquad (5\text{-}10)$$

We begin the stability analysis by assuming the rod is executing plane, steady-state, harmonic motion of the form

$$T_{2n}(\tau) = A_{1n} \sin 2\tau + A_{2n} \cos 2\tau . \qquad (5\text{-}11)$$

The Ritz averaging conditions show that the algebraic relations between the amplitude of the response and the frequency of the exciting force when $T_{3m}(\tau) \equiv 0$ are

$$\left(\frac{\left(2\omega_n^{(3)}\right)^2}{\omega^2} - 4\right)\bar{A}_{1n} - 2\, c_n \bar{A}_{1n}(\bar{A}_{1n}^2 + \bar{A}_{2n}^2) = 0 \qquad (5\text{-}12)$$

$$\left(\frac{\left(2\omega_n^{(3)}\right)^2}{\omega^2} - 4\right)\bar{A}_{2n} - 2c_n\bar{A}_{2n}(\bar{A}_{1n}^2 + \bar{A}_{2n}^2) = \frac{8\bar{B}_b\varphi_n}{\beta_n \ell} . \qquad (5\text{-}13)$$

Note that in equations (5-12) and (5-13), as before, we have used the notation

$$\left(2\omega_n^{(3)}\right)^2 = \frac{4\beta_n^{(3)}}{\alpha}$$

$$b_n = \frac{4\gamma_n \ell}{\alpha}$$

$$c_n = -\frac{\delta_n \ell^2}{\alpha}$$

$$\bar{B}_b = \frac{B_b}{\ell} .$$

One can note by direct substitution into equations (5-12) and (5-13) that $\bar{A}_{2n} = 0$, $\bar{A}_{1n} \neq 0$ is not a solution, nor is $\bar{A}_{1n} = \bar{A}_{2n} = 0$. Algebraic manipulation further shows that $\bar{A}_{1n} \neq 0$, $\bar{A}_{2n} \neq 0$ is also not a possible solution; hence, the only solution is $\bar{A}_{2n} \neq 0$, $\bar{A}_{1n} = 0$. That is, the solution is given by $T_{2n}(\tau) = \bar{A}_{2n} \cos 2\tau$. Since $\bar{A}_{1n} = 0$, we shorten the notation to $T_{2n}(\tau) = \bar{A}_n \cos 2\tau$. Now this solution reduces equations (5-12) and (5-13) to

$$\left(\frac{\left(2\omega_n^{(3)}\right)^2}{\omega^2} - 4\right)\bar{A}_n - 2c_n\bar{A}_n^3 = \frac{8\bar{B}_b\varphi_n}{\beta_n \ell} . \qquad (5\text{-}14)$$

Solving for ω^2, we find

$$\frac{\omega^2}{\left(2\omega_n^{(3)}\right)^2} = \frac{1}{\frac{8\bar{B}_b\varphi_n}{\beta_n \ell \bar{A}_n} + 2c_n\bar{A}_n^2 + 4} . \qquad (5\text{-}15)$$

A graph of equation (5-15) for $n = 1,2,3$, is shown in Figure 10. One should keep in mind that damping, which is always present in physical

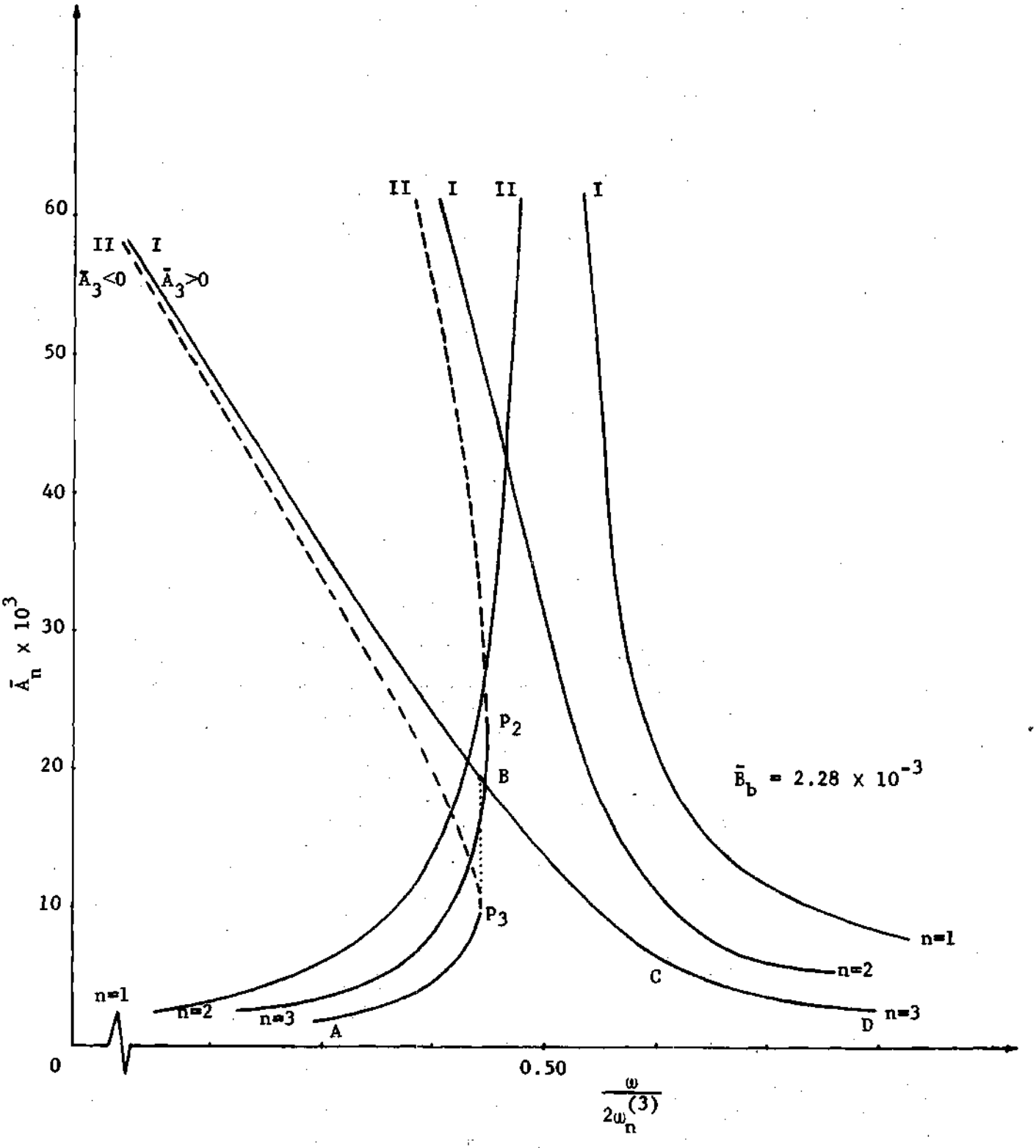

Figure 10. The Response Relation for Plane Motion of the Transversely Excited Rod, n = 1,2,3.

problems, causes the two branches of the response relation to merge in the manner shown in Appendix D. The source of the numbers used to plot Figure 10 is the example problem at the end of this chapter.

It is well-known (see [1] and others) that the dashed curves shown in Figure 10 represent motions which are unstable with respect to small amplitude perturbations in the direction of the planar response. These dashed portions are located by determining point P which is the point at which the response curve has a vertical tangent. This general type of response is like that of systems governed by the Duffing equation and has been extensively studied. For example, consider the curves for the $n = 3$ case, and notice that as the exciting frequency is increased, the planar amplitude increases along path A P_3 to the point of vertical tangency; here an upward amplitude jump occurs. Now the rod responds with an amplitude given by point B. The amplitude then decreases along path B C D as frequency is further reduced.

For decreasing values of the exciting frequency, the planar amplitudes increase along path D C B E until the point is reached at which damping (which is not taken into account here) causes the dashed and solid line portions of the response curve to merge. At that frequency, a downward amplitude jump occurs to a value of the amplitude given by A.

The stability of the planar response to out-of-plane perturbations is determined, as before, by letting

$$\bar{T}_{2n}(\tau) = T_{2n}(\tau) + 0 = A_n \cos 2\tau \qquad (5\text{-}16)$$

$$\bar{T}_{3m}(\tau) = 0 + x_{3m}(\tau) \ , \qquad (5\text{-}17)$$

substituting these into equations (5-12) and (5-13), making use of the fact that $T_{2n}(\tau)$ is a solution to equation (5-10), and neglecting terms of higher order than the first in x_{3m}. The stability equation is

$$x''_{3m}(\tau)+\left(\frac{\left(2\omega_m^{(2)}\right)^2}{\omega^2}-4c_{mn}\bar{A}_n^2\cos 4\tau\right)x_{3m}(\tau)=0\ . \tag{5-18}$$

Letting $\zeta = 4\tau$, we find that

$$\frac{d^2x_{3m}(\zeta)}{d^2\zeta}+(\epsilon_1+\epsilon_2\cos\zeta)x_{3m}(\zeta)=0\ , \tag{5-19}$$

where

$$\epsilon_1=\frac{\left(2\omega_m^{(2)}\right)^2}{16\omega^2} \tag{5-20}$$

$$\epsilon_2=-\frac{1}{4}c_{mn}\bar{A}_n^2\ . \tag{5-21}$$

Elimination of ω^2 from equations (5-20) and (5-21) is accomplished by using equation (5-15) in equations (5-20) and (5-21). Then the parametric equations (with $\bar{A}_n$ as the parameter) for the response curve in the ϵ_1,ϵ_2-plane are

$$\epsilon_2=-\frac{1}{4}c_{mn}\bar{A}_n^2\ . \tag{5-23}$$

$$\epsilon_1 = \frac{1}{8}\frac{\omega_m^{(2)^2}}{\omega_n^{(3)^2}}\left(\frac{4\bar{B}_b\varphi_n}{\beta_n \ell \bar{A}_n} + c_n\bar{A}_n^2 + 2\right). \tag{5-22}$$

Notice now that the above equations no longer describe a straight line in the ϵ_1,ϵ_2-plane, even when m = n and $\omega_m^{(2)} = \omega_n^{(3)}$ as was the case for the axially excited rod. Note also in equations (5-22) and (5-23) that $\frac{4\bar{B}_b\varphi_n}{\beta_n \ell}$ depends only on n, ℓ, and B_b and that c_n and c_{mn} depend only on n, m, and ℓ. In other words, the value of $(\bar{A}_n)_{cr.}$ does not depend on E, M, and the shape of the cross-section but is a function only of m, n, ℓ, B_b, and $\frac{\omega_m^{(2)}}{\omega_n^{(3)}}$.

For the special case of m = n and $I_2 = I_3$, equations (5-22) and (5-23) reduce to

$$\epsilon_1 = \frac{1}{8}\left(\frac{4\bar{B}_b\varphi_n}{\beta_n \ell \bar{A}_n} + c_n\bar{A}_n^2 + 2\right) \tag{5-24}$$

$$\epsilon_2 = -\frac{1}{4}c_n\bar{A}_n^2 . \tag{5-25}$$

When considering the parametrically excited rod, it was easy to eliminate ϵ_1 between the equation describing ϵ_1 as a function of $\bar{A}_n$ and the equation for the boundary of the principal stability region. This operation yielded $(\bar{A}_n)_{cr.}$ which is the value of the planar amplitude for

which instability occurs. In the present cases, $(\bar{A}_n)_{cr.}$ can not be so readily determined as it is the solution to a cubic equation. This cubic, which is found by solving $\epsilon_1 = \frac{1}{4} \pm \frac{1}{2}\epsilon_2$ along with equations (5-22) and (5-23), is

$$\left(c_n \pm c_{mn}\frac{\omega_n^{(3)^2}}{\omega_m^{(2)^2}}\right)\bar{A}_n^3 + 2\left(1 - \frac{\omega_n^{(3)^2}}{\omega_m^{(2)^2}}\right)\bar{A}_n + \frac{4\bar{B}_b\varphi_n}{\beta_n \ell} = 0 . \qquad (5\text{-}26)$$

For the special case m = n and $\omega_m^{(2)} = \omega_n^{(3)}$, equation (5-26) simplifies to

$$\bar{A}_n^{(3)} + \frac{2\bar{B}_b\varphi_n}{\beta_n \ell} = 0 \qquad (5\text{-}27)$$

when intersections with $\epsilon_1 = \frac{1}{4} + \frac{1}{2}\epsilon_2$ are sought, and to

$$\frac{4\bar{B}_b\varphi_n}{\beta_n \ell} = 0 \qquad (5\text{-}28)$$

when intersections with $\epsilon_1 = \frac{1}{4} - \frac{1}{2}\epsilon_2$ are sought. Condition (5-28) is possible only if $\bar{B}_b = 0$ which is not a situation being considered; therefore, intersections with $\epsilon_1 = \frac{1}{4} - \frac{1}{2}\epsilon_2$ do not occur. Furthermore, the only real root of equation (5-27) is a negative one. This means, in the above special case, that the branch of the response curve which is in phase with the forcing function (branch II in Figure 10) never crosses a stability boundary. Only the out-of-phase branch (branch I in Figure 10) gives rise to a loss of planar stability.

If one maps the stability boundaries on the amplitude-frequency plane, a clear picture of how the response curves relate to the principal instability zone can be obtained. To determine the equations for the stability boundaries, we eliminate ϵ_1 and ϵ_2 between equations (5-20) and (5-21) and the equations $\epsilon_1 = \frac{1}{4} \pm \frac{1}{2}\epsilon_2$. This yields

$$\frac{\omega^2}{\left(2\omega_m^{(2)}\right)^2} = \frac{1}{2(2 + c_{mn}\,\bar{A}_n^2)} \tag{5-29}$$

for the boundary given by $\epsilon_1 = \frac{1}{4} - \frac{1}{2}\,\epsilon_2$ and

$$\frac{\omega^2}{\left(2\omega_m^{(2)}\right)^2} = \frac{1}{2(2 - c_{mn}\,\bar{A}_n^2)} \tag{5-30}$$

for the boundary given by $\epsilon_1 = \frac{1}{4} + \frac{1}{2}\,\epsilon_2$. Note that the above stability boundaries are independent of $\bar{B}_b$. Figures 11, 12, and 13 show the principal instability zone superposed on the $\frac{\omega}{2\omega_n^{(3)}}$, $\bar{A}_n$-plane when n = 1,2,3 for the special case m = n and $\omega_m^{(2)} = \omega_n^{(3)}$. The physical constants are given in the example problem which follows. It is interesting to note, for the above mentioned special case, that the stability boundary given by $\epsilon_1 = \frac{1}{4} - \frac{1}{2}\,\epsilon_2$ has the same equation in the $\frac{\omega}{2\omega_n^{(3)}}$, $\bar{A}_n$-plane as does the "backbone" or "free" oscillation curve found from equation (5-15) by setting $\bar{B}_b = 0$.

Referring to Figure 13, as an example, we see how the nonlinear jump in amplitude phenomenon comes into play with respect to nonplanar motions. If frequency is increased, a point progresses along the response curve from A to P where the jump phenomenon occurs. After the jump, the point is at B, which lies in a region for which plane motion is unstable when disturbed in a nonplanar direction. Hence, at point B, one observes the rod moving simultaneously in the (1), (2)-plane and the (1), (3)-plane. Now if frequency is decreased beginning at C, a point follows the response curve from C to D where again plane motion becomes unstable.

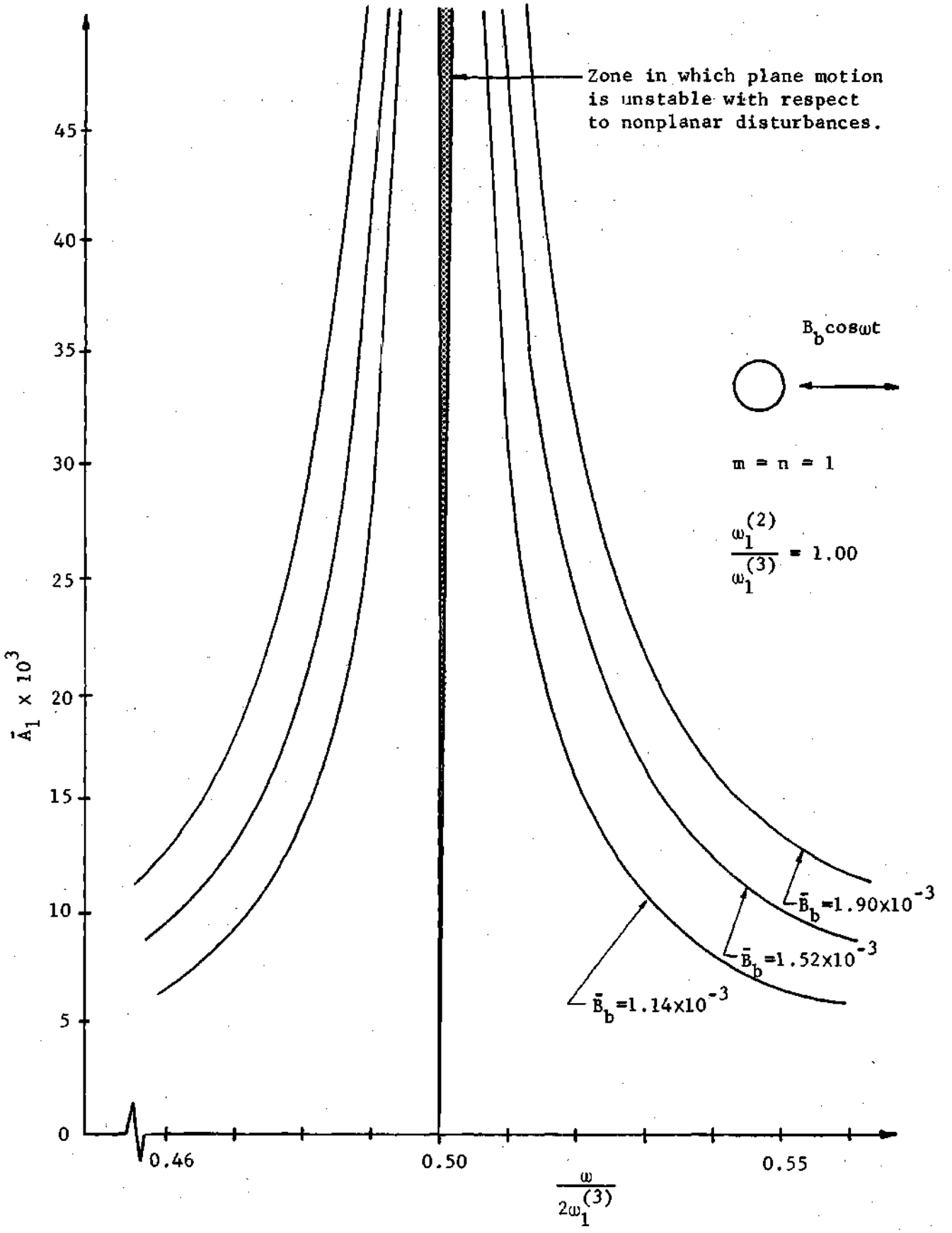

Figure 11. Response Equations and Stability Boundaries for the Transversely Excited Rod, m = n = 1.

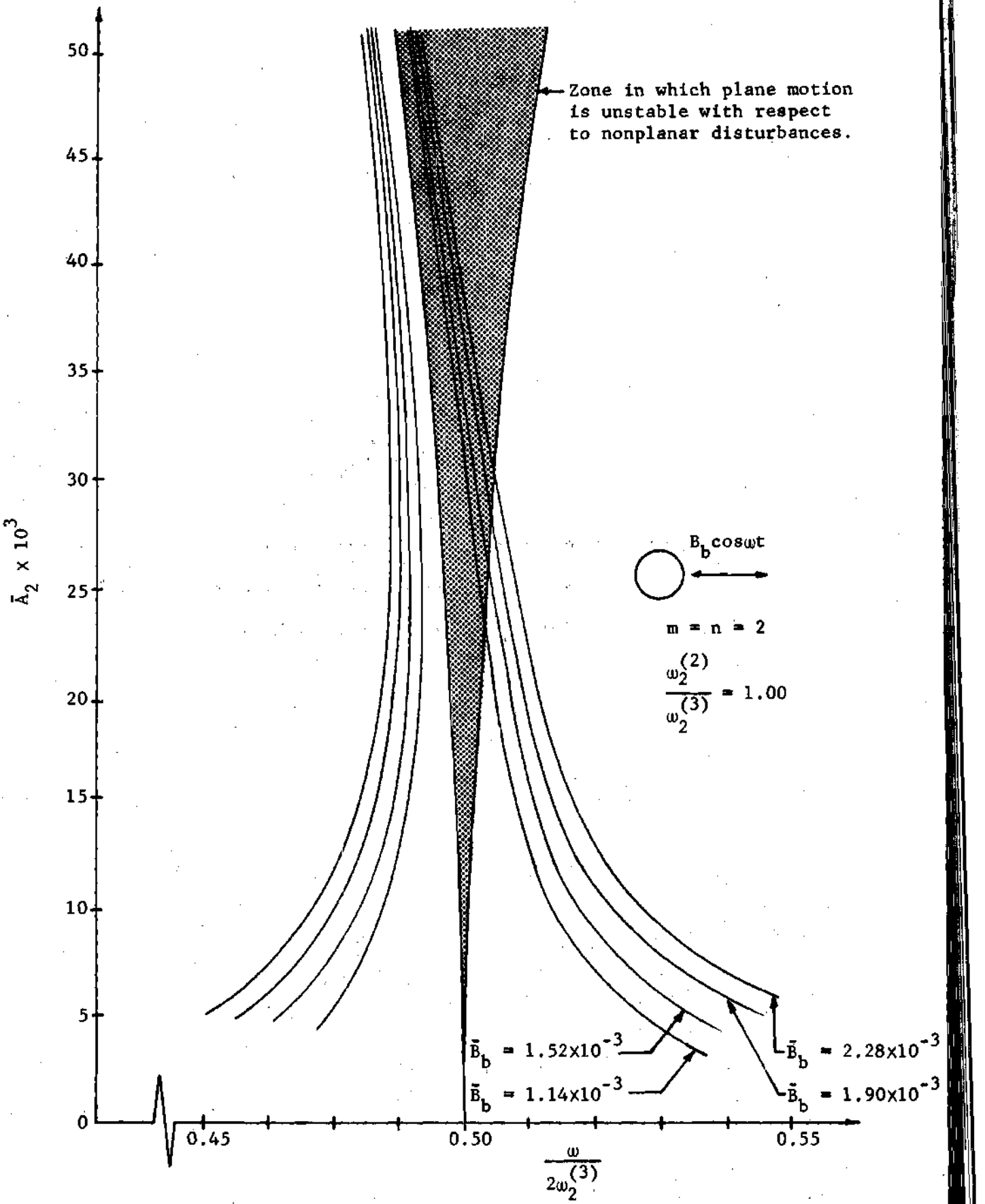

Figure 12. Response Equations and Stability Boundaries for the Transversely Excited Rod, m = n = 2.

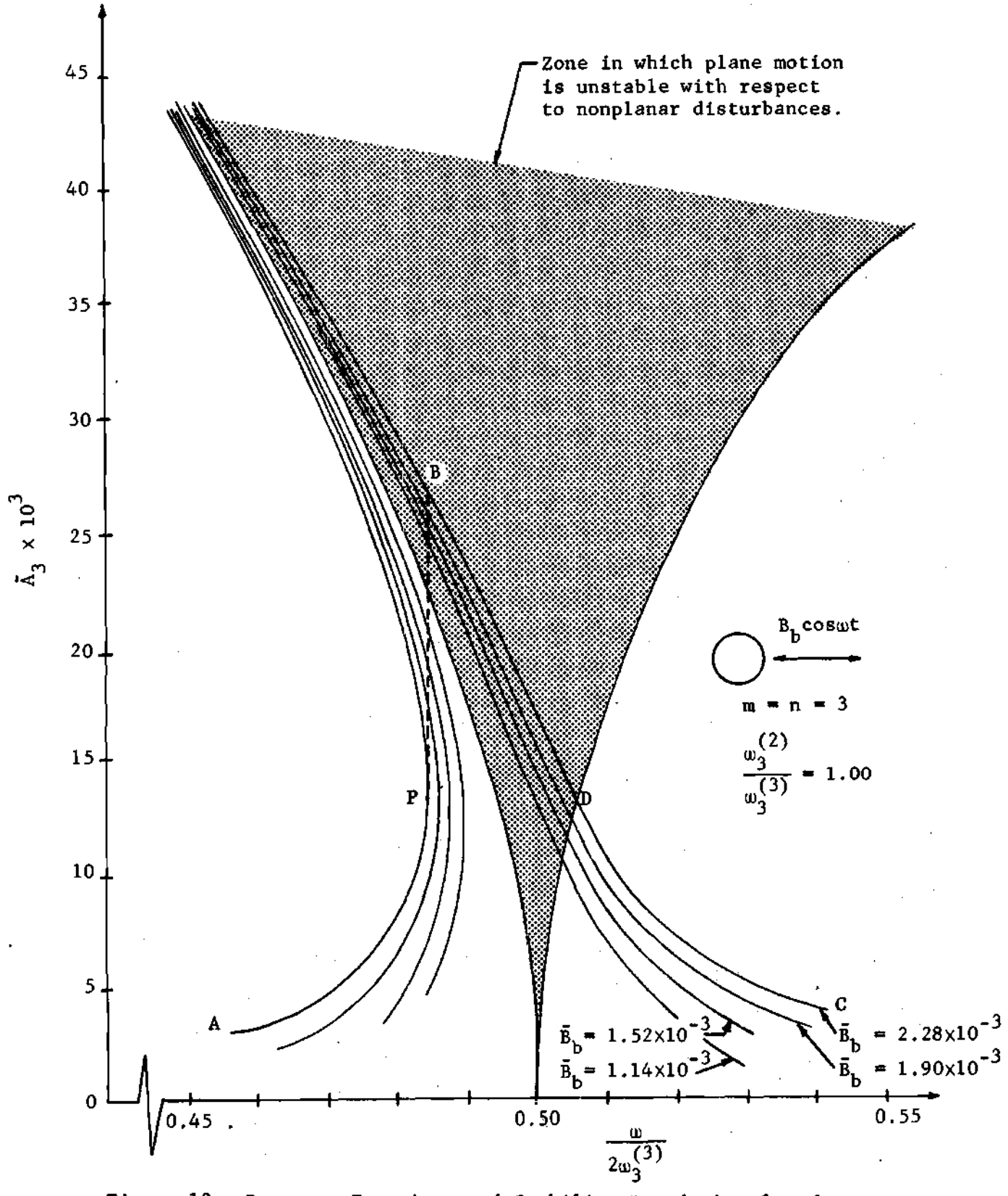

Figure 13. Response Equations and Stability Boundaries for the Transversely Excited Rod, m = n = 3.

Therefore, the jump phenomenon causes the motion represented by segment BD of the response curve to be unstable with respect to nonplanar perturbations. For all points on segment BD, then, plane motion is unstable.

In Figures 14 and 15, the effect of varying the natural frequency ratio is indicated. Note that, with no damping present, the response curve always passes through the instability region. As the difference between the natural frequency ratio and unity increases, the zone in which the response curve passes through the instability region becomes more narrow. The presence of damping, however, prevents the instability zone from extending all the way down to the $\frac{\omega}{2\omega_n^{(3)}}$ axis; therefore, with damping present, the likelihood of nonplanar motion decreases as the difference in the natural frequency ratio and unity increases. In Appendix D, we qualitatively indicate the influence of damping.

We conclude this chapter by pointing out that this problem is analogous to the elastic string excited transversely as studied by Murthy and Ramakrishna. That is, a steady-state harmonic solution of the form

$$v(S,t) = T_{2n}(t)X_n(S) = a_{n2}X_n(S)\cos\omega t$$
$$w(S,t) = T_{3n}(t)X_n(S) = a_{n3}X_n(S)\sin\omega t$$

can be found for the directly excited rod. This solution form, as we discussed in Chapter IV, accounts for a "whirling motion" by prescribing a phase difference of $\frac{\pi}{2}$ between motions in the x_1,x_2-plane and the x_1,x_3-plane.

The particular rod used to obtain the response curves and stability boundaries shown in Figures 10, 11, 12, and 13 is described by the following constants:

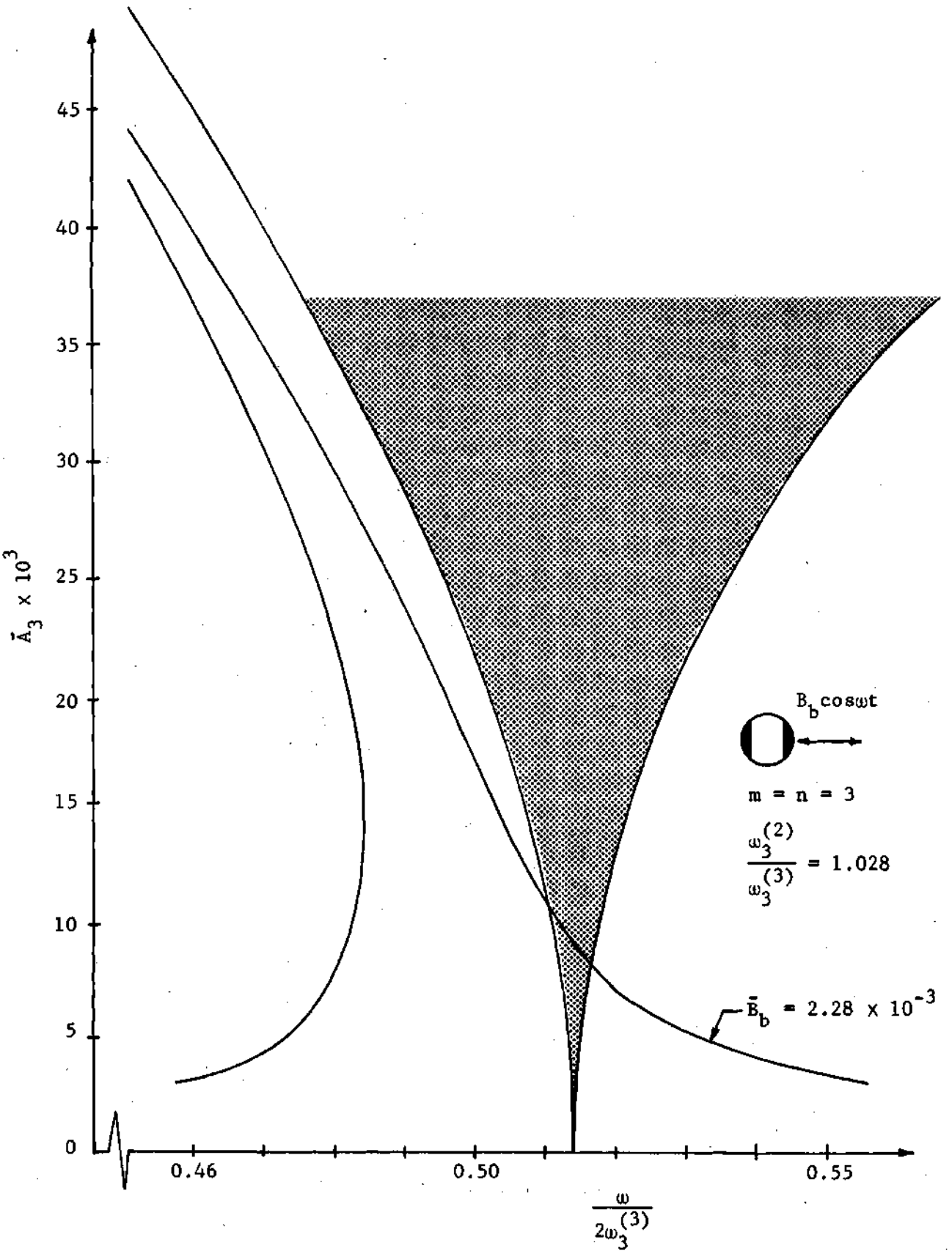

Figure 14. Effect of Varying the Natural Frequency Ratio for the Transversely Excited Rod, $\frac{\omega_n^{(2)}}{\omega_n^{(3)}} > 1$.

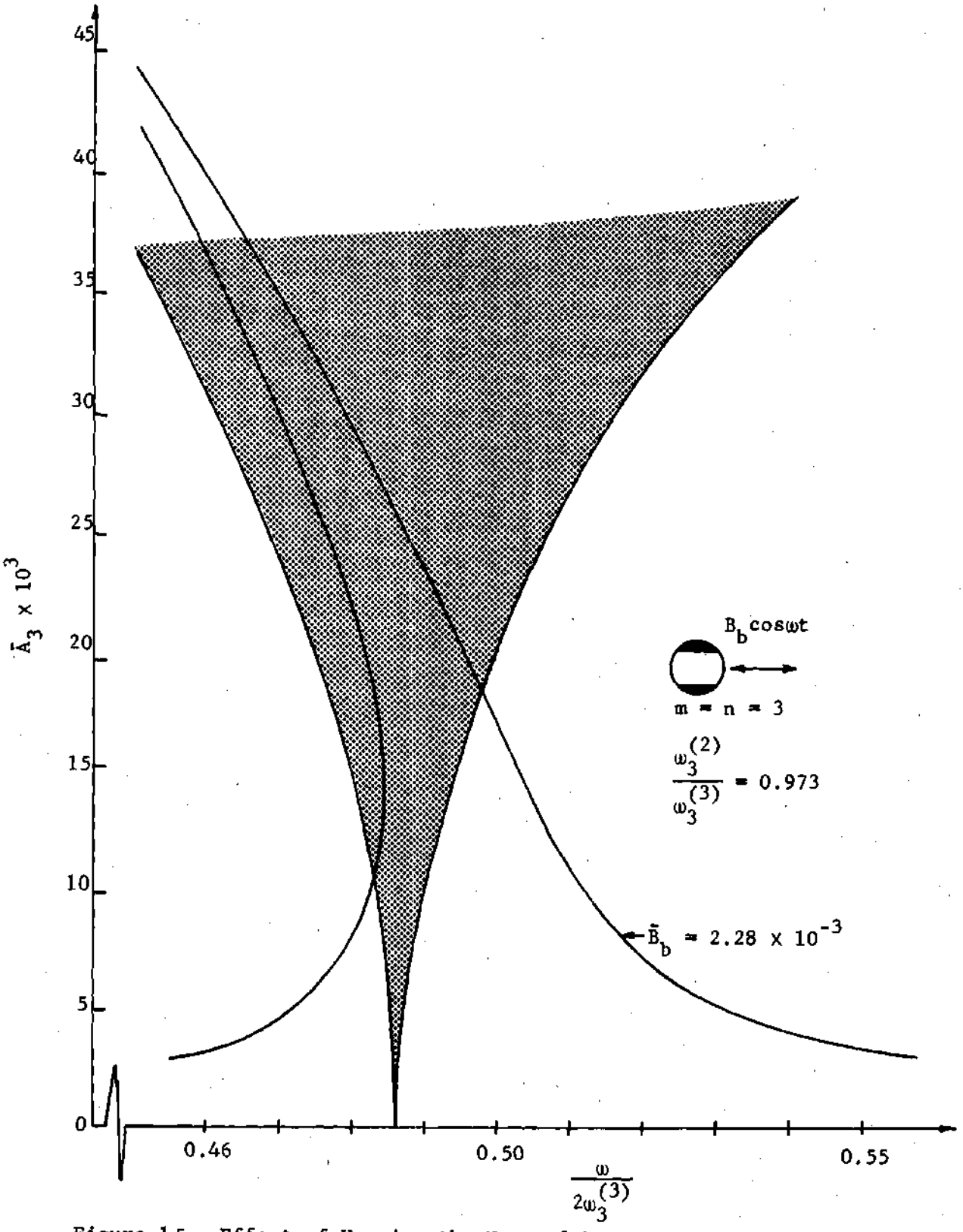

Figure 15. Effect of Varying the Natural Frequency Ratio for the Transversely Excited Rod, $\frac{\omega_n^{(2)}}{\omega_n^{(3)}} < 1$.

ℓ = 32.9 inches

Cross-section: circular

Diameter: 0.188 inches

$E = 30 \times 10^6$ psi

B_b = 0.075 inches

Specific weight of the material = 485 lb/ft^3.

These same data, except for the circular cross-section, are used to determine the information shown in Figures 14 and 15. In the latter graphs, the rod originally had a diameter of 0.188 inches, but parallel flats of material are considered removed from two sides to give the indicated natural frequency ratios.

CHAPTER VI

THE EXPERIMENTS

The purpose of the experiments is to test the validity of the foregoing analysis that predicts the inception of nonplanar responses of elastic rods. We are interested primarily in whether or not parametrically induced nonplanar motions are present and the conditions under which one might expect them. With these objectives in mind, the experiments were designed to be fundamentally of a qualitative nature. However, data on both the amplitude and frequency at which the planar response loses its stability when disturbed in a direction normal to the plane is also presented.

The device employed to harmonically excite the rod was an All American vibration fatigue testing machine, Model 25-VP-T, equipped with independent amplitude and frequency controls. The amplitude range for this machine is 0 - 0.075 inches and the frequency range is 5 - 100 cycles per second. Frequency measurements were taken from a digital recorder that received its signal from a capacitance displacement pickup positioned above the shaker table. Rod response amplitude measurements were made using a steel rule supported closely behind the free end of the rod. This method proved satisfactory since the amplitudes to be measured were large: in fact, the peak-to-peak displacement at the free end was between one-half and 6 inches.

Small electrodynamic vibration exciters of the type currently marketed by MB Electronics are not well suited for exciting nonplanar motions in rods such as these. This is particularly true for the case of the

transversely excited rod. The moving head of the exciter is not sufficiently rigid with respect to torques applied about its longitudinal axis. The nonplanar motions which interest us apply just such a torque to the shaker head and, since the shaker head is weak with respect to torque vectors about its longitudinal axis, the shaker head acts as a vibration absorber for the nonplanar oscillations. The author found it impossible to excite the nonplanar motions of the transversely excited rod with the electrodynamic exciter. No difficulties of this sort were experienced with the mechanical fatigue testing machine.

Similar but not so serious difficulties were experienced with the electrodynamic exciter in the case of the axially excited rod. The rod responded in the qualitative manner described in Chapter IV but the response amplitudes were diminished due to lack of rigidity of the shaker head. Consequently, the mechanical fatigue testing machine was used for all the experiments.

The specimens were made from 0.188 inch diameter steel drill rod having a useable length after clamping of 32.9 inches. Some rods were used in their original circular cross-section form while others had parallel flats ground on two sides by a surface grinder. All rods were carefully selected for initial straightness. The rods were rigidly clamped by means of shaped blocks to the specimen table of the shaker.

The Axially Excited Rod

The testing procedure for rods excited in the axial direction was as follows. The exciting frequency was slowly and continuously increased along path OLA (refer to Figure 7, page 37) until point A was reached.

At point A, a vertical amplitude jump to point B occurred. The frequency which corresponded to points A and B was measured (ω_A) and the steady-state x_1,x_2-plane response amplitude ($\bar{A}_{n_B}$) after the jump to point B was measured. Frequency was further increased (and a corresponding decrease in amplitude was witnessed) until the frequency at point D was reached. At point D, a vertical amplitude jump and a 90° plane-shift to point E was observed. Both the frequency at point D (ω_D) and the steady-state amplitude of the x_1,x_3-plane response at point E ($\bar{A}_{n_{E_{inc.}}}$, the amplitude at E when frequency is increased) were measured. The exciting frequency was then slowly raised until the x_1,x_3-plane response amplitude decreased to zero. The frequency which corresponded to the return to the straight configuration (ω_G) was measured at this point.

The exciting frequency was then slowly lowered along path HG until point G was reached; the frequency at G (ω_G) for which x_1,x_3-plane motions began was again recorded. The frequency ω_G obtained by increasing frequency was averaged with the frequency ω_G obtained by decreasing frequency and the average value is recorded in Table 2. The two values were substantially the same. Frequency was further decreased (and the response amplitudes increased) until the frequency which corresponds to point E was reached. At point E, a downward amplitude jump to point D with a corresponding 90° plane shift to x_1,x_2-plane oscillations was observed. Both the amplitude at E ($\bar{A}_{n_{E_{dec.}}}$, the amplitude at E when frequency is decreased) and the frequency at E (ω_E) were measured as was the x_1,x_2-plane response amplitude at D($\bar{A}_{n_D}$). If frequency was decreased still more, the x_1,x_2-plane amplitudes increased until damping caused a downward amplitude jump to the original straight configuration.

The above data were acquired for four rods, each having a different natural frequency ratio. Also, two different values of the base excitation amplitude A_b were used for each of the four rods. Because of the limited frequency range of the testing machine, only the second mode could be excited. In Table 2, we present the experimental data for these four rods and compare it to the theoretical values of the amplitudes and frequencies. Damping was not included in the theoretical calculations since it had only a small theoretical effect so long as the response amplitude was small (see Appendix D). All amplitudes reported are measured at the free end and all are non-dimensionalized by dividing by the rod length, $\ell = 32.9$ inches. All frequencies are non-dimensionalized by dividing by twice the theoretical natural frequency for the second mode.

The formulas used to calculate the amplitudes and frequencies tabulated in Table 2 are readily found from the equations in Chapter IV. They are:

$$(\bar{A}_{2_B})^2 = \frac{2}{c_2} b_2 \bar{A}_b \qquad \text{(from equation (4-37))} \tag{6-1}$$

$$(\bar{A}_{2_E})^2_{\text{inc.}} = (\bar{A}_{2_E})^2_{\text{dec.}} = \frac{1}{c_2}\left[b_2\bar{A}_b + 2\left(\frac{\omega_2^{(2)^2} - \omega_2^{(3)^2}}{\omega_2^{(2)^2} + \omega_2^{(3)^2}}\right)\right]$$

(from equation (4-49)) (6-2)

$$(\bar{A}_{2_D})^2 = \frac{1}{c_2}\left[b_2\bar{A}_b - 2\left(\frac{\omega_2^{(2)^2} - \omega_2^{(3)^2}}{\omega_2^{(2)^2} + \omega_2^{(3)^2}}\right)\right]$$

(from equation (4-50)) (6-3)

$$\omega_A^2 = \frac{2\left(\omega^{(3)}\right)^2}{2 + b_2\bar{A}_b} \qquad \text{(from equation (4-37))} \qquad (6\text{-}4)$$

$$\omega_D^2 = \omega_E^2 = 2\left(\omega_2^{(2)^2} + \omega_2^{(3)^2}\right) \qquad \text{(from equation (4-48))} \qquad (6\text{-}5)$$

$$\omega_G^2 = \frac{2\left(\omega_2^{(2)}\right)^2}{2 - b_2\bar{A}_b} \qquad \text{(from equation (4-38))}. \qquad (6\text{-}6)$$

The data in Table 2 indicates that the theory correctly models the qualitative response of the rod. However, the theoretical amplitudes are in all instances greater than the experimentally obtained amplitudes. The error increases as the amplitudes increase. Of course, a damping term tends to decrease the theoretical amplitudes, but we have shown in Appendix D that if it is assumed that damping forces are proportional to velocity, the effect only becomes noticeable for much larger amplitudes than those with which we are concerned. Possibly a nonlinear damping term would allow the theory to more accurately predict the response amplitudes. One should observe that the agreement between theory and experiments is better for the amplitude ratios $\frac{\bar{A}_{2_B}}{\bar{A}_{2_E}}_{\text{inc.}}$ and $\frac{\bar{A}_{2_D}}{\bar{A}_{2_E}}_{\text{inc.}}$ than for the amplitudes themselves.

Note that for the first three cases listed the amplitude $\bar{A}_{2_E}$ (the amplitude at E when frequency is being increased) is less than $\bar{A}_{2_E}$ for the experiments. These amplitudes theoretically should be the same provided that damping is not present. Also note that ω_D is greater than ω_E in the experiments; these, too, should be the same provided damping is absent. But even if damping proportional to velocity is included in the theory,

Table 2. Comparison of the Experiments With the Theory for the Axially Excited Rod; $m = n = 2$, $\ell = 32.9$ inches.

Parameters	Source of Data	$\frac{\omega_A}{2\omega_2^{(2)}}$	$\bar{A}_{2_B}$	$\frac{\omega_D}{2\omega_2^{(2)}}$	$\bar{A}_{2_E}$ inc.	$\frac{\omega_G}{2\omega_2^{(2)}}$	$\bar{A}_{2_E}$ dec.	$\frac{\omega_E}{2\omega_2^{(2)}}$	$\bar{A}_{2_D}$	$\frac{\bar{A}_{2_B}}{\bar{A}_{2_E}}$ inc.	$\frac{\bar{A}_{2_D}}{\bar{A}_{2_E}}$ inc.
$\bar{A}_b = 2.28 \times 10^{-3}$	Experiments	0.985	0.013	1.005	0.015	1.045	0.019	0.974	0.016	0.87	1.07
$\omega_2^{(2)}/\omega_2^{(3)} = 0.973$	Theory	0.967	0.033	0.993	0.027	1.020	0.027	0.993	0.019	1.22	0.70
$\bar{A}_b = 1.52 \times 10^{-3}$	Experiments	0.993	0.010	1.007	0.011	1.036	0.016	0.985	0.011	0.91	1.00
$\omega_2^{(2)}/\omega_2^{(3)} = 0.973$	Theory	0.974	0.022	0.993	0.023	1.013	0.023	0.993	0.013	0.96	0.57
$\bar{A}_b = 2.28 \times 10^{-3}$	Experiments	0.929	0.015	0.959	0.015	1.000	0.021	0.937	0.013	1.00	0.87
$\omega_2^{(2)}/\omega_2^{(3)} = 0.946$	Theory	0.954	0.033	0.987	0.030	1.020	0.030	0.987	0.013	1.10	0.43
$\bar{A}_b = 1.52 \times 10^{-3}$	Experiments	0.935	0.010	(1)	(3)	0.997	0.017	0.942	0.002	(3)	0.12
$\omega_2^{(2)}/\omega_2^{(3)} = 0.946$	Theory	0.960	0.022	(1)	(3)	1.013	0.027	0.987	(2)	(3)	(2)
$\bar{A}_b = 2.28 \times 10^{-3}$	Experiments	0.908	0.016	(1)	(3)	1.007	0.022	0.928	0.003	(3)	(3)
$\omega_2^{(2)}/\omega_2^{(3)} = 0.897$	Theory	0.929	0.033	(1)	(3)	1.020	0.036	0.974	(2)	(3)	(2)

(Continued)

Table 2. Comparison of the Experiments With the Theory for the Axially Excited Rod; $m = n = 2$, $\ell = 32.9$ inches. (Continuation)

Parameters	Source of Data	$\frac{\omega_A}{2\omega_2^{(2)}}$	$\bar{A}_{2_B}$	$\frac{\omega_D}{2\omega_2^{(2)}}$	$\bar{A}_{2_E}$ inc.	$\frac{\omega_G}{2\omega_2^{(2)}}$	$\bar{A}_{2_E}$ dec.	$\frac{\omega_E}{2\omega_2^{(2)}}$	$\bar{A}_{2_D}$	$\frac{\bar{A}_{2_B}}{\bar{A}_{2_E}}$ inc.	$\frac{\bar{A}_{2_D}}{\bar{A}_{2_E}}$ inc.
$\bar{A}_b = 1.52 \times 10^{-3}$	Experiments	0.917	0.010	(1)	(3)	1.000	0.017	0.940	(2)	(3)	(2)
$\omega_2^{(2)}/\omega_2^{(3)} = 0.897$	Theory	0.935	0.022	(1)	(3)	1.013	0.033	0.974	(2)	(3)	(2)
$\bar{A}_b = 2.28 \times 10^{-3}$	Experiments	0.894	0.015	(1)	(3)	1.003	0.022	0.926	(2)	(3)	(2)
$\omega_2^{(2)}/\omega_2^{(3)} = 0.861$	Theory	0.909	0.033	(1)	(3)	1.020	0.039	1.004	(2)	(3)	(2)
$\bar{A}_b = 1.52 \times 10^{-3}$	Experiments	0.900	0.010	(1)	(3)	0.997	0.020	0.948	(2)	(3)	(2)
$\omega_2^{(2)}/\omega_2^{(3)} = 0.861$	Theory	0.916	0.022	(1)	(3)	1.013	0.037	1.004	(2)	(3)	(2)

(1) In these cases, the rods were sufficiently detuned so that zone JDK, Figure 7, disappeared. Hence there is no frequency which corresponds to point D. See Figure 8.

(2) No amplitude exists at point D for the reason mentioned in (1). See Figure 8.

(3) The amplitude at E can not be reached by increasing frequency. See Figure 8.

the alteration to ω_D, ω_E, $\bar{A}_{n_{E_{dec.}}}$ and $\bar{A}_{n_{E_{inc.}}}$ is very small for the amount of damping indicated by the viscous damping hypothesis. Again, a nonlinear damping term might cause better agreement between theory and experiments. The fact that $\omega_D > \omega_E$ and $\bar{A}_{2_{E_{inc.}}} < \bar{A}_{2_{E_{dec.}}}$ indicates that the response relations and the stability boundaries should have the shape indicated in Figure 16 when damping is included.

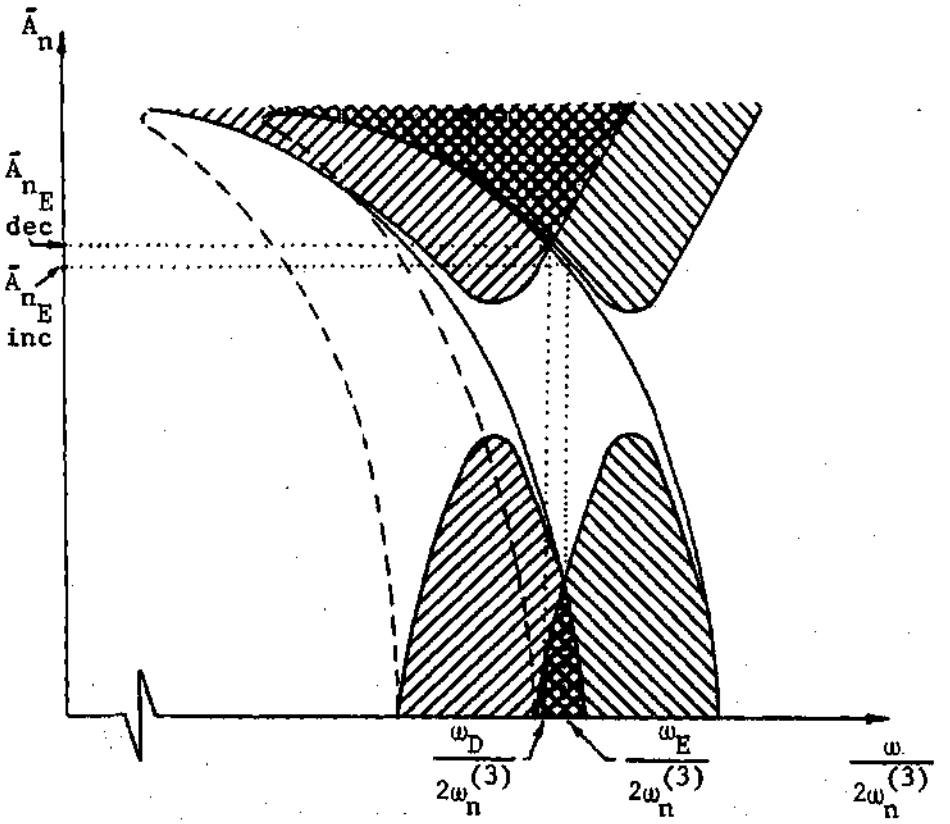

Figure 16. Shape of the Response Curves and Stability Boundaries as Suggested by the Experimental Data.

The Directly Excited Rod

Since we have shown that the planar response of the directly excited rod can become unstable with respect to nonplanar disturbances even when $\frac{\omega_n^{(2)}}{\omega_n^{(3)}} = 1$, we extend this set of experiments to include circular cross-section rods as well as the rods used for the axial excitation experiments.

Three rods were tested at various values of B_b; one had a circular cross-section, one had parallel flats on its sides and was excited in a direction parallel to the flats, and the third was excited in a direction perpendicular to the flats. Data is presented for the cases $m = n = 2$ and $m = n = 3$. It was not possible to excite the first mode since the testing machine could not be controlled at very low frequency. Situations for which $m \neq n$ were not observed in the laboratory. Figure 17, (a), (b), (c) indicates the general shape of the response curve and the stability boundary for the above mentioned cases.

The testing procedure for this method of excitation was basically the same as that outlined for the axially excited rod. The purpose of the tests is to determine the region of the $\bar{A}_n$, $\frac{\omega}{2\omega_m^{(2)}}$ - plane for which plane motion of the rod is unstable with respect to nonplanar disturbances. To accomplish this, the amplitude of the planar response and the corresponding frequency at points C and D were measured for rods of the type shown in Figure 17, (b). For rods shown in Figure 17, (c) the amplitudes and corresponding frequencies at points D, C, and B were measured. For the circular cross-section rods (Figure 17, (a)) only the amplitude and frequency at C and the frequency at B could be measured. No measurement

of the amplitude at B is recorded since point B corresponds to an unstable plane motion.

The comparison of the experimental data with the theory is shown in Table 3. Agreement between theoretical and experimental values is good for both amplitudes and frequencies. Note that the theory does an especially good job of predicting low values of amplitude. Damping has not been included in the theoretical calculations.

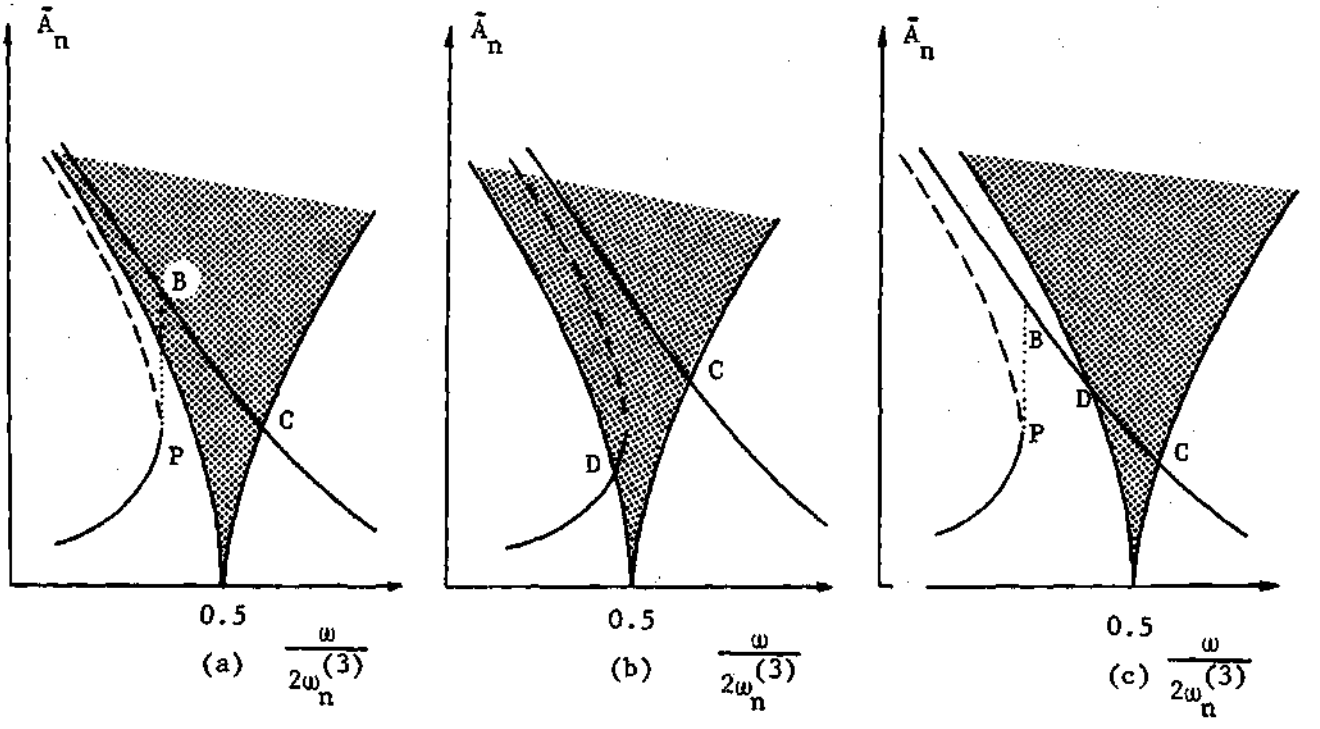

Figure 17. The Response Curves and Stability Zones for the Three Transversely Excited Rods Tested.

Table 3. Comparison of the Experiments with the Theory for the Transversely Excited Rod; $m = n = 2$ and $m = n = 3$, $\ell = 32.9$ inches.

Parameters	Source of Data	$\frac{\omega_B}{2\omega_n^{(3)}}$	$\frac{\omega_C}{2\omega_n^{(3)}}$	$\frac{\omega_D}{2\omega_n^{(3)}}$	$\bar{A}_{n_C}$	$\bar{A}_{n_D}$
$\bar{B}_b = 2.28 \times 10^{-3}$ $m = n = 2$ $\omega_2^{(2)}/\omega_2^{(3)} = 1.00$	Experiments	0.471	0.503	-	0.013	-
	Theory	0.488	0.504	-	0.015	-
$\bar{B}_b = 1.90 \times 10^{-3}$ $m = n = 2$ $\omega_2^{(2)}/\omega_2^{(3)} = 1.00$	Experiments	0.471	0.503	-	0.011	-
	Theory	0.489	0.504	-	0.014	-
$\bar{B}_b = 1.52 \times 10^{-3}$ $m = n = 2$ $\omega_2^{(2)}/\omega_2^{(3)} = 1.00$	Experiments	0.477	0.503	-	0.010	-
	Theory	0.491	0.503	-	0.013	-
$\bar{B}_b = 1.14 \times 10^{-3}$ $m = n = 2$ $\omega_2^{(2)}/\omega_2^{(3)} = 1.00$	Experiments	0.479	0.503	-	0.010	-
	Theory	0.492	0.502	-	0.012	-
$\bar{B}_b = 0.75 \times 10^{-3}$ $m = n = 2$ $\omega_2^{(2)}/\omega_2^{(3)} = 1.00$	Experiments	0.484	0.500	-	0.009	-
	Theory	0.494	0.502	-	0.010	-
$\bar{B}_b = 2.28 \times 10^{-3}$ $m = n = 3$ $\omega_3^{(2)}/\omega_3^{(3)} = 1.00$	Experiments	0.457	0.495	-	0.006	-
	Theory	0.484	0.506	-	0.007	-

(Continued)

Table 3. Comparison of the Experiments with the Theory for the Transversely Excited Rod; m = n = 2 and m = n = 3, ℓ = 32.9 inches. (Continuation)

Parameters	Source of Data	$\frac{\omega_B}{2\omega_n^{(3)}}$	$\frac{\omega_C}{2\omega_n^{(3)}}$	$\frac{\omega_D}{2\omega_n^{(3)}}$	$\bar{A}_{n_C}$	$\bar{A}_{n_D}$
$\bar{B}_b = 1.90 \times 10^{-3}$ m = n = 3 $\omega_3^{(2)}/\omega_3^{(3)} = 1.00$	Experiments	0.459	0.497	-	0.005	-
	Theory	0.486	0.505	-	0.006	-
$\bar{B}_b = 1.52 \times 10^{-3}$ m = n = 3 $\omega_3^{(2)}/\omega_3^{(3)} = 1.00$	Experiments	0.466	0.496	-	0.005	-
	Theory	0.488	0.504	-	0.006	-
$\bar{B}_b = 1.14 \times 10^{-3}$ m = n = 3 $\omega_3^{(2)}/\omega_3^{(3)} = 1.00$	Experiments	0.473	0.498	-	0.005	-
	Theory	0.490	0.503	-	0.005	-
$\bar{B}_b = 0.75 \times 10^{-3}$ m = n = 3 $\omega_3^{(2)}/\omega_3^{(3)} = 1.00$	Experiments	0.478	0.498	-	0.005	-
	Theory	0.492	0.502	-	0.005	-
$\bar{B}_b = 2.28 \times 10^{-3}$ m = n = 2 $\omega_2^{(2)}/\omega_2^{(3)} = 0.973$	Experiments	-	0.498	0.474	0.019	0.009
	Theory	-	0.496	0.485	0.023	0.007
$\bar{B}_b = 1.14 \times 10^{-3}$ m = n = 2 $\omega_2^{(2)}/\omega_2^{(3)} = 0.973$	Experiments	-	0.502	0.481	0.014	0.007
	Theory	-	0.504	0.476	0.020	0.005

Table 3. Comparison of the Experiments with the Theory for the Transversely Excited Rod; m = n = 2 and m = n = 3, ℓ = 32.9 inches. (Continuation)

Parameters	Source of Data	$2\omega_n^{(3)}$	$2\omega_n^{(3)}$	$2\omega_n^{(3)}$	$\bar{A}_{n_C}$	$\bar{A}_{n_D}$
$\bar{B}_b = 2.28 \times 10^{-3}$ m = n = 3 $\omega_3^{(2)}/\omega_3^{(3)} = 0.973$	Experiments	-	0.493	0.463	0.008	0.006
	Theory	-	0.497	0.482	0.009	0.005
$\bar{B}_b = 1.14 \times 10^{-3}$ m = n = 3 $\omega_3^{(2)}/\omega_3^{(3)} = 0.973$	Experiments	-	0.496	0.476	0.006	0.004
	Theory	-	0.496	0.484	0.008	0.003
$\bar{B}_b = 2.28 \times 10^{-3}$ m = n = 2 $\omega_2^{(2)}/\omega_2^{(3)} = 1.028$	Experiments	0.466	0.514	0.488	0.008	0.015
	Theory	0.488	0.515	0.512	0.007	0.009
$\bar{B}_b = 1.14 \times 10^{-3}$ m = n = 2 $\omega_2^{(2)}/\omega_2^{(3)} = 1.028$	Experiments	0.477	0.514	0.506	0.005	0.009
	Theory	0.492	0.515	0.513	0.004	0.005
$\bar{B}_b = 2.28 \times 10^{-3}$ m = n = 3 $\omega_3^{(2)}/\omega_3^{(3)} = 1.028$	Experiments	0.459	0.506	0.476	0.005	0.008
	Theory	0.484	0.516	0.510	0.004	0.005
$\bar{B}_b = 1.14 \times 10^{-3}$ m = n = 3 $\omega_3^{(2)}/\omega_3^{(3)} = 1.028$	Experiments	0.468	0.510	0.490	0.003	0.005
	Theory	0.490	0.515	0.513	0.002	0.003

CHAPTER VII

DISCUSSION OF THE RESULTS AND CONCLUSIONS

A study has been made of the conditions under which planar forced vibrations of a long slender elastic rod become unstable when disturbed in a nonplanar direction. Two specific problems are presented; they are the parametrically excited fixed-free rod undergoing planar subharmonic oscillations and the transversely forced fixed-free rod responding harmonically in the plane. In both cases we have shown that nonplanar motion is parametrically coupled to the planar response under certain circumstances. Although only one pair of end conditions has been mentioned, other forms of support can be accommodated in a similar manner.

There is apparently no study in the literature of the stability to nonplanar perturbations of a system which is executing parametrically induced plane subharmonic vibrations. In this sense, the present study of the axially excited rod is unique. The transversely excited elastic string analysis as presented by Murthy and Ramakrishna [15] is similar in many respects to our transversely excited elastic rod study. However, it is possible in our analysis to generate several quantitatively different responses by varying the natural frequency ratio for motions in the two principal planes.

Three nonlinear partial differential equation of motion are derived and they are reduced to a pair of nonlinear coupled ordinary ones by the use of Galerkin's approximate method. We show that a nonlinear approach

is necessary to the correct formulation of the problem since the essential coupling between planar and nonplanar motions exists only in the nonlinear terms of the differential equations. The response equations for plane motion are derived and the "variational method" is employed to test the stability of the assumed planar response to a small nonplanar disturbance.

The central issue is the result of the stability analysis. In both cases, the analysis shows that there are values of the base excitation amplitude and the driving frequency for which the plane subharmonic (in the case of the axially excited rod) solution and the plane harmonic (in the direct excitation case) solution are unstable when disturbed in a nonplanar manner.

As the exciting frequency of the axially forced rod is slowly increased from zero, the plane steady-state solution is stable until a critical frequency value is reached. At this frequency, an upward amplitude jump occurs and the plane of the response simultaneously changes by ninety degrees. For frequencies higher than the critical value, the plane solution is stable until the originally straight configuration is reached once more. When frequency is decreased, the plane response remains stable until the critical frequency is reached; then a downward amplitude jump takes place and the response plane again changes by ninety degrees. For lower than critical value frequencies, the plane solution remains stable until damping causes a return to the straight configuration.

Only when the natural frequency ratio is near unity does the amplitude jump and accompanying plane change occur both for increasing and decreasing frequency. The effect of increasing the detuning is to cause the response curves for plane motion to become more widely separated in

frequency. For large enough detuning, the jump from motion in one plane to motion in a perpendicular plane is eliminated. We have shown that if the detuning is sufficiently large and damping is considered, the two perpendicular plane motions can be separated by a region in which the straight configuration is stable.

When $m = n$ and $\omega_m^{(2)} = \omega_n^{(3)}$, the planar response is stable over the whole frequency range provided that damping, no matter how small, is considered. The writer suggests that this result has application to the problem of the vertical excitation of an upright, rigid, right circular cylindrical tank filled with a liquid. As mentioned in Chapter I, page 5, Dodge, Kana, and Abramson report that their experiments show no time-dependent rotation of the plane of the liquid motion, even for large amplitude sloshing. They did, however, observe the plane rotation when the tank was excited in a transverse direction. These results are similar to the ones we have obtained for the axially and transversely excited rods. It is conceivable that the plane shift and amplitude jump analogous to that obtained for the axially excited rod when $\omega_m^{(2)} \neq \omega_m^{(3)}$ could occur in an axially excited fluid tank having a nearly circular cross-section with unequal major and minor axes.

We show also that when $\omega_m^{(2)} \neq \omega_m^{(3)}$ a "whirling motion" of the rod can exist only at a single discrete value of the exciting frequency. This is tantamount to saying that the "whirling motion" does not occur for the axially excited rod since the discrete frequency value can never be precisely achieved in practice.

When the rod is driven transversely, the stability analysis leads us to the result that there are values of the driving frequency which

cause plane motion to be unstable. This holds true even when $m = n$ and $\omega_m^{(2)} = \omega_n^{(3)}$ and damping is present. For the $\omega_m^{(2)} = \omega_m^{(3)}$ case, plane motion remains stable as frequency is increased from zero until a critical frequency is reached. At this frequency an upward amplitude jump occurs and the planar response no longer is stable with respect to nonplanar disturbances. Upon increasing frequency further, stable plane motions return when a second critical frequency value is reached. When frequency is decreased, plane motions again become unstable when the abovementioned second critical frequency is reached. As the frequency is lowered further, plane motion remains unstable until a downward amplitude jump due to damping takes place and the stable planar response returns.

The effect of detuning the in-plane and out-of-plane natural frequencies is to shift the zone of instability for plane motion relative to the response curves. This effect is shown in Figures 14 and 15. The detuning can be large enough to cause the complete disappearance of the nonplanar motion when a small amount of damping is included in the analysis.

Damping is incorporated in the analysis by inserting a term proportional to velocity into the differential equations of motion. The effect on both problems is to limit the otherwise theoretically infinite response amplitudes and to decrease the region of planar instability. That is, damping has a stabilizing effect for this problem. The abovementioned damping model proved inadequate for predicting the planar response amplitudes for the axially excited rod.

The experiments show that the theory qualitatively predicts the correct rod response in both cases. However, a significant difference exists between theoretical and experimental amplitudes for the axially

excited rod. This discrepancy can not be accounted for by the addition to the theory of a damping term proportional to velocity. The laboratory results suggest that a nonlinear damping term might better the agreement between theory and experiments. For the transversely excited rod, the linear damping hypothesis shows good agreement between theoretical and experimental amplitudes. Critical frequencies are closely predicted by the theory for both cases.

It is possible that the use of more than a single term in the Galerkin approximation might lead to better agreement with the experiments for the axially excited rod. The higher order approximation, of course, leads to a more complicated algebraic system and conclusions would doubtlessly be difficult to make.

APPENDICES

APPENDIX A

DERIVATION OF THE SIMPLIFIED CURVATURE EXPRESSION AND SIMPLIFICATION OF THE BENDING POTENTIAL ENERGY FORMULA

In the first part of this appendix, the procedure for converting the curvature expression in Eulerian or spatial coordinates to an approximate formula using Lagrangian or material coordinates is shown. The Eulerian curvature expression (using the summation convention) is

$$\kappa(s,t) = \left[\frac{\partial^2 x_i(s,t)}{\partial s^2}\,\frac{\partial^2 x_i(s,t)}{\partial s^2}\right]^{\frac{1}{2}}, \quad i = 1,2,3 . \qquad \text{(A-1)}$$

We begin by changing the independent variables from the coordinates of the deformed configuration (s,t) to the coordinates of the undeformed configuration (S,t). The chain rule shows that

$$\frac{\partial x_i}{\partial S} = \frac{\partial x_i}{\partial s}\,\frac{\partial s}{\partial S} ,$$

and

$$\frac{\partial^2 x_i}{\partial S^2} = \frac{\partial^2 s}{\partial S^2}\,\frac{\partial x_i}{\partial s} + \left(\frac{\partial s}{\partial S}\right)^2 \frac{\partial^2 x_i}{\partial s^2} .$$

After some algebraic manipulation, the latter two equations yield

$$\frac{\partial x_i}{\partial s} = \left(\frac{\partial s}{\partial S}\right)^{-1} \frac{\partial x_i}{\partial S} \qquad \text{(A-2)}$$

$$\frac{\partial^2 x_i}{\partial s^2} = \left(\frac{\partial s}{\partial S}\right)^{-2} \frac{\partial^2 x_i}{\partial S^2} - \left(\frac{\partial s}{\partial S}\right)^{-3} \frac{\partial^2 s}{\partial S^2}\,\frac{\partial x_i}{\partial S}, \quad i = 1,2,3. \qquad \text{(A-3)}$$

The quantities $\frac{\partial s}{\partial S}$ and $\frac{\partial^2 s}{\partial S^2}$ can be calculated from the definition of extensional strain

$$\epsilon(S,t) = \frac{1}{2}\frac{ds^2 - dS^2}{dS^2} . \qquad (A\text{-}4)$$

Definition (A-4) gives

$$\frac{\partial s}{\partial S} = [1 + 2\epsilon(S,t)]^{\frac{1}{2}} . \qquad (A\text{-}5)$$

Hence,

$$\frac{\partial^2 s}{\partial S^2} = \frac{\partial \epsilon}{\partial S}[1 + 2\epsilon(S,t)]^{-\frac{1}{2}} . \qquad (A\text{-}6)$$

Using equations (A-5) and (A-6) in equations (A-2) and (A-3), we find that

$$\frac{\partial x_i}{\partial s} = [1 + 2\epsilon(S,t)]^{-\frac{1}{2}}\frac{\partial x_i}{\partial S}$$

and

$$\frac{\partial^2 x_i}{\partial s^2} = [1 + 2\epsilon(S,t)]^{-1}\frac{\partial^2 x_i}{\partial S^2} - [1 + 2\epsilon(S,t)]^{-2}\frac{\partial \epsilon}{\partial S}\frac{\partial x_i}{\partial S} . \qquad (A\text{-}7)$$

The coordinates x_1, x_2, x_3 can be changed to displacement components by noting that

$$\left.\begin{aligned} x_1(S,t) &= S + u(S,t) \\ x_2(S,t) &= v(S,t) \\ x_3(S,t) &= w(S,t) . \end{aligned}\right\} \qquad (A\text{-}8)$$

Furthermore, it can be shown that the expression for $\varepsilon(S,t)$ in terms of displacement components is [24]

$$\varepsilon(S,t) = u' + \frac{1}{2}(v'^2 + w'^2 + u'^2) \quad . \tag{A-9}$$

The final result is obtained by differentiating equation (A-8) and (A-9) a suitable number of times and by substituting the results, along with equation (A-7), into equation (A-1). The resulting curvature expression in terms of displacement components with S as an independent variable is

$$\begin{aligned}\kappa(S,t) = [(1+u')^2+v'^2+w'^2]^{-2}\Big[\Big\{[(1+u')^2+v'^2+w'^2]u'' \\ - \frac{1+u'}{2}\frac{\partial}{\partial S}[(1+u')^2+v'^2+w'^2]\Big\}^2 + \Big\{[(1+u')^2+v'^2+w'^2]v'' \\ - \frac{v'}{2}\frac{\partial}{\partial S}[(1+u')^2+v'^2+w'^2]\Big\}^2 + \Big\{[(1+u')^2+v'^2+w'^2]w'' \\ - \frac{w'}{2}\frac{\partial}{\partial S}[(1+u')^2+v'^2+w'^2]\Big\}^2\Big]^{\frac{1}{2}} \quad .\end{aligned} \tag{A-10}$$

An alternate form for equation (A-10) is

$$\begin{aligned}\kappa(S,t) = (1+2\varepsilon)^{-2}\Big\{\Big[(1+2\varepsilon)u'' - \frac{1+u'}{2}\frac{\partial}{\partial S}(1+2\varepsilon)\Big]^2 \\ + \Big[(1+2\varepsilon)v'' - \frac{v'}{2}\frac{\partial}{\partial S}(1+2\varepsilon)\Big]^2 \\ + \Big[(1+2\varepsilon)w'' - \frac{w'}{2}\frac{\partial}{\partial S}(1+2\varepsilon)\Big]^2\Big\}^{\frac{1}{2}} \quad .\end{aligned} \tag{A-11}$$

In the second part of this appendix, we present the steps which allow the bending potential energy expression

$$V_b(t) = \frac{1}{2}\int_0^{\ell} EI_{\eta}(S,t)\kappa^2(S,t)dS \tag{A-12}$$

to be approximated by

$$V_b(t) \doteq \frac{1}{2} \int_0^{\ell} E[I_3 v''^2(S,t) + I_2 w''^2(S,t)]dS \ . \qquad \text{(A-13)}$$

Figure 18 defines the angle ψ and shows the location of the bending axis η.

Making use of the fact that χ_2 and χ_3 are principal axes of inertia, the well-known transformation equation for moments of inertia is

$$I_\eta(S,t) = I_2 \sin^2\psi(S,t) + I_3 \cos^2\psi(S,t) \ . \qquad \text{(A-14)}$$

Now angle $\psi(S,t)$ can be determined by taking the dot product of the unit vector $\bar{j}$ at point S with the unit normal vector $\bar{n}$ at point S. The unit tangent vector $\bar{t}$ in Eulerian coordinates is

$$\bar{t} = \frac{\partial x_1}{\partial s}\,\bar{i} + \frac{\partial x_2}{\partial s}\,\bar{j} + \frac{\partial x_3}{\partial s}\,\bar{k} \ , \qquad \text{(A-15)}$$

and the unit normal vector $\bar{n}$ is

$$\bar{n} = \frac{1}{\kappa}\frac{\partial \bar{t}}{\partial s} = \frac{1}{\kappa}\left(\frac{\partial^2 x_1}{\partial s^2}\,\bar{i} + \frac{\partial^2 x_2}{\partial s^2}\,\bar{j} + \frac{\partial^2 x_3}{\partial s^2}\,\bar{k}\right) \ . \qquad \text{(A-16)}$$

Hence,

$$\cos\psi = \bar{n}\cdot\bar{j} = \frac{1}{\kappa}\frac{\partial^2 x_2}{\partial s^2} \ . \qquad \text{(A-17)}$$

By using equations (A-8) and (A-9) in the second of equations (A-3), it can be shown that

$$\frac{\partial^2 x_2}{\partial s^2} = (1+2\varepsilon)^{-2}\left[(1+2\varepsilon)v'' - v'\frac{\partial \varepsilon}{\partial S}\right] \ . \qquad \text{(A-18)}$$

Therefore,

$$\cos\psi = \frac{1}{\kappa}(1+2\varepsilon)^{-2}\left[(1+2\varepsilon)v'' - v'\frac{\partial \varepsilon}{\partial S}\right] , \qquad \text{(A-19)}$$

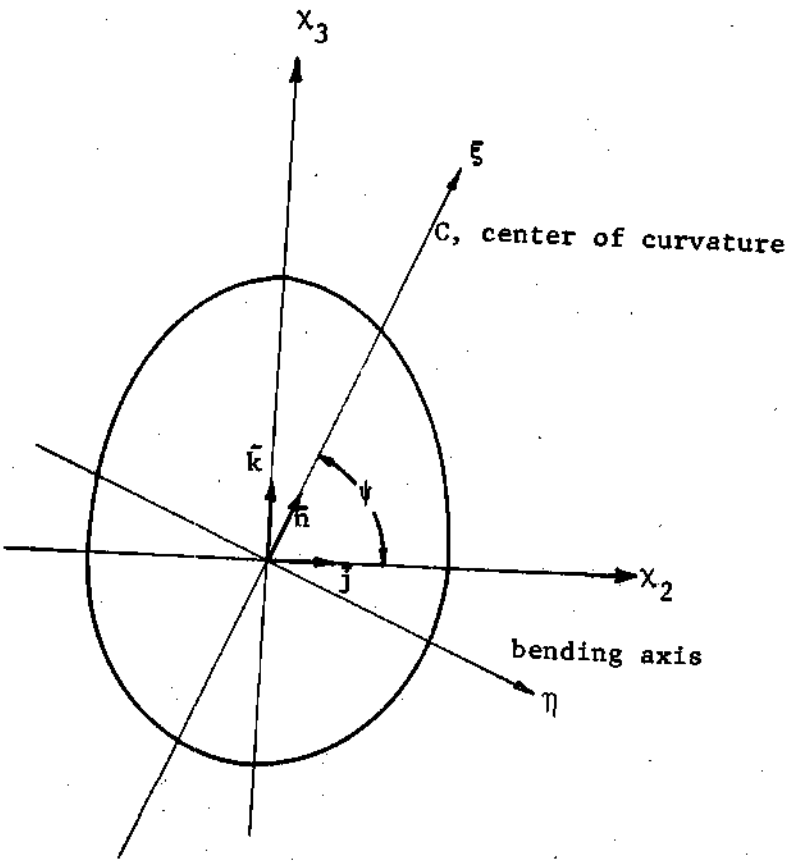

Figure 18. Location of Angle ψ and Axis η.

and the curvature κ is given by equation (A-11).

In order to simplify equation (A-19), we make use of the same approximations which where used in Chapter II to simplify the curvature formula. These are

$$\left.\begin{aligned} &|\epsilon(S,t)| \ll \tfrac{1}{2} \\ &\frac{\partial \epsilon(S,t)}{\partial S} \doteq 0 \\ &|u'(S,t)| \ll \tfrac{1}{2} \end{aligned}\right\} \qquad \text{for } 0 \le S \le \ell \text{ and } t \ge 0 . \qquad \text{(A-20)}$$

The first and second of equations (A-20) reduce equation (A-19) to

$$\cos \psi \doteq \frac{v''}{\kappa} .$$

Making use of the simplified curvature expression from Chapter II, we find

$$\cos \psi \doteq \frac{v''}{(v''^2+w''^2)^{\frac{1}{2}}} . \qquad \text{(A-21)}$$

The approximate bending potential energy formula can now be determined by applying equation (A-21) to equation (A-14) and the result to equation (A-12). The formula is

$$V_b(t) \doteq \frac{1}{2}\int_0^{\ell} E[I_2 w''^2(S,t) + I_3 v''^2(S,t)]dS . \qquad \text{(A-22)}$$

APPENDIX B

VALUES OF THE INTEGRALS WHICH RESULT FROM APPLYING THE GALERKIN METHOD

The following integrals appear in the text in Chapter III, page 17 and are evaluated using the integrals calculated by Young and Felgar [25]:

$$\alpha = M \int_o^{\ell} X_j^2(S)dS = M\ell \tag{B-1}$$

$$\beta_j^{(i)} = \int_o^{\ell} [EI_i X_j(S)X_j''''(S)dS \ , \quad \begin{matrix} i=2,\ j=m \\ \text{or} \\ i=3,\ j=n \end{matrix}$$

$$= EI_i \beta_j^4 \ell \tag{B-2}$$

$$\gamma_j = \int_o^{\ell} [MX_j(S)X_j'(S) - M(\ell-S)X_j(S)X_j''(S)]dS \ , \quad j=m,n$$

$$= 2M - \frac{1}{2} M\ell\varphi_j\beta_j(2-\varphi_j\beta_j\ell) \ . \tag{B-3}$$

The following integrals are calculated by numerical integration (Simpson's Rule) on the digital computer. Some results are tabulated in Tables 4 and 5.

$$\Delta_{ij} = \int_o^{\ell} \left[M\int_o^s X_j'^2(\xi)d\xi\right] X_i(S)X_i'(S)dS$$

$$- \int_o^{\ell} \left\{M\int_s^{\ell} [X_j'^2(\eta)d\eta]d\xi\right\} X_i(s)X_i''(S)dS \ , \quad j=m,n \ . \tag{B-4}$$

$$\delta_j = \int_o^{\ell} \left[M \int_o^s X_j'^2(\xi) d\xi \right] X_j(S) X_j'(S) dS$$

$$- \int_o^{\ell} \left\{ M \int_s^{\ell} \left[\int_o^{\xi} X_j'^2(\eta) d\eta \right] d\xi \right\} X_j(S) X_j''(S) dS \ , \quad j=m,n \ . \qquad \text{(B-5)}$$

It is convenient to form the dimensionless numbers

$$c_n = \frac{\delta_n \ell^2}{\alpha}$$

$$c_{mn} = \frac{\Delta_{mn} \ell^2}{\alpha}$$

and tabulate these rather than δ_n and Δ_{mn}.

Table 4. Values of b_n and c_n.

n	b_n	c_n
1	6.28	4.60
2	34.6	145
3	99.8	998

$$b_n = \frac{4\gamma_n \ell}{\alpha}$$

$$c_n = \frac{\delta_n \ell^2}{\alpha}$$

Table 5. Values of c_{mn}

m	n	c_{mn}
1	2	25.2
1	3	66.7
2	3	369

$$c_{mn} = \frac{\Delta_{mn} \ell^2}{\alpha}$$

Note: It can be shown that $c_{mn} = c_{nm}$.

APPENDIX C

A SUMMARY OF THE RITZ AVERAGING METHOD

The Ritz averaging method is identical to the Galerkin method. However, the latter is most generally used to solve static boundary value problems or, if the problem is represented by a partial differential equation with time and space as independent variables, it is used on only the space variable. The Ritz averaging method is used to determine an approximate solution for steady-state vibration problems. Both methods are useful for obtaining approximate quantitative information about problems governed by nonlinear differential equations.

Suppose the differential equation is

$$N[q(t)] = 0 \ , \qquad \text{(C-1)}$$

where N is a differential operator (not necessarily linear), t is the independent variable, and q is the dependent variable for which an approximate solution is sought. According to the Ritz averaging method, a set (not necessarily orthogonal) of coordinate functions $\psi_i(t)$ is selected and the approximate solution $\bar{q}(t)$ is represented by a linear combination of a finite number of these coordinate functions. That is

$$\bar{q}(t) = \sum_{i=1}^{n} a_i \psi_i(t) \ . \qquad \text{(C-2)}$$

The constants a_i are determined from the following set of algebraic equations:

$$\int_{t_o}^{t_1} N[\bar{q}(t)]\psi_i(t)dt = 0 , \quad i = 1, 2, \ldots, n . \tag{C-3}$$

The integration (or averaging) is usually taken over one period of the oscillation.

In this thesis, only one term approximations are used. Since our problem is close to a linear problem, we select an approximation of the form $\bar{q}(t) = A \cos (t-\theta)$, where A and θ are constants to be determined. An equivalent form for this approximation (and the one which is actually used) is

$$\bar{q}(t) = B \cos t + C \sin t , \tag{C-4}$$

where B and C are the constants to be determined.

Using the Ritz averaging conditions (C-3), we find the following:

$$\int_{o}^{2\pi} N[\bar{q}(t)]\cos t \, dt = 0$$

$$\int_{o}^{2\pi} N[\bar{q}(t)]\sin t \, dt = 0 . \tag{C-5}$$

These furnish two algebraic equations (which may be nonlinear and coupled) for the determination of B and C.

An advantage of both the Ritz averaging method and the Galerkin method is that is is only necessary to know the differential equation; one need not know a corresponding variational expression as is required in the Rayleigh-Ritz method. A more complete discussion of the Ritz averaging method and related methods is given by Klotter [27]. The reader is also referred to a comprehensive discussion by Finlayson and Scriven [31].

APPENDIX D

ADDITION OF DAMPING

Our purpose in this appendix is to indicate the qualitative effect of damping on the response curves and the stability zones for nonplanar disturbances. That we must limit our attention only to qualitative damping effects is dictated by the fact that there is currently no direct systematic method by which the complex subject of energy dissipation in engineering structures can be studied.

There are at least three different sources of damping effects in this rod problem. There is the dissipation of energy due to internal friction, the resistance imparted by the surrounding air to the motion of the rod through it, and the external loss of energy due to relative motion between the rod and its support system. In short, a meaningful mathematical model of damping for this system is difficult to construct. However, some particular trends can be found by adding certain suitable terms to the equations of motion for the undamped problem and then by making adjustments based on experimental data to these terms so that the theoretical result shows acceptable agreement with the experiments. We proceed with this indirect method.

The Axially Excited Rod

Assume that damping forces are directly proportional to velocity. Then the equations of motion for the axially excited rod (equations (3-4) and (3-5)) take the form

$$\alpha\ddot{T}_{2n} + 2\epsilon_n \dot{T}_{2n} + (\beta_n^{(3)} + \gamma_n A_b \omega^2 \cos\omega t)T_{2n}$$

$$+ \delta_n T_{2n}(T_{2n}\ddot{T}_{2n} + \dot{T}_{2n}^2) + \Delta_{nm} T_{2n}(T_{3m}\ddot{T}_{3m} + \dot{T}_{3m}^2) = 0 \qquad \text{(D-1)}$$

$$\alpha\ddot{T}_{3m} + 2\epsilon_m \dot{T}_{3m} + (\beta_m^{(2)} + \gamma_m A_b \omega^2 \cos\omega t)T_{3m}$$

$$+ \delta_m T_{3m}(T_{3m}\ddot{T}_{3m} + \dot{T}_{3m}^2) + \Delta_{mn} T_{3n}(T_{2n}\ddot{T}_{2n} + \dot{T}_{2n}^2) = 0 \ . \qquad \text{(D-2)}$$

Introducing dimensionless time $\tau = \frac{\omega t}{2}$ and setting $T_{3m}(\tau) \equiv 0$ gives the equation which governs the planar response of the rod:

$$T''_{2n} + \frac{4\epsilon_n}{\alpha\omega} T'_{2n} + \left(\frac{4\beta_n^{(3)}}{\alpha\omega^2} + \frac{4\gamma_n A_b}{\alpha} \cos 2\tau\right)T_{2n}$$

$$+ \frac{\delta_n}{\alpha} T_{2n}(T_{2n}T''_{2n} + T'^2_{2n}) = 0 \ . \qquad \text{(D-3)}$$

We introduce the previously used dimensionless quantities along with the dimensionless number

$$\frac{f_n}{\omega} = \frac{4\epsilon_n}{\alpha\omega} \qquad \text{(D-4)}$$

to get

$$T''_{2n} + \frac{f_n}{\omega} T'_{2n} + \left[\frac{\left(2\omega_n^{(3)}\right)^2}{\omega^2} + b_n \bar{A}_b \cos 2\tau\right]T_{2n}$$

$$+ c_n T_{2n}(T_{2n}T''_{2n} + T'^2_{2n}) = 0 \ . \qquad \text{(D-5)}$$

The Ritz averaging method, using the solution form (4-1), gives the algebraic equations of the damped planar response:

$$\left[\bar{A}_n^2 - \frac{2}{c_n}\left(\frac{\left(2\omega_n^{(3)}\right)^2}{\omega^2} - 1 - \frac{b_n\bar{A}_b}{2}\right)\right]\bar{A}_{1n} + \frac{2f_n}{c_n\omega}\bar{A}_{2n} = 0 \qquad \text{(D-6)}$$

$$-\frac{2f_n}{c_n\omega}\bar{A}_{1n} + \left[\bar{A}_n^2 - \frac{2}{c_n}\left(\frac{\left(2\omega_n^{(3)}\right)^2}{\omega^2} - 1 + \frac{b_n\bar{A}_b}{2}\right)\right]\bar{A}_{2n} = 0 \,. \qquad \text{(D-7)}$$

Elimination of $\bar{A}_{1n}$ and $\bar{A}_{2n}$ from equations (D-6) and (D-7) shows that the amplitude-frequency relation is

$$\frac{\omega^4}{\left(2\omega_n^{(3)}\right)^4} - \frac{\left[4\left(c_n\bar{A}_n^2 + 2 - \frac{f_n^2}{\left(2\omega_n^{(3)}\right)^2}\right)\right]}{\left[c_n^2\bar{A}_n^4 + 4c_n\bar{A}_n^2 + 4 - b_n^2\bar{A}_b^2\right]}\frac{\omega^2}{\left(2\omega_n^{(3)}\right)^2} + \frac{4}{c_n^2\bar{A}_n^4 + 4c_n\bar{A}_n^2 + 4 - b_n^2\bar{A}_b^2} = 0 \,. \qquad \text{(D-8)}$$

For small values of $\left(\frac{f_n}{2\omega_n^{(3)}}\right)^2$ and for small values of $\bar{A}_n$, the effect of damping on the response curves is small if handled in the above manner. To see that this is true, we solve equation (D-8) for $\frac{\omega^2}{\left(2\omega_n^{(3)}\right)^2}$ and find that

$$\frac{\omega^2}{\left(2\omega_n^{(3)}\right)^2} = \frac{2\left(c_n\bar{A}_n^2 + 2 - \frac{f_n^2}{\left(2\omega_n^{(3)}\right)^2}\right) \pm 2\sqrt{b_n^2\bar{A}_b^2 - \frac{2f_n^2}{\left(2\omega_n^{(3)}\right)^2}c_n\bar{A}_n^2 + 2 - \frac{f_n^2}{2\left(2\omega_n^{(3)}\right)^2}}}{c_n^2\bar{A}_n^4 + 4c_n\bar{A}_n^2 + 4 - b_n^2\bar{A}_b^2} \qquad \text{(D-9)}$$

For the rods used in this study, the dimensionless parameters are in the ranges

$$10^{-5} < \left(\frac{f_n}{2\omega_n^{(3)}}\right)^2 < 10^{-4}$$

$$0 \leq c_n \bar{A}_n^2 < 1$$

$$10^{-2} < (b_n \bar{A}_b)^2 < 10^{-1} .$$

Then, by referring to the numerator of the right-hand side of equation (D-9), one sees that damping has little effect on the response provided the parameters are in the intervals listed above.

For large values of $\bar{A}_n$, damping has an important qualitative effect on the response relation (D-8); it causes the two formerly separate branches to become joined at high values of $\bar{A}_n$. The branches become joined when the discriminant of quadratic equation (D-8) is zero. That is, the branches come together when

$$\bar{A}_n^2 = \frac{1}{2c_n}\left[\frac{b_n^2\bar{A}_b^2 + \left(\frac{f_n}{2\omega_n^{(3)}}\right)^4 - 2\left(\frac{f_n}{2\omega_n^{(3)}}\right)^2}{\left(\frac{f_n}{2\omega_n^{(3)}}\right)^2}\right] . \qquad \text{(D-10)}$$

Therefore, linear viscous damping has little qualitative or quantitative effect on the response curves until $\bar{A}_n$ becomes large enough to be near the value given by equation (D-10). Equation (D-8) is shown in Figure 19.

Because the linear damping term has such a negligible effect on the response curves for small values of $\bar{A}_n$ and $\left(\frac{f_n}{2\omega_n^{(3)}}\right)^2$ and because the plane shift described in Chapter IV occurs for relatively low values of

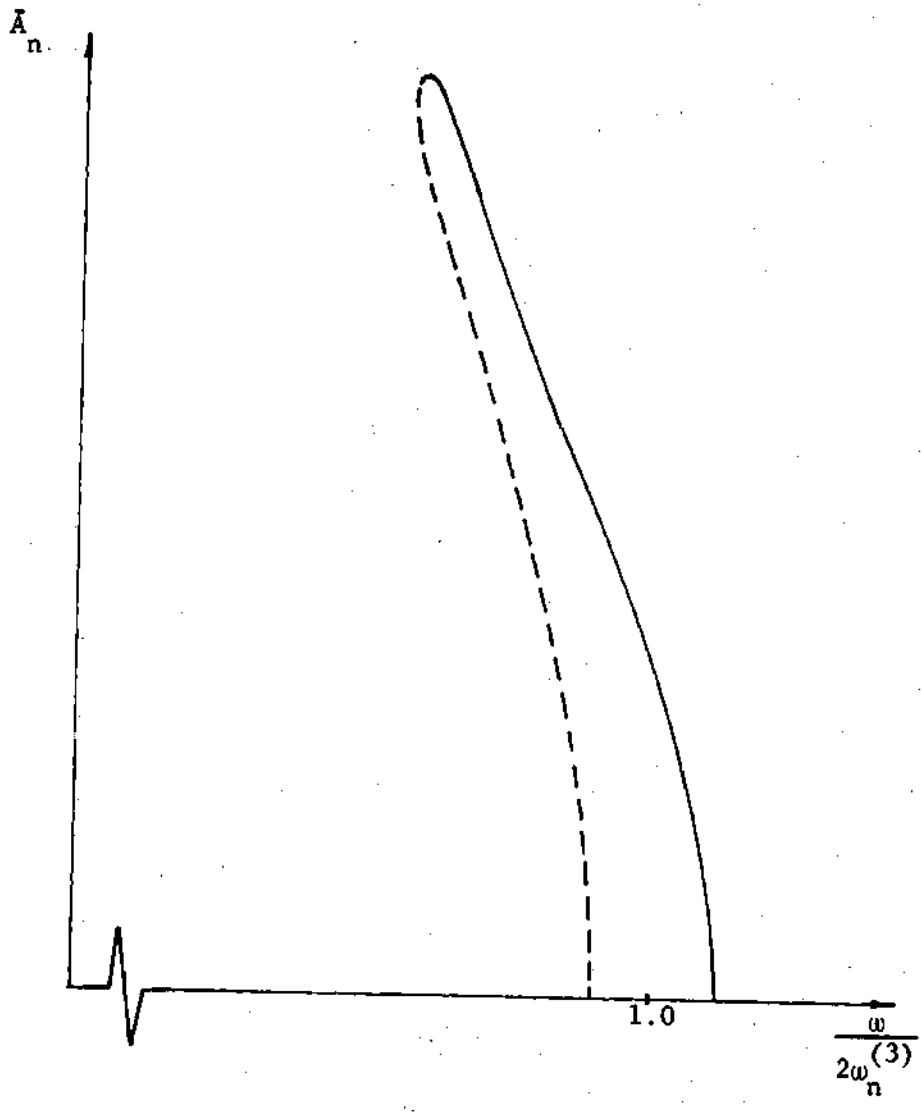

Figure 19. Effect of Damping on the Response Curves for the Axially Excited Rod.

$\bar{A}_n$ when $\frac{\omega_n^{(2)}}{\omega_n^{(3)}}$ is near unity, we do not include the damping term in the response equation. That is, we only include the effect of damping on the zones for which plane motion is unstable with respect to nonplanar disturbances.

To determine the equation of the boundaries of the instability zone, we follow Bolotin [10], Chapter 2, §8 and §9. The result of applying an analysis for stability of the planar response to nonplanar perturbations (see equation (4-24)) is

$$x''_{3m}(\tau) + \frac{f_n}{\omega} x'_{3m}(\tau) + \left[\frac{\left(2\omega_m^{(2)}\right)^2}{\omega^2} + (b_m \bar{A}_b - c_{mn}\bar{A}_n^2)\cos 2\tau\right] x_{3m}(\tau) = 0 \qquad \text{(D-11)}$$

where $x_{3m}(\tau)$ is a small disturbance in the x_3-direction. As is known from the theory of the Mathieu equation, solutions which correspond to points on the principal stability boundary have period $\frac{4\pi}{\omega}$, so we seek a solution to equation (D-11) in the form

$$x_{3m}(\tau) = \sum_{k=1,3,5,\ldots}^{\infty} (a_k \sin k\tau + b_k \cos k\tau) \; . \qquad \text{(D-12)}$$

Substituting this into equation (D-11) and equating coefficients of like terms in sin $k\tau$ and cos $k\tau$, we obtain an infinite system of homogeneous linear algebraic equations for the determination of the a_k and b_k. By setting the determinant of the coefficient matrix equal to zero, one finds an infinite determinant which describes the boundary. By keeping

only the k = 1 term we find that the boundary equations are approximated by

$$\frac{(\omega)^2}{\left(2\omega_m^{(2)}\right)^2} = \left[1 \pm \frac{\omega^4}{4\left(2\omega_m^{(2)}\right)^4}\left(b_m\bar{A}_b - c_{mn}\bar{A}_n^2\right)^2 - \left(\frac{\Delta_n}{\pi}\right)^2\right]^{\frac{1}{2}} \qquad \text{(D-13)}$$

where Δ_n is the logarithmic decrement defined by

$$\Delta_n = \frac{1}{T} \ln \frac{T_{2m}(\tau)}{T_{2m}(\tau+T)} .$$

T is the period of the steady state response.

In the elementary theory of vibrations, one shows that the logarithmic decrement Δ_n is related to the damping constant $2\epsilon_n$ approximately by

$$\Delta_n = \frac{2\pi\epsilon_n}{\alpha\omega_n^{(3)}} . \qquad \text{(D-14)}$$

A graph of equation (D-13) with $\Delta_n = 0.02$ and the other physical parameters given in Chapter IV is shown in Figure 20.

It is now apparent that the effect of damping is to shrink the regions of instability. There is, however, no fundamental qualitative difference in the manner in which the axially excited rod responds (except for the joining of the two branches of the response curve). The discussion in Chapter IV of how the rod reacts to increasing and decreasing excitation frequencies is still valid with damping included.

As a final observation on the effect of damping on the axially excited rod, we note that damping is responsible for causing the special case m = n, $\omega_n^{(3)} = \omega_m^{(2)}$ to execute stable plane motion for all values of ω.

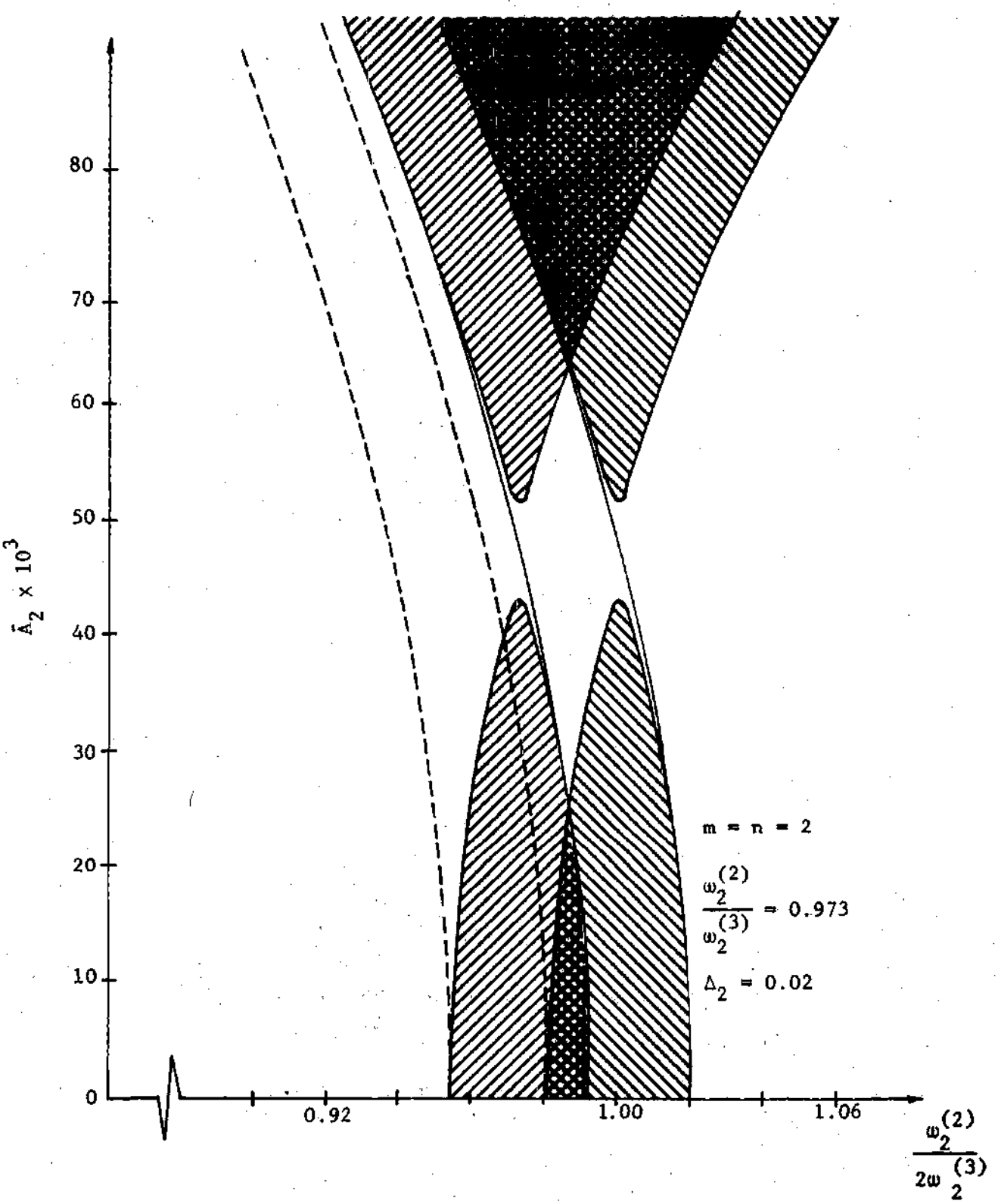

Figure 20. Effect of Damping on the Instability Region for the Axially Excited Rod.

This can be attributed to the fact that damping shrinks the size of the instability zones so that the response curves now lie entirely within the region which is stable with respect to nonplanar disturbances. The response curves and stability boundaries for this special case are shown in Figure 21.

We reemphasize that this mathematical model of damping which assumes that damping forces are proportional to velocity is useful only for determining qualitative trends in the case of the axially excited rod. It is inadequate for predicting the amplitude of the response for a given frequency; it is expecially inaccurate when amplitudes are large. Equation (D-10), for example, gives far greater values for the maximum response amplitude than can be obtained in the laboratory.

Evidence of the inadequacy of the linear damping model is that the logarithmic decrement when calculated by the formula

$$\Delta_n = \frac{1}{T} \ln \frac{T_{2m}(\tau)}{T_{2m}(\tau+T)}$$

proved to increase strongly with amplitude using data taken during the experimental phase of this research.

The Directly Excited Rod

The analysis for this case proceeds along the same lines as discussed for the axially excited rod. The damped equations of motion are (see equations (5-6) and (5-7)):

$$\alpha\ddot{T}_{2n} + 2\epsilon_n\dot{T}_{2n} + \beta_n^{(3)}T_{2n} + \delta_n(T_{2n}\ddot{T}_{2n}+\dot{T}_{2n}^2)T_{2n} + \Delta_{nm}(T_{3m}\ddot{T}_{3m}+\dot{T}_{3m}^2)T_{3m}$$

$$= \frac{2\omega^2 MB_b\varphi_n}{\beta_n}\cos\omega t \qquad \text{(D-15)}$$

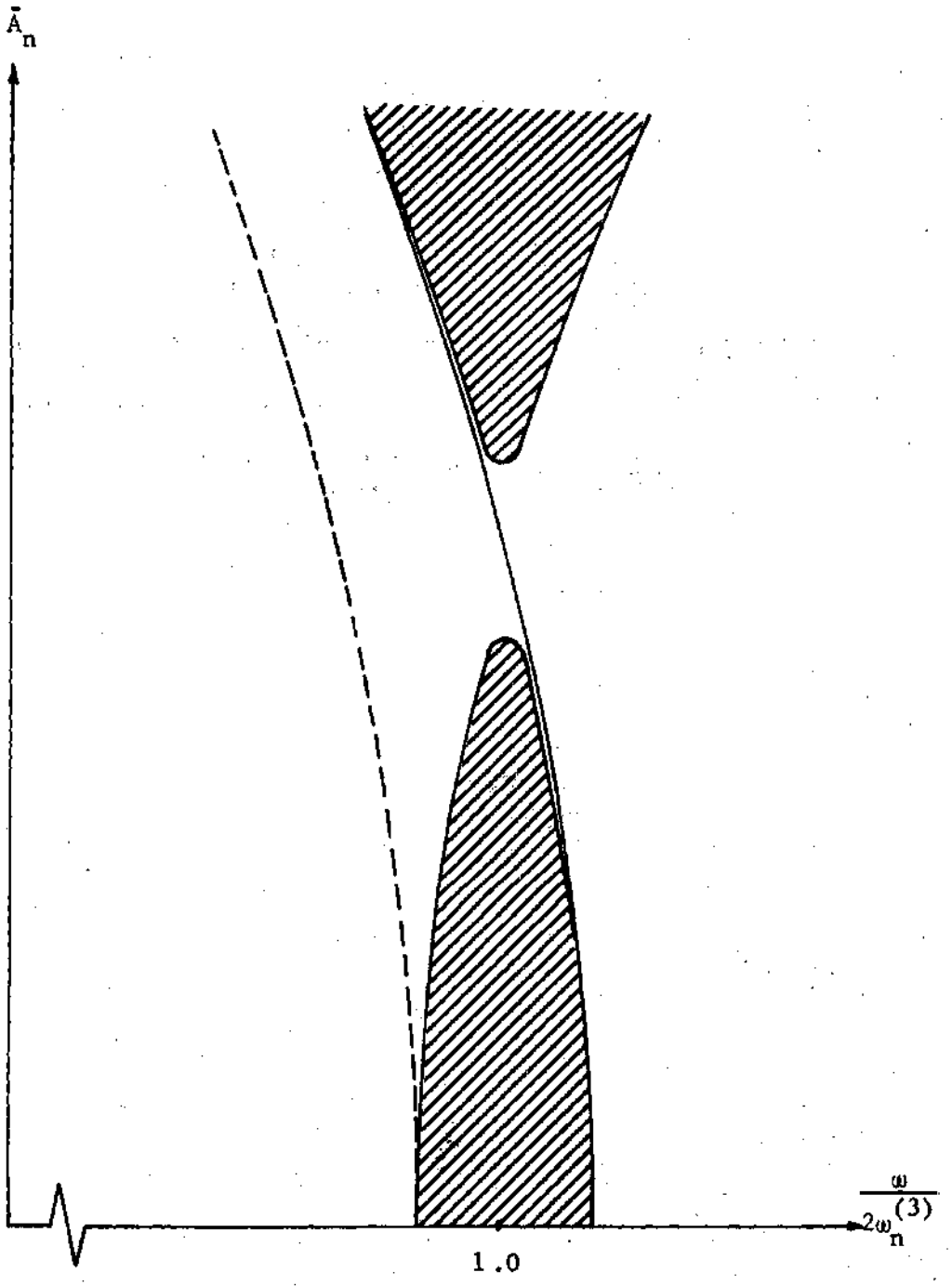

Figure 21. Effect of Damping on the Instability Region for the Axially Excited Rod When m = n and $\omega_n^{(3)} = \omega_m^{(2)}$.

$$\alpha\ddot{T}_{3m} + 2\epsilon_m\dot{T}_{3m} + \beta_m^{(2)}T_{3m} + \delta_m(T_{3m}\ddot{T}_{3m}+\dot{T}_{3m})T_{3m}$$

$$+ \Delta_{mn}(T_{2n}\ddot{T}_{2n}+\dot{T}_{2n}^2)T_{3m} = 0 \ . \qquad \text{(D-16)}$$

The Ritz averaging method using the assumed solution

$$T_{2n}(\tau) = A_{1n} \sin 2\tau + A_{2n} \cos 2\tau$$

$$T_{3m}(\tau) \equiv 0$$

shows that

$$\left[\frac{\left(2\omega_n^{(3)}\right)^2}{\omega^2} - 4 - 2c_n\bar{A}_n^2\right]\bar{A}_{1n} - \frac{2f_n}{\omega}\bar{A}_{2n} = 0 \qquad \text{(D-17)}$$

$$\frac{2f_n}{\omega}\bar{A}_{1n} + \left[\frac{\left(2\omega_n^{(3)}\right)^2}{\omega^2} - 4 - 2c_n\bar{A}_n^2\right]\bar{A}_{2n} = \frac{8\bar{B}_b\varphi_n}{\beta_n\ell} \ . \qquad \text{(D-18)}$$

Solving these for $\bar{A}_{1n}$ and $\bar{A}_{2n}$ and using the fact that $\bar{A}_n^2 = \bar{A}_{1n}^2+\bar{A}_{2n}^2$, we find the response curve for plane motion in the x_1,x_2-plane is given by

$$\left[c_n^2\bar{A}_n^6 + 4c_n\bar{A}_n^4 + 4\bar{A}_n^2 - \left(\frac{4\bar{B}_b\varphi_n}{\beta_n\ell}\right)^2\right]\frac{\omega^4}{\left(2\omega_n^{(3)}\right)^4}$$

$$- \bar{A}_n^2\left[c_n\bar{A}_n^2 + 2 - \frac{f_n^2}{\left(2\omega_n^{(3)}\right)^2}\right]\frac{\omega^2}{\left(2\omega_n^{(3)}\right)^2} + \frac{1}{4}\bar{A}_n^2 = 0 \ . \qquad \text{(D-19)}$$

It is worth noting that this equation is quite similar to the one found by Anand [33] in his analysis of the nonlinear string excited in transverse direction with viscous damping included.

Again we note that for small damping values and low response

amplitudes, the effect of damping on the response curves is small when it is assumed that the effect of damping is proportional to velocity. This becomes evident when equation (D-19) is solved for $\frac{\omega^2}{\left(2\omega_n^{(3)}\right)^2}$:

$$\frac{\omega^2}{\left(2\omega_n^{(3)}\right)^2} =$$

$$= \frac{\bar{A}_n^2\left(c_n\bar{A}_n^2 + 2 - \frac{f_n^2}{\left(2\omega_n^{(3)}\right)^2}\right) \pm \bar{A}_n\sqrt{\left(\frac{4\bar{B}_b\varphi_n}{\beta_n\ell}\right)^2 - \bar{A}_n^2\frac{2f_n^2}{\left(2\omega_n^{(3)}\right)^2}\left(c_n\bar{A}_n^2+2 - \frac{f_n^2}{2\left(2\omega_n^{(3)}\right)^2}\right)}}{2\left[c_n^2\bar{A}_n^6 + 4c_n\bar{A}_n^4 + 4\bar{A}_n^2 - \left(\frac{4\bar{\beta}_b b_n}{\beta_n\ell}\right)^2\right]}$$

(D-20)

For our study of the stability of the planar response, the dimensionless parameters have values in the ranges

$$10^{-5} < \frac{f_n^2}{\left(2\omega_n^{(3)}\right)^2} < 10^{-4}$$

$$0 \le \bar{A}_n < 3 \times 10^{-2} \quad \text{(for transition into the instability zone)}$$

$$2 \times 10^{-7} < \left(\frac{4\bar{B}_b\varphi_n}{\beta_n\ell}\right)^2 < 3 \times 10^{-6} .$$

For these values, the effect of damping on the response curves is slight; this can be seen from the numerator of the right-hand side of equation (D-20).

For larger values of $\bar{A}_n$, both the quantitative and qualitative effect of damping becomes significant. In fact, by setting the discriminant of equation (D-19) equal to zero, we see as before that the two

response curve branches join when the amplitude takes on the value

$$\bar{A}_n^2 = \frac{1}{c_n} - \left[1 + \frac{f_n^2}{4\left(2\omega_n^{(3)}\right)^2} + \sqrt{1 + c_n \frac{\left(2\omega_n^{(3)}\right)^2}{2f_n^2} \left(\frac{4\bar{B}_b \varphi_n}{\beta_n \ell}\right)^2 - \frac{f_n^2}{2\left(2\omega_n^{(3)}\right)^2} \left(1 - \frac{1}{8} \frac{f_n^2}{\left(2\omega_n^{(3)}\right)^2}\right)} \right] . \quad \text{(D-21)}$$

For the values of $\bar{B}_b$ used in the experiments, the response amplitudes are well below this peak value, hence damping has little effect on the response curves in our zone of interest. With this in mind, we have neglected damping from the portion of the analysis involving the response relation and have considered only its effect on the stability boundaries.

For the directly excited rod, the assumption that damping forces are proportional to velocity gives much closer quantitative agreement between theory and experiments than does the same assumption for the axially excited rod. In fact, response relation (D-20) models the actual laboratory data reasonably well even for large values of $\bar{A}_n$. Furthermore, the maximum amplitude predicted by equation (D-21) is only about 50% higher than the experimental maximum amplitude. No attempt was made to gain better agreement between theoretical response amplitudes and experimental response amplitudes for either the axially or directly excited rods since it is not our objective in this study to verify the response relations; our purpose here is to predict the stability of the planar response to nonplanar perturbations.

A procedure identical with the previously outlined one shows that

the equations for the stability boundaries are given by

$$\frac{\omega^2}{\left(2\omega_m^{(2)}\right)^2} = \frac{1 \pm \left[1 - \left(1 + \frac{\Delta_n^2}{\pi^2}\right)\left(1 - \frac{1}{4} c_{mn}^2 \bar{A}_n^4\right)\right]^{\frac{1}{2}}}{4\left(1 - \frac{1}{4} c_{mn}^2 \bar{A}_n^4\right)} . \qquad \text{(D-22)}$$

Figure 12 of Chapter V is repeated with this altered stability zone taken into account in Figure 22. Once again note that no new qualitative information appears and the discussion of the rod response given in Chapter V holds equally well for the damped case. One should observe however, that as the detuning increases (that is, when $\omega_m^{(2)}/\omega_m^{(3)}$ is not near unity) the presence of damping can cause the complete disappearance of the planar instability phenomenon. A situation of this kind is shown in Figure 23.

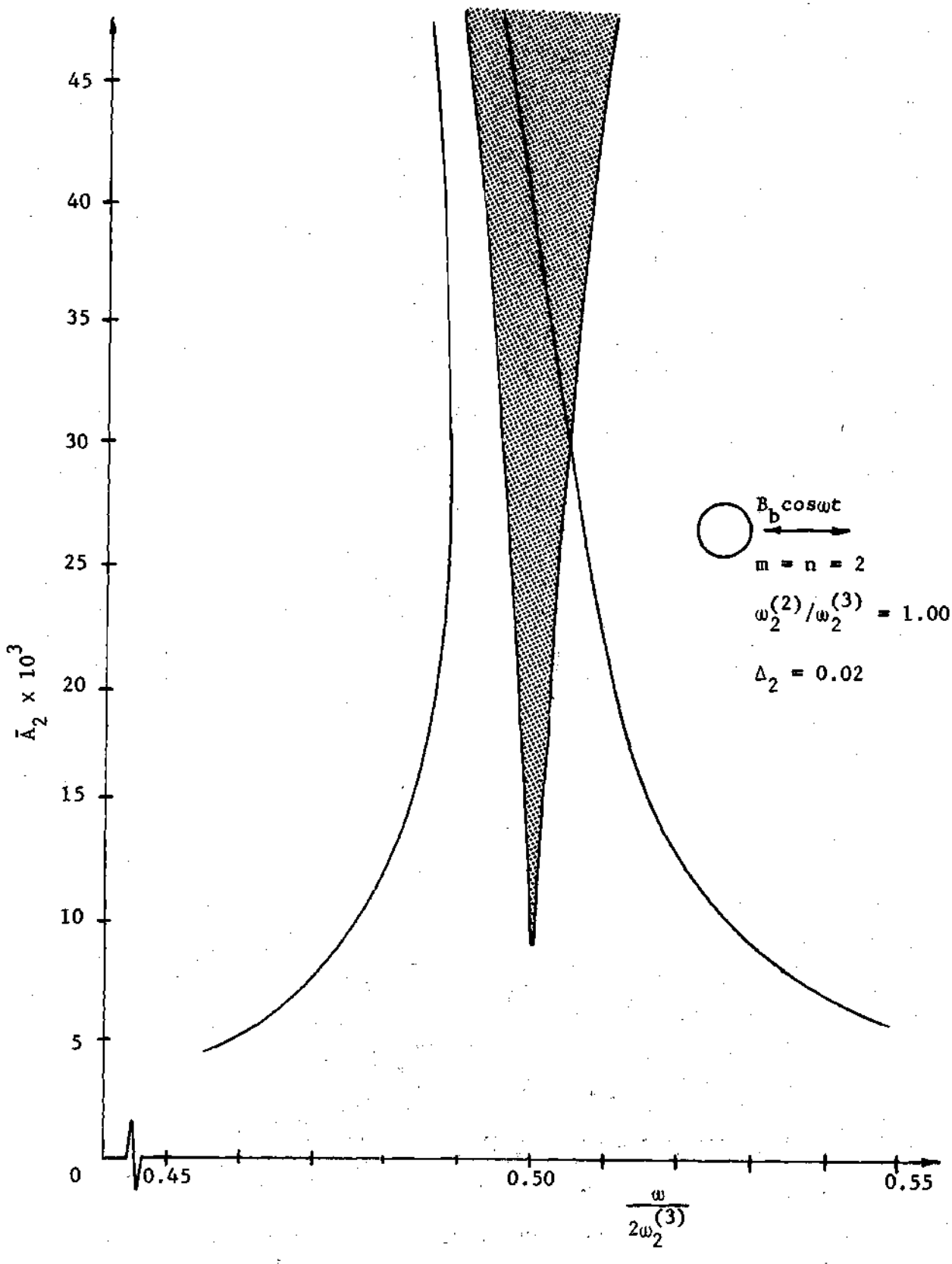

Figure 22. Effect of Damping on the Instability Region for the Transversely Excited Rod.

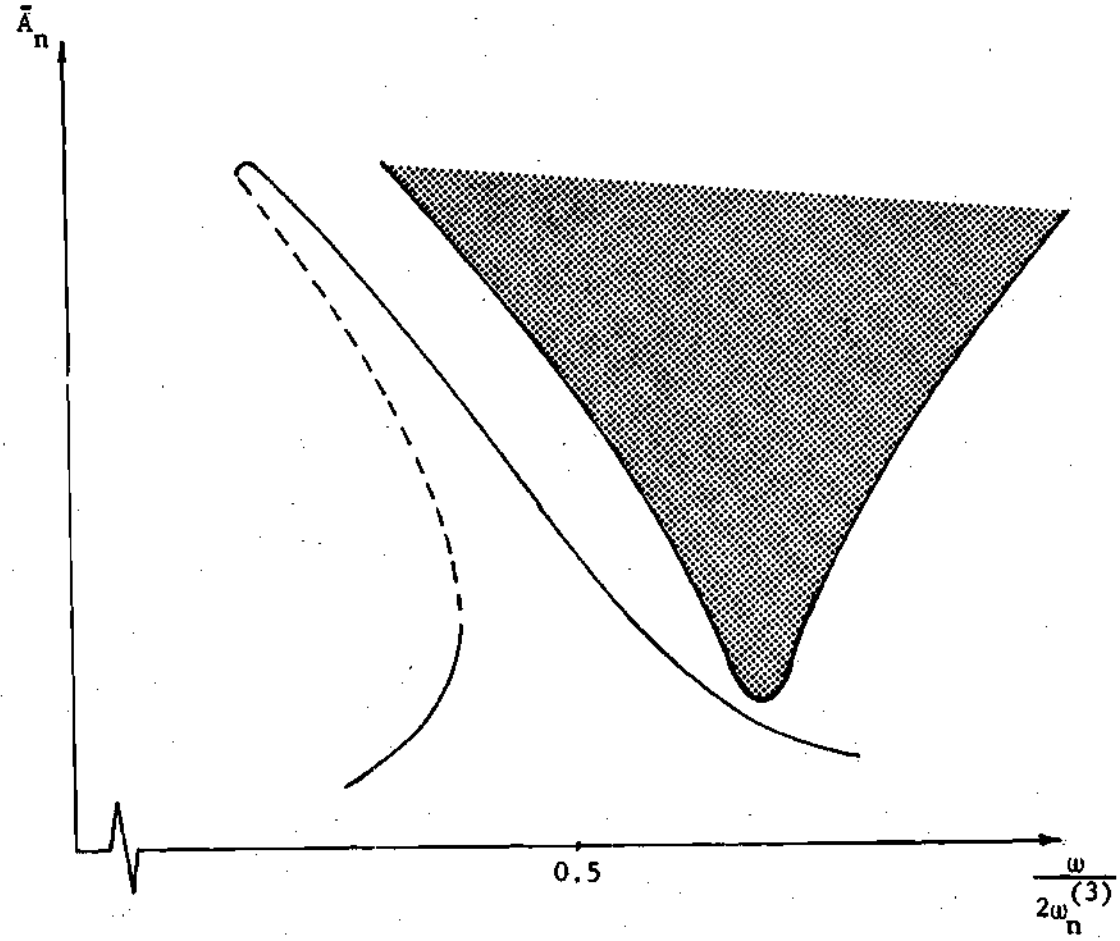

Figure 23. The Combined Effect of Large Detuning and Damping On the Instability Region for the Transversely Excited Rod.

LITERATURE CITED

1. J. J. Stoker, Nonlinear Vibrations, Interscience Publishers, New York, 1950.

2. Ye. A. Beylin and G. Yu. Dzhaneldize, "A Survey of Writings on the Dynamic Stability of Elastic Bodies," Prikladnaya Matematika i Mekhanika (Applied Mathematics and Mechanics), Vol. 16, 1952, pp. 635-648.

3. R. M. Evan-Iwanowski, "On the Parametric Response of Structures," Applied Mechanics Reviews, Vol. 18, No. 9, September 1965, pp. 699-702.

4. M. Faraday, "On a Peculiar Class of Acoustical Figures; and on Certain Forms Assumed by Groups of Particles Upon Vibrating Elastic Surfaces," Philosophical Transactions of the Royal Society, London, England, May, 1831, pp. 299-340.

5. F. Melde, "Über Erregung stehender Wellen eines faden-förmigen Körpers," Annalen der Physik und Chemie, Vol. 109, Series 2, 1859, pp. 193-215.

6. Lord Rayleigh, "On the Maintenence of Vibrations by Forces of Double Frequency, and on the Propagation of Waves Through a Medium Endowed With a Periodic Structure," The London, Edinburgh, and Dublin Philosophical Magazine and Journal of Science, Series 5, Vol. 24, 1887, pp. 145-159.

7. N. M. Beliaev, "Stability of Prismatic Rods Subject to Variable Longitudinal Forces," Collection of Engineering Construction and Structural Mechanics, Leningrad, Put', 1924.

8. S. Lubkin and J. J. Stoker, "Stability of Columns and Strings Under Periodically Varying Forces," Quarterly of Applied Mathematics, Vol. 1, July, 1943, pp. 215-236.

9. I. I. Gol'denblat, Contemporary Problems of Vibrations and Stability of Engineering Structures, Stroiizdat, Moscow, 1947.

10. V. V. Bolotin, The Dynamic Stability of Elastic Systems, Gostekhizdat, Moscow, 1956. (English translation by V. I. Weingarten, et. al., Holden-Day, Inc., San Franscisco, 1964).

11. H. A. Evensen and R. M. Evan-Iwanowski, "Effects of Longitudinal Inertia Upon the Parametric Response of Elastic Columns," Journal of Applied Mechanics, March, 1966, pp. 141-148.

12. R. F. Henry and S. A. Tobias, "Modes at Rest and Their Stability in Coupled Non-Linear Systems," Journal of Mechanical Engineering Science, Vol. 3, No. 2, 1961, pp. 163-173.

13. S. A. Tobias, "Free Undamped Non-Linear Vibrations of Imperfect Circular Discs," Proceedings of the Institution of Mechanical Engineers, London, Vol. 171, No. 22, 1957, pp. 691-715.

14. J. W. Miles, "Stability of Forced Oscillations of a Spherical Pendulum," Quarterly of Applied Mathematics, Vol. 20, No. 1, April, 1962, pp. 21-32.

15. G. Murthy and B. Ramakrishna, "Nonlinear Character of Resonance in Stretched Strings," Journal of the Acoustical Society of America, Vol. 38, September, 1965, pp. 461-471.

16. J. W. Miles, "Stability of Forced Oscillations of a Vibrating String," Journal of the Acoustical Society of America, Vol. 38, July-December, 1965, pp. 855-861.

17. R. Hemp and P. Sethna, "The Effect of High Frequency Support Oscillations on the Motion of a Spherical Pendulum," Journal of Applied Mechanics, June, 1964, pp. 351-354.

18. R. Hemp and P. Sethna, "Non-Linear Oscillations of a Gyroscopic Pendulum with an Oscillating Point of Suspension," Les Vibrations Forces Dans Les Systemes Non-Lineaires, Colloques Internationaux Du Centre National De La Recherche Scientifique, No. 148, Marseille, September, 1964.

19. W. H. Quick, "Theory of the Vibrating String as an Angular Motion Sensor," Journal of Applied Mechanics, September, 1964, pp. 523-534.

20. S. G. Ebner, "Elastic Oscillations of Imperfect Columns of Thin-Walled Open Sections Subjected to Axial Periodic Loads," Ph.D. Thesis, University of Colorado, 1968.

21. W. K. Tso, "Parametric Torsional Stability of a Bar Under Axial Excitation," Journal of Applied Mechanics, March, 1968, pp. 13-19.

22. D. A. Evensen, "A Theoretical and Experimental Study of the Nonlinear Flexural Vibrations of Thin Circular Rings," NASA Technical Report, NASA TR R-227, December, 1965.

23. F. Dodge, D. Kana, and H. N. Abramson, "Liquid Surface Oscillations in Longitudinally Excited Rigid Cylindrical Containers," AIAA Journal, Vol. 3, No. 4, April, 1965, pp. 685-695.

24. I. S. Sokolnikoff, Mathematical Theory of Elasticity, Second Edition, McGraw-Hill Book Company, Inc., New York, 1956, p. 31.

25. D. Young and R. P. Felgar, "Tables of Characteristic Functions Representing Normal Modes of Vibration of a Beam," Engineering Research Bulletin No. 4913, Bureau of Engineering Research, The University of Texas, July, 1949.

26. M. L. Moody, "The Parametric Response of Imperfect Columns," Developments in Mechanics, Vol. 4, Proceedings of the Tenth Midwestern Mechanics Conference, 1967, pp. 329-346.

27. K. Klotter, "Non-Linear Vibration Problems Treated by the Averaging Method of W. Ritz," Proceedings of the 1st U. S. National Congress of Applied Mechanics, June, 1951, J. W. Edwards, Ann Arbor, Michigan, 1952, pp. 125-131.

28. J. J. Stoker, "On the Stability of Mechanical Systems," Communications on Pure and Applied Mathematics, Vol. VIII, 1955, pp. 133-142.

29. N. W. McLachlan, Ordinary Non-Linear Differential Equations in Engineering and Physical Sciences, Second Edition, Oxford at the Clarendon Press, 1958.

30. W. J. Cunningham, Nonlinear Analysis, McGraw-Hill Book Company, Inc., New York, 1958.

31. B. A. Finlayson and L. E. Scriven, "The Method of Weighted Residuals-A Review," Applied Mechanics Reviews, Vol. 19, No. 9, September, 1966, pp. 735-748.

32. J. A. Shiflett, "On the Nonlinear Steady State Transverse Vibration of a Cantilever Column with a Sinusoidal Longitudinal End Displacement," Masters Thesis, Georgia Institute of Technology, August, 1968.

33. G. V. Anand, "Nonlinear Resonance in Stretched Strings with Viscous Damping," The Journal of the Acoustical Society of America, Vol. 40, 1966, pp. 1517-1528.

VITA

Edward Charles Haight, Jr. was born on August 25, 1941 in New Orleans. He attended the public schools of New Orleans and Ponchatoula, Louisiana and graduated from Ponchatoula High School in 1959. Ed received from Louisiana State University a Bachelor of Science in Civil Engineering in 1963 and a Master of Science in Engineering Mechanics in 1965. He entered the School of Engineering Mechanics at Georgia Tech in September, 1965.

In 1963 he married Judith Patricia McClellan of Ponchatoula. They have two children: Ned, born in 1967 and Ann, born in 1968.